



Supplementary Materials for

Immune Correlates Analysis of the mRNA-1273 COVID-19 Vaccine Efficacy Trial

Peter B. Gilbert[†], David C. Montefiori[†], Adrian B. McDermott[†], Youyi Fong, David Benkeser, Weiping Deng, Honghong Zhou, Christopher R. Houchens, Karen Martins, Lakshmi Jayashankar, Flora Castellino, Britta Flach, Bob C. Lin, Sarah O’Connell, Charlene McDanal, Amanda Eaton, Marcella Sarzotti-Kelsoe, Yiwen Lu, Chenchen Yu, Bhavesh Borate, Lars W. P. van der Laan, Nima S. Hejazi, Chuong Huynh, Jacqueline Miller, Hana M. El Sahly, Lindsey R. Baden, Mira Baron, Luis De La Cruz, Cynthia Gay, Spyros Kalams, Colleen F. Kelley, Michele P. Andrasik, James G. Kublin, Lawrence Corey, Kathleen M. Neuzil, Lindsay N. Carpp, Rolando Pajon, Dean Follmann, Ruben O. Donis[‡], and Richard A. Koup[‡] on behalf of the Immune Assays; Moderna, Inc.; Coronavirus Vaccine Prevention Network (CoVPN)/Coronavirus Efficacy (COVE); and United States Government (USG)/CoVPN Biostatistics Teams

Correspondence to: pgilbert@fredhutch.org

[†] Contributed equally. [‡] Contributed equally.

This PDF file includes:

Materials and Methods
Supplementary Text S1 and S2
Figs. S1 to S30
Tables S1 to S9
References (39-53)

Table of Contents

Materials and Methods	6
Composition of Research Teams	6
Immune Assays Team.....	6
Moderna, Inc. Team.....	6
Coronavirus Vaccine Prevention Network (CoVPN)/Coronavirus Efficacy (COVE) Team	7
CoVPN/COVE Team (cont'd): COVE Trial Investigators and Study Teams.....	10
United States Government (USG)/Coronavirus Prevention Network (CoVPN) Biostatistics Team.....	20
Trial design and COVID-19 endpoint evaluated for correlates	20
Laboratory methods	20
Solid-phase electrochemiluminescence S-binding IgG immunoassay (ECLIA).....	20
Neutralization assay.....	21
Ethics	22
Bridging of binding antibody assay readouts and neutralizing antibody assay readouts to the WHO International Standard for anti-SARS-CoV-2 immunoglobulin.....	22
Summary values for WHO anti-SARS-CoV-2 IgG (20/136).....	23
Statistical methods	24
Case-cohort sets included in correlates analyses	24
Covariate-adjustment.....	25
Correlates of risk in vaccine recipients.....	25
Correlates of protection: controlled vaccine efficacy and mediation.....	25
Hypothesis testing.....	26
Calibration of ID50 and ID80 titers between the Duke neutralization assay on COVE trial samples and the Monogram PhenoSense neutralization assay performed on AstraZeneca COV002 samples	26
Sensitivity analysis comparing correlate of protection results between COV002 and COVE	26
Software and data quality assurance.....	27
Research reproducibility approach	27
Table S1. Demographics and clinical characteristics of baseline SARS-CoV-2 negative per-protocol trial participants in the immunogenicity subcohort and thus have Day 1, 29, 57 antibody marker data	28
Table S2. Sample sizes of baseline SARS-CoV-2 negative per-protocol vaccine recipients included in immune correlates analyses, by baseline sampling strata and case/non-case strata	29

Fig. S1. (A) Day 29 marker case-cohort set and (B) Day 57 marker case-cohort set.....	30
Fig. S2. Flowchart of study participants from enrollment to the Day 29 and Day 57 case-cohort sets of baseline SARS-CoV-2 negative per-protocol participants.....	31
Fig. S3. Phases of the COVE trial, timing of mRNA-1273 doses and blood sampling, and the two time periods for diagnosis of COVID-19 endpoints (“Intercurrent” and “Post Day 57”).	32
Table S3. Meso-Discovery (MSD) and pseudovirus neutralization assay limits of the four antibody markers evaluated as immune correlates.	33
Fig. S4. For each antibody marker, correlations of Day 29 levels with Day 57 levels in baseline SARS-CoV-2 negative per-protocol vaccine recipients in the immunogenicity subcohort.	34
Fig. S5. Correlations of Day 29 antibody markers in baseline SARS-CoV-2 negative per-protocol vaccine recipients in the immunogenicity subcohort.	35
Fig. S6. Correlations of Day 57 antibody markers in baseline SARS-CoV-2 negative per-protocol vaccine recipients in the immunogenicity subcohort.	36
Fig. S7. A) Anti-RBD IgG concentration and B) pseudovirus neutralization ID80 titer by COVID-19 outcome status.	37
Fig. S8. Marker values (spike IgG, RBD IgG, ID50, ID80) by COVID-19 outcome status in placebo recipients.....	38
Fig. S9. Day 29 marker data points from baseline SARS-CoV-2 negative per-protocol vaccine recipients in the Day 29 marker case-cohort set.	39
Fig. S10. Day 57 marker data points from baseline SARS-CoV-2 negative per-protocol vaccine recipients in the Day 57 marker case-cohort set.	40
Fig. S11. Inverse probability sampling (IPS)-weighted empirical reverse cumulative distribution function curves for each Day 57 marker (spike IgG, RBD IgG, ID50, ID80) and application of the Siber (2007) method (27) for estimating a threshold of perfect vs. no protection.....	41
Fig. S12. Inverse probability sampling (IPS)-weighted empirical reverse cumulative distribution function curves for each Day 29 marker (spike IgG, RBD IgG, ID50, ID80) and application of the Siber (2007) method (27) for estimating a threshold of perfect vs. no protection.....	42
Fig. S13. Day 29 and Day 57 antibody markers (spike IgG, RBD IgG, ID50, ID80) vs. number of days from Day 29 visit until COVID-19 primary endpoint diagnosis for per-protocol baseline SARS-CoV-2 negative vaccine recipient breakthrough cases.....	43
Fig. S14: Covariate-adjusted cumulative incidence of COVID-19 by Low, Medium, High tertile of Day 57 IgG concentration or pseudovirus neutralization titer. (A) Anti-RBD IgG concentration; (B) ID80 titer.....	44
Supplementary Text S1	45
Baseline covariates adjusted for in immune correlates analyses, including the baseline COVID-19 risk score	45
Table S4. Individual baseline variables input into the Superlearner model for predicting occurrence of COVID-19 in baseline SARS-CoV-2 negative per-protocol placebo recipients.¹.....	45
Table S5. Learning algorithm-screen combinations (14 in total) used as input to the Superlearner model in baseline negative per-protocol placebo recipients.....	46

Table S6. Weights assigned by Superlearner to each individual learner in the COVID-19 prediction modeling of the placebo arm.....	47
Table S7. Predictors in learners assigned positive weight by Superlearner in the COVID-19 prediction modeling of the placebo arm.	48
Fig. S15. (A) Cross-validated receiver operating characteristic curve for the two top-performing learners, Superlearner, and the Discrete Superlearner models classifying COVID-19 outcome occurrence in baseline SARS-CoV-2 negative per-protocol placebo recipients, with cross-validated area under the curve (CV-AUC) summarizing classification performance. (B) Receiver operating characteristic curve for the Superlearner upon applying the model built from placebo recipients to baseline SARS-CoV-2 negative per-protocol vaccine recipients, with AUC in parentheses summarizing classification performance.	50
Fig. S16. Superlearner model predicted probabilities of the COVID-19 endpoint starting 7 days post Day 57 visit by case vs. non-case (i.e., control) status, for baseline SARS-CoV-2 negative per-protocol vaccine recipients in the Day 57 marker case-cohort set.....	51
Fig. S17. Covariate-adjusted hazard ratios of COVID-19 per 10-fold increase in each Day 29 antibody marker in baseline SARS-CoV-2 negative per-protocol vaccine recipients overall and in subgroups.....	52
Figure S18. Covariate-adjusted cumulative incidence of COVID-19 by Low, Medium, High tertile of Day 29 IgG concentration or pseudovirus neutralization titer in baseline SARS-CoV-2 negative per-protocol participants.....	53
Fig. S20. Covariate-adjusted risk of COVID-19 by the level of each Day 57 marker (spike IgG, RBD IgG, ID50, ID80), estimated with a generalized additive model, in baseline SARS-CoV-2 negative per-protocol vaccine recipients.....	55
Fig. S21. Covariate-adjusted risk of COVID-19 by the level of each Day 29 marker (spike IgG, RBD IgG, ID50, ID80), estimated with a generalized additive model, in baseline SARS-CoV-2 negative per-protocol vaccine recipients.....	56
Fig. S22. Further analyses of Day 29 ID50 level as a correlate of risk and as a correlate of protection.....	57
Fig. S23. Further analyses of Day 57 ID80 level as a correlate of risk and analysis as a correlate of protection.....	58
Fig. S24. Further analyses of Day 57 anti-spike IgG level as a correlate of risk and as a correlate of protection.....	59
Fig. S25. Further analyses of Day 57 anti-RBD IgG level as a correlate of risk and as a correlate of protection.....	60
Fig. S26. Further analyses of Day 29 ID80 level as a correlate of risk and as a correlate of protection.....	61
Fig. S27. Further analyses of Day 29 anti-spike IgG level as a correlate of risk and as a correlate of protection.....	62
Fig. S28. Further analyses of Day 29 anti-RBD IgG level as a correlate of risk and as a correlate of protection.....	63
Supplementary Text S2: Controlled vaccine efficacy sensitivity analysis and mediation analysis ...	64

Controlled vaccine efficacy sensitivity analysis to assess robustness of the effect of antibody marker on preventing COVID-19 to unmeasured confounding.....	64
Table S8. Sensitivity analysis to assess Day 57 and Day 29 antibody markers categorized as upper vs. lower tertiles as controlled vaccine efficacy CoPs against COVID-19.....	65
Mediation analysis	66
Table S9. Table of mediation effect estimates for quantitative markers with 95% confidence intervals.....	66
Fig. S29. Vaccine efficacy with sensitivity analysis by Day 57 (A) anti-spike IgG level, (B) anti-RBD IgG level, (C) ID50 level, or (D) ID80 level.....	68
Fig. S30. Vaccine efficacy with sensitivity analysis by Day 29 (A) anti-spike IgG level, (B) anti-RBD IgG level, (C) ID50 level, or (D) ID80 level.....	69

Materials and Methods

Composition of Research Teams

Immune Assays Team

(PubMed listed, and ordered alphabetically by affiliation)

Affiliation	Team Members
Biomedical Advanced Research and Development Authority (BARDA), Washington, DC	Oleg Borisov, Flora Castellino, Brett Chromy, Mark Delvecchio, Ruben O. Donis, Tremel Faison, Corey Hoffman, Christopher Houchens, Tom Hu, Chuong Huynh, Pennie Hylton, Lakshmi Jayashankar, Aparna Kolhekar, James Little, Karen Martins, Jeanne Novak, Carol Sabourin, Evan Sturtevant, Xiaomi Tong, John Treanor, Danielle Turley, Leah Watson
Boston Consulting Group, Boston, MA	Gian King, Andrew Li, Najaf Shah, Smruthi Suryaprakash, Jue Xiang Wang
Division of AIDS, NIAID, NIH, Bethesda, MD	Patricia D'Souza
Division of MID (Microbiology and Infectious Diseases), NIAID, NIH, Bethesda, MD	Janie Russell
Duke University, Durham, NC	David Beaumont, Kendall Bradley, Jiayu Chen, Xiaoju Daniell, Thomas Denny, Elizabeth Domin, Amanda Eaton, Kelsey Engel, Wenhong Feng, Juanfei Gao, Hongmei Gao, Kelli Greene, Sarah Hiles, Leihua Liu, Kristy Long, Kellen Lund, Charlene McDanal, David C. Montefiori, Marcella Sarzotti-Kelsoe, Francesca Suman, Haili Tang, Jin Tong, Olivia Widman
The Tauri Group, an LMI company - Contract Support for U.S. Department of Defense (DOD) Joint Program Executive Office for Chemical, Biological, Radiological and Nuclear Defense (JPEO-CBRND) Joint Project Manager for Chemical, Biological, Radiological, and Nuclear Medical (JPM CBRN Medical), Fort Detrick, Maryland, USA	Christopher S. Badorrek, Gregory E. Rutkowski
Vaccine Research Center, NIAID, NIH, Bethesda, MD	Akua Abrah, Obrimpong Amoa-Awua, Manjula Basappa, Robin Carroll, Erykah Coe, Jevone Fentress, Britta Flach, Suprabhath Gajjala, Nazaire Jean-Baptiste, Richard A. Koup, Bob C. Lin, Adrian McDermott, Christopher Moore, Mursal Naisan, Muhammed Naqvi, Sandeep Narpala, Sarah O'Connell, Abhinaya Srikanth, Clare Whittaker, Weiwei Wu

Moderna, Inc. Team

(PubMed listed, ordered alphabetically)

Affiliation	Team Members
Moderna, Inc., Cambridge, MA	Weiping Deng, Shu Hahn, Jacqueline Miller, Rolando Pajon, Honghong Zhou

Coronavirus Vaccine Prevention Network (CoVPN)/Coronavirus Efficacy (COVE) Team

(PubMed listed, and ordered alphabetically by institution affiliation)

Affiliation/Funding*	Study Group	Location
AB Clinical Trials	Atoya Adams, MD, MBA, Eric Miller	Las Vegas, NV
Accel Research Sites	Bruce G. Rankin DO, John Hill MD, Steven Shinn MD, Marshall Nash MD	DeLand, FL
Advanced Clinical Research	Sinikka L. Green MD, Colleen Jacobsen, Jayasree Krishnankutty, Sikhongi Phungwayo	Cedar Park, TX
Alliance for Multispecialty Research	Richard M. Glover, II MD, Drs. Stacy Slechta, Troy Holdeman, Robyn Hartvickson, Amber Grant	Newton, KS
Alliance for Multispecialty Research	Terry L. Poling MD, Terry D. Klein MD, Thomas C. Klein MD, Tracy R. Klein MD	Wichita, KS
Alliance for Multispecialty Research	William B. Smith MD, Richard L. Gibson MD, Jennifer Winbigler MD, Elizabeth Parker PA	Knoxville, TN
Baptist Health Center for Clinical Research	Priyantha N. Wijewardane, MD, Eric Bravo MD, Jeffrey Thessing MD, Michelle Maxwell APRN, Amanda Horn APRN	Little Rock, AR
Baylor College of Medicine, NIAID 1UM1AI148575-01S2	Hana El Sahly MD, Jennifer Whitaker MD, Catherine Mary Healy MD, Christine Akamine MD	Houston, TX
Benchmark Research	Laurence Chu, MD, R. Michelle Chouteau, MD	Austin, TX
Benchmark Research	Michael J. Cotugno MD, George H. Bauer, Jr. MD	Metairie, LA
Benchmark Research	Greg Hachigian MD, Masaru Oshita MD, Michael Cancilla NP, Deborah Murray NP, Kristen Kiersey NP	Sacramento, CA
Benchmark Research	William Seger MD, Mohammed Antwi, Allison Green, Anthony Kim	Fort Worth, TX
Brigham and Women's Hospital, NIAID UM1AI069412, NCATS UL1RR025758	Lindsey R Baden MD, Michael Desjardins MD, Jennifer A Johnson MD, Amy Sherman MD, Stephen R Walsh MD	Boston, MA
Carolina Institute for Clinical Research	Judith Borger DO, Ryan Starr DO, Scott Syndergaard DO, Nafisa Saleem MD	Fayetteville, NC
Centex Studies	Joel Solis MD, Martha Carmen Medina PA-C, Westly Keating PA-C, Edgar Garcia PA-C, Cynthia Bueno PA-C	McAllen, TX
Clinical Research Atlanta	Nathan Segall MD, Nathan Segall, Jon Finley, Mildred Stull	Stockbridge, GA
Clinical Trials of Texas	Douglas Scott Denham DO, Thomas Weiss MD, Ayoade Aworo DNP, Parke Hedges MD	San Antonio, TX
Coastal Carolina Research Center	Cynthia Becher Strout MD, Rica Santiago, Yvonne Davis, Patty Howenstine, Alison Bondell	Mount Pleasant, SC
Cornell Clinical Trials Unit - Weill Cornell Uptown & Weill Cornell Chelsea, NIAID UM1AI068619, NCAT UL1TR002384	Kristin Marks MS MD, Grant Ellsworth, MS, MD, Tina Wang, MD, Timothy Wilkin, MD, MPH, Mary Vogler, MD, Carrie Johnston, MD, MS	New York, NY
Covid19 Prevention Network (CoVPN, NIAID-NIH)	Michele P Andrasik, Jessica G Andriesen, Gail Broder, Lawrence Corey, Niles Eaton, Kathleen M Neuzil, Huub G Gelderblom, James G Kublin, Rachael McClennen, Nelson Michael, Merlin Robb, Carrie Sopher	Seattle, WA
DM Clinical Research	Vicki E. Miller MD, MPH, Fredric Santiago MD, Blanca Gomez FNP-C, Insiya Valika PA-C, Amy Starr FNP-C	Tomball, TX
Emory University – Ponce de Leon Clinical Research Site, NIAID 3UM1AI068614-14S1	Colleen Kelley MD MPH, Valeria D Cantos MD, Sheetal Kandiah MD MPH, Carlos del Rio MD	Atlanta, GA
Emory University – Hope Clinic, NIAID 1UM1AI148576-01	Nadine Rouphael MD, Paulina Rebolledo, Srilatha Edupuganti, Daniel Sans Graciaa	Decatur, GA
Emory University School of Medicine, NIAID 1UM1AI148576-01	Evan J Anderson MD, Andres Camacho-Gonzalez MD, Satoshi Kamidani MD, Christiana A Rostad MD, Meghan Teherani MD	Atlanta, GA
George Washington University, NIAID UM1AI068619	David Joseph Diemert MD, Elissa Malkin, Marc Siegel, Afsoon Roberts, Gary Simon	Washington, DC
Hackensack University Medical Center	Bindu Balani MD, Carolene Stephenson, Steven Sperber, Cristina Cicogna	Hackensack, NJ
Henry Ford Health System	Marcus J. Zervos MD, Paul Kilgore MD, MPH, Mayur Ramesh MD, Erica Herc MD, Kate Zenlea MPH	Detroit, MI
Hope Research Institute	Abram Burgher MD, Ann Marie Milliken	Phoenix, AZ
Hope Research Institute	Joseph D. Davis MD, Brendan Levy, Sandra Kelman	Chandler, AZ
Hope Research Institute	Matthew W. Doust MD, Denise Sample, Sandra Erickson	Phoenix, AZ
J. Lewis Research	Shane Glade Christensen MD, Christopher Matich, James Longe, John Witbeck	Salt Lake City, UT
J. Lewis Research	James Todd Peterson MD, Alexander Clark, Gerald Kelty, Issac Pena-Renteria	Salt Lake City, UT

Affiliation/Funding*	Study Group	Location
Jacksonville Center for Clinical Research	Michael J. Koren MD, Darlene Bartilucci MD, Jeffery Jacqmein MD, Alpa Patel MD, Carolyn Tran MD	Jacksonville, FL
Javara	Christina Kennelly MD, Robert Brownlee, Jacob Coleman, Hala Webster	Charlotte, NC
Johnson County Clin-Trials	Carlos A. Fierro MD, Natalia Leistner, Amy Thompson, Celia Gonzalez	Lenexa, KS
Kaiser Permanente Washington Health Research Institute, NIAID 1UM1AI148373-01	Lisa A Jackson MD MPH, Janice Suyehira MD	Seattle, WA
Laguna Clinical Research Associates	Milton Haber MD, Maria M. Regalado MD, Veronica Procasky RN JD, Alisha Lutat	Laredo, TX
Lynn Health Science Institute	Carl P. Griffin MD, Raymond Cornelison, William Schnitz, Shanda Gower	Oklahoma City, OK
Lynn Institute of the Rockies	Ripley R. Hollister MD, Jeremy Brown DO, Melody Ronk PA-C	Colorado Springs, CO
M3 Wake Research	Wayne Lee Harper MD, Lisa Cohen DO, Lynn Eckert PA-C, Matthew Hong MD	Raleigh, NC
MediSync Clinical Research Hattiesburg Clinic	Rambod Rouhbakhsh MD, MBA, Elizabeth Danford MD, John Johnson MD, Richard Calderone MD	Petal, MS
Meridian Clinical Research	Shishir Kumar Khetan MD, Oyebisi Olanrewaju AC-CRNP, Nan Zhai NP-C, Kimberly Nieves AC-CRNP, Allison O'Brien AC-CRNP	Rockville, MD
Meridian Clinical Research	Paul Simon Bradley MD, Amanda Lilienthal MSN NP-C, Jim Callis PA-C	Savannah, GA
Meridian Clinical Research	Adam Benson Brosz MD, Andrea Clement PA, Whitney West APRN, Luke Friesen PA, Paul Cramer APRN	Grand Island, NE
Meridian Clinical Research	Frank Steven Eder MD, Ryan Little FNP, Victoria Engler FNP, John Tarbox FNP, Heather Rattenbury-Shaw DO	Binghamton, NY
Meridian Clinical Research	David Jon Ensz MD, Tavane Harrison, Allie Oplinger	Dakota Dunes, SD
Meridian Clinical Research	Brandon James Essink MD, Jay Meyer MD, Frederick Raiser, III MD, Kimberly Mueller APRN, Roni Gray PA	Omaha, NE
Meridian Clinical Research	Keith William Vrbicky MD, Charles Harper MD, Chelsie Nutsch MD, Wendell Lewis III MD, Cathy Laflan MD	Norfolk, NE
Meridian Clinical Research	Jordan L. Whatley MD, Nicole Harrell MD, Amie Shannon MD, Crystal Rowell APRN, FNP-C, Christopher Dedon APRN, FNP-C	Baton Rouge, LA
NIH	Mamodikoe Makhene MD MPH	Bethesda, MD
New Horizons Clinical Research	Gregory Mark Gottschlich MD, Kate Harden PA-C, Melissa Gottschlich PA-C, Mary Smith MSN, FNP-C, Richard Powell MD	Cincinnati, OH
Optimal Research	Murray A. Kimmel DO, Simmy Pinto MD	Melbourne, FL
Optimal Research	Timothy P. Vachris MD, Mark Hutchens MD, Stephen Daniels DO, Margaret Wells MD	Austin, TX
Optimal Research	Mimi Van Der Leden MD, PhD, Peta Gay Jackson Booth MD	Rockville, MD
Palm Beach Research Center	Mira Baron MD, Pamela Kane DO, Shannen Seversen PA-C, Mara Kryvicky PA-C, Julia Lord PA-C	West Palm Beach, FL
Paradigm Clinical Research Center	Jamshid Saleh MD, Matthew Miles, Rafael Lupercio	Redding, CA
Quality of Life Medical & Research Centers	John W. McGettigan Jr. MD, Walter Patton MD, Riemke Brakema MD, Karin Choquette MSN, ABNP-C, Jonlyn McGettigan MSN, RN	Tucson, AZ
Rancho Paseo Medical Group	Judith L. Kirstein MD, Marcia Bernard NP	Banning, CA
Rapid Medical Research	Mary Beth Manning MD, Joan Rothenberg MD, Toby Briskin MD, Denise Roadman PAC, Sharita Tedder-Edwards FNP	Cleveland, OH
Research Centers of America	Howard I. Schwartz MD, Surisday Mederos, Barbara Corral, Jennifer Schwartz, Nelia Sanchez-Crespo	Hollywood, FL
Rutgers New Jersey Medical School, NIAID UM1AI068619	Shobha Swaminathan MD, Amesika Nyaku MD MS, Tilly Varughese MD, Michelle DallaPiazza MD	Newark, NJ
Saint Louis University, NIAID 1UM1AI148685-01	Sharon E Frey MD, Irene Graham MD, Getahun Abate MD PhD MSc, Daniel Hoft MD PhD	St. Louis, MO
St. Vincent's Health System	Leland N. Allen III MD, Leslie Anne Edwards MSN, CRNP, William Simpson Davis Jr., MS PA-C, Jessica Maria Mena, PA	Birmingham, AL
Suncoast Research Group	Mark E. Kutner MD, Jorge Caso MD, CPI, Maria Hernandez Moran APRN, Marianela Carvajal APRN, Janet Mendez APRN	Miami, FL
Sundance Clinical Research	Larkin T. Wadsworth III MD, Horacio Marafioti, Lyly Dang, Jennifer Berry, Lauren Clement	St. Louis, MO
Synexus Clinical Research	Michael Ryan Adams MD, Leslie Iverson PA	Murray, UT
Synexus Clinical Research	Joseph Lee Newberg MD, Laura Pearlman MS, MD, MBA	Chicago, IL
Synexus Clinical Research	Paul Joseph Nugent DO, Leonard Singer	Cincinnati, OH

Affiliation/Funding*	Study Group	Location
Synexus Clinical Research	Michele Diane Reynolds MD, Jennifer Bashour MD, Robert Schmidt MD	Dallas, TX
Synexus Clinical Research	Neil Parmanand Sheth MD, Kenneth Steil DO	Glendale, AZ
Synexus Clinical Research	Ramy Joseph Toma MD, William Kirby MD, Pink Folmar MD, Samantha Williams NP	Birmingham, AL
Synexus Clinical Research	Judith White MD, Robert Meyer MD, Sejal Patel MD, Prity Patel APRN	Orlando, FL
Tekton Research	Paul Pickrell MD, Stefanie Mott FNP-C, Carol Ann Linebarger MD, Hussain Malbari MD, David Pampe MD	Austin, TX
Texas Center for Drug Development	Veronica G. Fragoso MD, Lisa Holloway MD, Cecilia McKeown-Bragas MD, Teresa Becker MD, Vicki Miller MD	Houston, TX
Trial Management Associates	Barton G. Williams MD, William H. Jones MD	Wilmington, NC
VA Greater Los Angeles Healthcare System	Michael Lewis MD, Elham Ghadishah, Joseph Yusin, Mai Pham	Los Angeles, CA
University of California Los Angeles, NIAID UM1AI068619	Jesse L Clark MD, Steven Shoptaw PhD, Michele Vertucci PA, NP, Will Hernandez NP	Los Angeles, CA
University of California San Diego, NIAID UM1AI068636	Stephen A. Spector MD, Amaran Moodley MD, Jill Blumenthal MD, Lisa Stangl NP, Karen Deutsch NP	La Jolla, CA
University of Chicago	Kathleen M. Mullane DO PharmD, David Pitrak MD, Cheryl Nuss FNP, Judy Pi PharmD	Chicago, IL
University of Cincinnati, NIAID UN1AI068619	Carl Fichtenbaum MD, Margaret Powers-Fletcher PhD, Michelle Saemann RN, Sharon Kohrs RN	Cincinnati, OH
University of Colorado Denver, Anschutz Medical Campus, NIAID UM1AI068636	Thomas B. Campbell MD, Andrew Lauria, Jose Castillo Mancilla, Hillary Dunlevy	Aurora, CO
University of Illinois at Chicago – Project WISH, NIAID UM1AI068619	Richard M Novak MD, Andrea Wendrow, Scott Borgetti, Ben Ladner	Chicago, IL
University of Maryland School of Medicine, NIAID 1UM1AI148689-01	Karen L Kotloff MD, Matthew Laurens, Milagritos Tapia, Lisa Chrisley, Cheryl Young	Baltimore, MD
University of Miami, NIAID 3UM1AI068614-14S1	Susanne Doblecki-Lewis MD, Maria Luisa Alcaide, Jose Gonzales-Zamora, Stephen Morris	Miami, FL
University of North Carolina at Chapel Hill, NIAID UM1AI068619	Cynthia Gay MD MPH, David Wohl MD, Joseph Eron, Jr. MD	Chapel Hill, NC
University of Pennsylvania, NIAID 3UM1AI068614-14S1	Ian Frank MD, Debora Dunbar, David Metzger, Florence Momplaisir	Philadelphia, PA
University of Pittsburgh Medical Center, NIAID 1UM1AI148452-01	Judith Martin MD, Alejandro Hoberman MD, Timothy Shope MD MPH, Gysella Muniz MD	Pittsburgh, PA
University of Texas Medical Branch, NIAID 1UM1AI148575-01	Richard Rupp MD, Amber Stanford PA-C, Megan Berman MD, Laura Porterfield MD	Galveston, TX
VA Greater Los Angeles Healthcare System	Michael Lewis MD, Elham Ghadishah, Joseph Yusin, Mai Pham	Los Angeles, CA
Vanderbilt University Medical Center, NIAID 1UM1AI148452-01	Clarence Buddy Creech II MD, Shannon Walker MD, Stephanie Rolsma MD PhD, Robert Samuels, Isaac Thomsen MD	Nashville, TN
Vanderbilt University Medical Center, NIAID 3UM1AI068614-14S1	Spyros Andrews Kalams MD, Greg Wilson MD	Nashville, TN
Velocity Clinical Research	Gregg H. Lucksinger MD, Kevin Parks MD, Ryan Israelsen MD, Jaleh Ostovar FNP-C, Kary Kelly FNP-C	Medford, OR
Velocity Clinical Research, San Diego	Jeffrey Scott Overcash MD, Hanh Chu, Kia Lee, Karla Zepeda	La Mesa, CA
VitaLink Research	Luis I. De La Cruz MD, Steve Clemons, Elizabeth Everette, Suzanna Studdard	Greenville, SC
VitaLink Research	Gowdhami Mohan MD, Stefanie Tyson, Alyssa-Kay Peay, Danyel Johnson	Anderson, SC
VitaLink Research-Spartanburg	Gregory J. Feldman MD, May-Yin Suen, Jacqueline Muenzner, Joseph Boscia, Farhan Siddiqui	Spartanburg, SC
Wake Forest University Health Sciences	John Sanders MD, PhD, James Peacock MD, Julio Nasim MD	Winston Salem, NC
WR-Clinical Research Center of Nevada	Michael L. Levin MD, Julie Hussey MSN APRN FNP-C, Marcy Kulic MD	Las Vegas, NV
WR-ClinSearch	Mark Montgomery McKenzie MD, Teresa Deese, Erica Osmundsen, Christy Sweet	Chattanooga, TN
WR-Global Medical Research	Valentine Mbepson Ebuh MD MA MSc, Elwaleed Elnagar MD, Georgette Ebuh DNP APRN FNP-C, Genevieve Iwuala FNP	Dallas, TX
WR-Medical Center for Clinical Research	Laurie J. Han-Conrad MD, Todd Simmons MD, Denis Tarakjian MD	San Diego, CA

*Funding of institutions by the National Institute of Allergy and Infectious Diseases (NIAID) and/or research support by the National Center for Advancing Translational Science (NCATS) as indicated. All other institutions were funded by Office of the Assistant Secretary for Preparedness and Response, Biomedical Advanced Research and Development Authority. The content of this publication is solely the responsibility of the authors and does not necessarily represent the official views of the funding sources.

CoVPN/COVE Team (cont'd): COVE Trial Investigators and Study Teams

Principal Investigator	Study Team	Institution	Location
Atoya Adams, MD, MBA	Miriah Campbell, Eric Miller, Daisy Langarica, Alia Bober, Diana Giraldo	AB Clinical Trials	Las Vegas, NV
Michael Ryan Adams, MD	Leslie Iverson, Andryelle Toledo, Melinda Bullington, Alicia Hanten, Carolyn Taylor, Shannon Wright, Chase Carnahan, Rachel Law, Natalie Smith, Julie Taylor, Jared-Robert Blake, Stefanie Vasconez, Courtney Jensen	Synexus Clinical Research	Murray, UT
Leland N. Allen III, MD	Leslie Anne Edwards, William Simpson Davis, Jr., Ronald Meza, Jordan Stauffer, John Farringer, Faith Holmes, Rhonda Buzbee, Cristina Velez, Huse Lisa, Lisa Huse, Camelia Speegle, Gregory Prestage, Mary Perez, Jessica Space, Matthew Todd, Jessica McDowell, Marha Bunnell-Pollak, Jackie Ziegler, Jasmine Ali, Dumitru Sirbu, Kellie Williams, Logan Sawyer, Richelle Chambliss, Samantha Blackmon, Stephanie Brennan, Tiffany Gibbs, Alexandria Anderson, Caitlin Roll, Candace Robinson, Zachary McCoy, Jessica Bartlett, Kimberly Cornelison, Chris Bovell, Vincent Baglini, Christy Greenhalgh, Jessica Maria Mena, David House, Matt Honold, Esteban Zurita	St. Vincent's Health System	Birmingham, AL
Evan J. Anderson, MD	Kathleen Stephens, Francine Dyer, Maya Stagg, Aaliyah Carron, Austin Lu, Julia Barton, Sy Tran, Leisa Bower, Esther Park, Jianguo Xu, Rebecca Gonzalez, Vy Ngo, Mike Shepard, Lezly Roxxette Zepeda, Karen Sytsma, Sandra Rojas-Honan, Felicia Glover, Susan Rogers, Theda Gibson, Christina A. Rostad, Andres Camacho-Gonzalez, Teresa Ball, Satoshi Kamidani, Mehgan Farah Teherani, Vikash Patel, Etza Peters, Peggy Kettle, Lisa Macoy, Cindy Lubbers, Amber Samuel, Laila Hussaini, Kathryn Zaks, Caroline Ciric, Meg Taylor, Oliver Smith, Amy Muchinsky, Sydney Biccum, Laura Clegg, Dean Kleinhenz, Angelle Ijeoma, Hannah Huston	Emory University School of Medicine	Atlanta, GA
Lindsey Baden, MD	Xhoi Mitre, Jon Gothing, Bruce Bausk, Jessica Cauley, Natalie Izaguirre, Lewis Novack, Michael Seaman, Katherine Yanosick, Henry Rutherford, Jung Hyun Kim, Dominique Betterbed, Kathleen Garvey, Lauren Clore, Alexander Mills, Deepesh Duwadi, Alessandra Setaro, Kyl Bowman, Kevin McManus, Sidali Beriane, Fadi Ghantous, Christy Lavine, Jasper Ophel, Joseph Sapiente, Jessica Doring, Tessa Speidel, Lauren Garneau, Robert Dannemiller, Kirquenie Rolle, Mulika Chhorn, Bailey McCarthy, Hana Flaxman, Milenko Tanasijevic, Cameron Nutt, Javier Barria, Andre Avila-Paz, Buteau Malhaika, Tong Alexandra, Tenaizus Woods, Bethany Evans, Hannah Jin, LaKeisha Gandy, Stephanie St. Pierre, Carolyn Darcy, Michael Corrado, James Maguire, Adetoun Okenla, Tamara Roldon Sevilla, David Kubiak, Cassandre Titus, Movita Harrigan, Maria Alvarado, Rose Theodat, Amy Sherman, Laura Platt, Kirsten Goodman, Laura Nicholson, Wilfredo Matias, Emily Koleske, Ruth Rodriguez, Nicole Taikeff, Jun Bai Park Chang, Julia Klopfer, Phoebe Cunningham, Elizabeth Sampson, Karen Magsipoc, Maureen Macgowan, Lauren Donahue, Haley Schram, Noah Abasciano, Megan Powell, Janet Morgan, Yazed Alsowaida, Olivia Riccardi, Neha Limaye, Virginia Loudermilk, Austin Kim, Kevin Zinchuk, Caitlin Grant, Charles Kelly, David Mellace, Jamie Myers, Erika Gribb, Jose Licon, Monica Feeley, Stephen R Walsh, Jennifer A Johnson, Ann Woolley, Alexis Liakos, Jane Kleinjan, Jon Gothing, Nicolas Issa, Michael Desjardins, Raphael Dolin, Alka Patel, Opeyemi Talabi, Christin Price, Paulette Chandler, Elizabeth W Karlson, Allison P Moriarty	Brigham and Women's Hospital	Boston, MA
Bindu Balani, MD	Smith Kerowyn, Sergio Garcia, Charo Valdez, Shelly Chin, Caitlin DiBello, Silvia Lara, Chika Ekweghari, Abena Roberts, Abimbola Coker, Marie-Therese Estanbouli, Greg Eskinazi, Michael Tortoriello, Jay Elkareh, Meral Karakoc, Olga Spathis, Patrice Hassoun, Carolene Stephenson, Steven Sperber, Kaur Harveen, Cristina Cicogna, Ciaran Mannion	Hackensack University Medical Center	Hackensack, NJ
Mira Baron, MD	Pamela Kane, Maria Bermudez, Shannen Seversen, Mara Kryvicky, Julia Lord, Terri Barr, Daisy Acevedo, Elena Acosta, Delta Anderson, Alexandra Arango, Anne Bauer, Joshua Egbehor, Tim Flanary, Audrey Haber, Carol Henao, Patti Isaacson, Peter Jacob, Sakaiya Jackson, Karen Kodes, Ludovic La-Branche, Kimarie Lee-Russell, Carol Liso, Cristina Liso, Stephanie Morse, Michelle Navarrette, Christy Norcross, Nora Norcross, Annette Pitts, Mary Sergalis, David Scott, Tytiana Spearman, Danielle Theodore, Brian Thomas, Jennifer Torres	Palm Beach Research Center	West Palm Beach, FL
Judith Borger, DO	Jennifer Angell, Nicole Austin, Deanna Benz, Lucian Cappoli, Nicole Davis, Lynn Eckert, Kathryn Hostetter, Stephanie Keating, Jeanette Mangual-Coughlin, Avia McClain-Stocker, Ifeanyi Momodu, Cheryl Norris, Brennan Opanasenko, Stacey Saldua, Nafisa Saleem, Amy Sheets, Ryan Starr, Scott Syndergaard, Jennifer Thomas, Michelle Wallace, Jeffery Pemberton, Mitchell Arildsen, Dan Tomita	Carolina Institute for Clinical Research	Fayetteville, NC
Paul Simon Bradley, MD	Taja Adams, Stephanie Ailey, Kira Bell, Shanice Bennett, Vincent Bernades, Jim Callis, Bounphone Chanthavong, Taryn Collett, Anne Crouch, Shannon Davis, Morgan Deal, Mimi Duncan, Brandon Essink, Laura Falcone, Debra Gabrielson, Brooke Halpern, Anyfa Hanna, Cassie Heisey, Dawn Kalloniatis, Andrew Kimball, Jeanette Lee, Amanda Lilienthal, Ginny McNew, Crystal Neely, Kay Lynn Olmsted, Nicole Osborn, Chevon Roberts, Pechoka Sanders, Cynthia Seedorf, Kathryn Stoddard, Jonathan Whelan, Stella Yoon	Meridian Clinical Research	Savannah, GA

Principal Investigator	Study Team	Institution	Location
Adam Benson Brosz, MD	Rhonda Richter, Debra Gabrielson, Kayla Flege, Ashley Bell, Karen Jo Johnson, Paul Cramer, Jessica Stanton, Andrea Clement, Whitney West, Laura Falcone, Amanda Friesz, Kathy Osborne, Summer Tophoj, Kimber Breeden, Susan Newman, Douglas Herbek, Lindsey Mettenbrink, Luke Friesen, Alison Pierce	Meridian Clinical Research	Grand Island, NE
Abram Burgher, MD	Stephanie Catanzaro, Shauna Harrell, Magen Hess, Nate Alderson, Bettie D'Nise Corcoran, Norma Frederick, Adrian Alejo, Brian DeCraene, Karen Wakefield, Scarlett Hammett, Susan DeCraene, Ann Marie Milliken, Neil Pearson, Donald Terral Harper	Hope Research Institute	Phoenix, AZ
Thomas B. Campbell, MD	Andrew Lauria, Jenelynn Kimble, Steven Johnson, Matin Krsak, Andrew Monte, Patrisha Adkins, Michelle Barron, Suzanne Fiorillo, Amy Harrison, Anderson Victoria, Nga Le, Sara Berech, Jose Castillo-Mancilla, Kristine Erlandson, Laurel Ware, Josie Marshall, Stephen Bartlett, Hillary Dunlevy	University of Colorado Denver, Anschutz Medical Campus	Aurora, CO
Shane Glade Christensen, MD	Christopher Mickelson, Jessica Shaw, Emily Raming, Amy Nelson, Gabrielle Lewis, Jenessa Folsom, Mikaela Jones, Dylan Owen, Rachel Pugmire, Jennifer Bradley, Anjanette Kemp, Krista Marti, Allyson Christensen, Madison Ellis, Holly Anderson, Emily Bloomquist, Ross Brunetti, Thomas Conner, Jr., Gina Cox, Diana Grazulis, Wesley Lewis, James Longe, Christopher Matich, Bryan Nelson, Sarah Scott, John Witbeck, Stephen Wood	J. Lewis Research	Salt Lake City, UT
Laurence Chu, MD	Jennifer Bacchi, Maria Barrientes, Lamar Box, Christian Casas, R. Michelle Chouteau, Katherine Davis, Tandra Dora, Cindy Duran, Pamela Fidler, Ruth Fitch, Brooke Harris, Isaiah Knight, Jennifer Leyva, Michelle Listz, Jennifer Montes, Javier Perez, Jessica Ruff, Dean Skiles, Sean Turnbow, Francesca Vigil, Breana Wade, Kelly Weber	Benchmark Research	Austin, TX
Jesse L. Clark, MD	Sandy MacNicol, Somaieh Talebi, Timothy Hall, Steven Shoptaw, Emery Chang, Michael Li, David Goodman, Paul Adamson, Oladunni Adeyiga, Inez Bentancourt, Susan Reed, Christopher Blades, Jasmin Tavares, Demetria Villanueva, Simone Riley, Jonathan Veloz, Schuyler Thomas, Will Hernandez, Jennifer Baughman, Mitchell Stern, Michele Vertucci	University of California, Los Angeles	Los Angeles, CA
Michael J. Cotugno, MD	Kyra Lawson, Kim Harper, Edwin Adamson, George H. Bauer Jr., Julie Bilich, Brenda Lawson, Brandon Illickal, Lois Eaglin, Heather Salisbury, Jeff Segner	Benchmark Research	Metairie, LA
Clarence Buddy Creech II, MD	Shanda Phillips, Naomi Kown, Katherine Sokolow, Wendy Winn, Katherine Wright, Shannon Walker, Stephanie Rolsma, Anna Gallion, April Hanlotxomphou, Deborah Myers, Robert Adkisson, Natalia Jimenez, Cindy Trimmer, Roberta Winfrey, Matthew Donio, John Oleis, Donna Torr, Shelly McGehee, Robert Samuels, Sandra Yoder, Eric Brady, Isaac Thomsen, Madeleine Guy, Emma Alexander, Lana Howard, Krisha Alexander, Shane Moore, Tacora Wright, Tara Evans, Ursula Powell, Jenna Caserta, Valerie Mitchell, Meryk Moore, Melissa Lehman, Diane Anders, Constance Dotye, Crystal Rice, Lamar Bowman, Sherri Hails, Monique Bennett, Nicki Soper, Leigh Howard	Vanderbilt University Medical Center	Nashville, TN
Joseph D. Davis, MD	Sandra Kelman, Sandra Braden, Sabrina Bolland, Mia Munoz, Jose Barocio, Brendan Levy, Dhwani Shah, Neil Pearson, Stephanie Catanzaro, Nathan Alderson, Susan DeCraene, Maureen Godfrey, Skyla Clark	Hope Research Institute	Chandler, AZ
Luis I. De La Cruz, MD	Amy Ford, Taylor Wilson, Cindy Smith, Austin Lambert, Erin Zeiler, Kaelyn Rowland, Marlee Smith, Suzanna Studdard, Zandra Hamilton, Meredith Benfield, Sara Poff, David Godwin, Elizabeth Everette, Steven Clemons, Kayla Peay, Stephanie Gilreath	VitaLink Research	Greenville, SC
Douglas Scott Denham, DO	Thomas Weiss, Parke Hedges, Ayoade Avworo, Kay Scroggins, Leisel Koerber, Antonio Gutierrez, Nathan Cortez, Andrea Gomez, Darlington Akahara, Michelle Smith, Kristy Trevino, Beatriz Herrera, Shaiane Dickerson, Kerry de Jesus, Matthew Korte, Cynthia Ramos, Reanna Martinez, Erica Leal, Shakera Flores, Paul Esparza, Brian Hemming, Melinda Axton, D'Andre White, Terri Perez, Carolina Coronado, Rebecca Many, Clayton Stone, Kimberly Evans, Anshumaan Maharaj, Stephen Brick, Steffanie Barrera, Staci Poettgen, Dawn Killian, Gerardo Pena, Karol Perez, Victoria Hernandez, Kevin Martinez, Amy Griffith, Nolan Payton, Quincey Hogue, Jamie Padilla, Emily Mendez, Lily Hays, Maristelle Co, Nicholas Trinidad, Ismael Rodriguez, Amy Lewis, Cindi Nellis, Lele Simmons, Marissa Johnson	Clinical Trials of Texas	San Antonio, TX
David Joseph Diemert, MD	Linda Witkin, Aimee Desrosiers, DeEnna Wedding, Bertran Walton, LaKeisha Queen, Ryan Mouton, Caroline Thoreson, Manya Magnus, Jennifer Wald, Erika Faust, Nicholas Heredia, Robbie Kattappuram, Hira Qadir, Chelsea Ware, Hannah Yellin, Kegan Dasher, Daniel Mullen, Jeanne Jordan, Taylor Ladson, Madison Lintner, Kaitlyn Macnair, Bitana Saintilma, Kelly Thomas, Samantha Walker, Neha Rampally, Madhu Balachandran, Elissa Malkin, David Parenti, Hana Akseled, Marc Siegel, Gary Simon, Afsoon Roberts, Aileen Chang	George Washington University	Washington, DC

Principal Investigator	Study Team	Institution	Location
Susanne Doblecki-Lewis, MD	Maria Luisa Alcaide, Jose Gonzalez-Zamora, Stephen Morris, Yimy Puerto, Annie Salvarrey, Claudia Balgas, Claudia Santos, Katherine King, Brahian Steven Erazo, Mayra Fernandez, Leopoldo Cordova-Garcia, Elisa Corzo-Sanchez, Edgar Fernandez, Loreta Padron, Stefani Ann Butts, Kenia Moreno, Juan Casuso, Maria de Pilar Valanzasca, Thomas Tanner, Marilyn Fernandez, Mary Aloise, Inza Patton, Vivian Pastrana, Sendy Puerto, Irma Barreto Ojeda, Junlin Long, Barbara Huang, Gilianne Narcisse, Vanessa Perez	University of Miami	Miami, FL
Matthew W. Doust, MD	Denise Sample, Sandra Erickson, Nate Alderson, Adrian Alejo, Stephanie Catanzaro, Susan DeCraene, Cassie Enrico, Sandra Erickson, Alex Guereque, Shauna Harrell, Shana Harshell, Stephanie Junker, Stephanie Laufenberg, Madison Mikulak, Makayla Morra, Nicole Olson, Neil Pearson, Jasmin Redden, Monique Romo, Denise Sample, Dhvani Shah, Sahara Vega, Emma Kar	Hope Research Institute	Phoenix, AZ
Valentine Mbepson Ebu, MD	Elwaleed Elnagar, Georgette Ebu, Genevieve Iwuala, Catina Adams, Marissa Cervenka, Ezgar Del Real, Shraddha Dubal, Elwaleed Elnagar, Jenifer Fiette, Kathy Harrell, Genevieve Iwuala, Vicki Martinez, Robert Miranda, Brennan Opanasenko, Destiny Robinson, Liz Ruiz, Amy Sheets, Shoniece Wallace	WR-Global Medical Research	Dallas, TX
Frank Steven Eder, MD	Ryan Little, Victoria Engler, John Tarbox, Heather Rattenbury-Shaw, Deborah Hubish, Jessie Taylor, Debra Gabrielson, Jessica Fellows, Jennifer Molstead, Kathe Olmstead, Ashley Conover, Tammy Kohn, Chelsea Briar, Corrine Young, Collen McVannan, Kelli Quick, Shaylyne Hubanks, Kimber Breeden, Ann Marie Sampson, Traci Hull, Tarin Gordon, Susan Owen, Kate Macarak, Tonya Rackett, Jacob Blattstein, Partidge Jane Aton, Nicole Croft, Carolyn Grausgruber, Rebecca Miller, Ryan Little, Victoria Engler, John Tarbox, Heather Rattenbury-Shaw, Nathan Kimball, Courtney Heisey, Ginny McNew, Abigail Wine, Cindi VanKuren, Jared Frick, Tammy Dennis, Andrew Kimball	Meridian Clinical Research	Binghamton, NY
Hana M. El Sahly, MD	Jennifer A. Whitaker, C. Mary Healy, Christine Akamine, Wendy A Keitel, Robert L Atmar, Annette Nagel, Sandra Francisco, Thea Marie Cordero, Janet Brown, Jennifer Christensen, Caroline Doughty-Skierski, Connie Rangel, Carrie Kibler, Coni Cheesman, Lisreina Toro, Chanei Henry, Chianti Wade Bowers, Pedro Piedra, Kathy Bosworth, Kayla Burrell, Jesus Banay, Tykel Eddy, Trent Davis, Shetel Anassi, Yvette Rugeley, Olga Rybina-Willis	Baylor College of Medicine	Houston, TX
David Jon Ensz, MD	Pamela Allen, Taylor Bergh, Kimber Breeden, Avery Dunn, Brandon Essink, Debra Gabrielson, Rylea Gulick, Tavane Harrison, Courtney Heisey, Andrew Kimball, Shelby Klaschen, Jessica Knight, Makayla Langston, Meagan Miller, Allie Oplinger, Heather Persinger, Alison Pierce, Kathryn Stoddard, Kayla Sturgeon, Jamie Thompson, Melissa Wiseman	Meridian Clinical Research	Dakota Dunes, SD
Brandon James Essink, MD	Jay Meyer, Frederick Raiser, Kimberly Mueller, Roni Gray, Riley Brockman, Tabitha Campbell, Carrie Essink, Laura Falcone, Roni Gray, Linda Layton, Jay Meyer, Kimberly Mueller, Tiffany Nemecek, Frederick "Fritz" Raiser, III, Jessica Satorie, Chelsea Steinmetz, Nicole Osborn, Cassie Heisey, Maria Nguyen	Meridian Clinical Research	Omaha, NE
Gregory J. Feldman, MD	May-Yin Suen, Brittany Cooksey, Madison Fowler, Sarah Chynoweth, Gary Clemons, Laura Jolly, Charlie Jordan, Heather Allison, Steve Clemons, Amber Brittany Belcher, Allison Kelly, Marsha Gossett, Wendy Taylor, Amy Witt, Kendal Nelson, Jeffrey Witt, Jacqueline Muenzner, Elizabeth Everette, Supinder Channa, Allison Ayers, Joseph Boscia, Farhan Siddiqui	VitaLink Research-Spartanburg	Spartanburg, SC
Carl J. Fichtenbaum, MD	Maggie Powers-Fletcher, Michelle Saemann, Sharon Kohrs, Kimberly Mullins, Lindsay Davis, Moises Huaman, Angela Snyder, Kristin Weghorn, Brenda Miller, Elizabeth Costea, Lisa Schira, Romana Saeed, Helen Shelton, Kathleen Ballman, Laura Browning-Cho, Sherry Donaworth, Chris Goddard, Jeanine Goodin, Elizabeth Niederegger, Lisa Hachey, Tamara Maus, Pam Fletcher, Makayla Bishop, Victoria Straughn, Shaina Homer, Carrie Christofield, Dana Burns, Jason Mayes, Kelly Windholtz, Lisa Proffitt, Faizan Qureshi, Michelle O'Neil, Arustamyan Lisa, Sarah Trentman, Eva Whitehead, Jennifer Baer, Linda Hinds, Jaasiel Chapman, D'Vaughn House, Gary Frazier, Judy Houston, Lisa Altenau, Mary Burns, Dorice Smith, Justin Ragle, Eric Mueller, Cynthia Nypaver, Jaime Robertson, Anissa Moussa, Geronimo Fera Garzon, Sierra Bennett, Marlana Petrie	University of Cincinnati	Cincinnati, OH
Carlos A. Fierro, MD	Mazen Zari, Celia Gonzalez, Natalia Leistner, Mary Easley, Mary Provost, Krista Estrada, Ann Geier, Amy Thompson, Heather Barker, Karol Moore, Kelly Moen, Monica Atwood, Amber Wolf, Brandi Dickerson, Manyoohn Rinehart, Dina Hammine, Angela Eichler, Casey Johnson, Nathan Arthur	Johnson County Clin-Trials	Lenexa, KS
Veronica G. Fragoso, MD	Lisa Holloway, Cecilia McKeown-Bragas, Teresa Becker, Vicki Miller, Leena Mir, Elton Oliveira, Moez Talpur, Enya Rentas-Sherman, Gabriela Maria Becerra, Dewayne Hicks, Robert Krbashyan, Shakira Barr, Ashraf Jafri, Herman Ortiz, Zohair Harianawala, Chandra Tobin, Norma Gonzalez, Saji Perinjilil, Khorshid Amirhosravi, Tracy Kowalski, Biman Goswami, Waheeda Sureshababu, Amy Anderson, Berenice Ferrero, Simeen Khan, Chen-Ho Yang, Nazanin Zarinkamar, Scott Ward, Crystal Reese, Miyosha Lewis, Olga Konshina, Lorrian Yates, Joel Cano, Quiana Wilson, Kara	Texas Center for Drug Development, Inc.	Houston, TX

Principal Investigator	Study Team	Institution	Location
	Sikes, Diana Chehab, Joanna Quezan, Maryam Rabbani, Sadaf Batla, Abbyssinia Moges, Diego Carrington, Matthew Joseph, Laura Grissanty, Dean Jang, Dustin McFadden, Misbah Baloch, Elisa Morales, Abdeali Dalal, Frances Saubon, William Fernandez, Jenny Toress, Blessing Felix, Zain Rizvi		
Ian Frank, MD	Annet Davis, Eileen Donaghy, Nicole Sundo, Juan Ramirez, Laura Schankel, Dana Brown, Katharine Bar, Dana Brown, Christopher Chianese, Gillain Constantino, Dovie Watson, Kathleen Degnan, Helen Koenig, William Short, Petra Alexander, Eileen Mergliano, Jie Ho, Michele Wisniewski, Debora Dunbar, Liani Santini-Lopez, Rosemarie Kappes, Angela Cabassa, Tammy Chen, Berry SotoVega, Deborah Kim, Devon Cliett, Kate Kearns, Jillian Baron, Vivian Leung, Florence Momplaisir, Sarah Wood, Tameka Matthews, David Metzger, Richard Tustin	University of Pennsylvania	Philadelphia, PA
Sharon E. Frey, MD	Irene Graham, Getahun Abate, Daniel Hoft, Heather Douds, Cassandra Zehenny, Joan Siegner, Helay Hassas, Kim Cooper, Shirley Dettlebach, Sabrina DiPiazza, Carol Duane, Linda Eggemeyer-Sharpe, Lauren Foreman, Jerry Hutter, Ryan Kerr, Kate Liefer, Tracy Montauk, Karla Mosby, Janice Tennant, Nicole Purcell, Kiana Wilder, Kathleen Chirco, Sharon Irby-Moore, Kathleen Koehler, Melissa Loyet, Thomas Pacatte, Susan Stewart, Azra Blazevic, Tamara Blevins, Chase Colbert, Christopher Eickhoff, Lainej Mejjia Jauregui, Keith Meyer, Krystal Meza, Amanda Nethington, Huan Ning, Brittany Williams, Mei Xia, Yinyi Yu, Stanley Dublin, Mary Pat Eastman, Eric Eggemeyer, Mikayla Frye, Michelle Harris, Aleshia McCoy, Donna Duncan, Gwendolyn Tatum, Nicole Purcell, Kiana Wilder, Tammy Grant, Claudia Castillo Paredes, Rong Hou, Jin Wang, Qian Wang, Sarah George	Saint Louis University	St. Louis, MO
Cynthia Gay, MD	David Wohl, Joseph Eron, Jr., Andrew Thorne, Michelle Floris-Moore, Christopher Hurt, David Wohl, Chidinma Okafor, Janette Goins, Ulrike Adam, Ekundayo Nylander-Thompson, Anna Furlong, XinHong Ao, Kathy Guerrero, Melinda Hart, Kathleen Loeven, Rachael Mossey, Esther Speight, Rachel White, Chloe Twomey, Kristen Gray, Miriam Chicurel-Bayard, Susanne Henderson, Patti Vasquez, April Welch, Camille O'Reilly, Maureen Furlong, Noshima Darden-Tabb, Elizabeth DuBose, Marie Oriol, Dynesha Perry, Maria Stetson, Maria Bullis, Shelby Turner, Ebony Harrington, Michael Herce, Suzanne Blevins, Alexander Bradley, Susan Pedersen, Becky Straub, Sandra Barnhart, Felicia Barriga Munante, Nazneen Howerton, Tenvan Keller, Mandy Tipton, Abigail Riddick, Kristi Kirkland, Maggie Harman, Tania Hossain, Centhla Washington, Erin Hoffman, Carolina Pastrana Medina, William Johnson, Samantha Earnhardt, Amy James Loftis, Catherine Kronk, Yaa Ofori-Marfoh, Julie A Nelson, Nicole Maponga, Lina Rosengren-Hovee, William Zhao, Jennifer Thompson, Sarah Law, Holly Milner, Jonathan Oakes, Rachel Cook, Erin Cardot, Oesa Vinesett, Victoria Rucinski, Joy Wannamaker, Tanailly Giralto Smith, Eliza DuBose, Chidinma Okafor	University of North Carolina at Chapel Hill	Chapel Hill, NC
Richard M. Glover, II, MD	Stacy Slechta, Troy Holdeman, Robyn Hartvickson, Amber Grant, Jennifer Bennett, Lindsey Brewer, Janelle Brown, Kelsey Burden, Melissa Burton, Brianna Burton, Jordan Danby, Sheri Duncan, Amber Grant, Robyn Hartvickson, Lisa Hemmelgam, Sherry Henning, Jeri King, Riley King, Colton King, April Kitterman, Shannen Lassiter, Cayla Lawless, Janna Martinez, Ragene Moore, Marissa Mueller, Aaron Nguyen, Justin Phillips, Jordan Reheis, Rebecca Ring, Katherine Saengerhausen, Shannon Thomas, Dylan Thomas, Cindy Thome, Denae Villines, Amber Wenzel, Eileen Wilbert, Avi Woods, Caressa Presley, Brianna Newport, Olivia Allen, Miranda Santiago, Cheryl Sauerwein, Jill Longstaff, Sadie Allen, Candace Heckart	Alliance for Multispecialty Research	Newton, KS
Gregory Mark Gottschlich, MD	Melissa Gottschlich, Steven Anderson, Gregory Mark Gottschlich II, Mary Woeste, Kate Harden, Cindy Young, Michael Pordy, Audrius Ruksenas, Lacy Baird, Kim Krogman, Lori Stanton, Melissa Fuson, Mason Urban, Christine Watson, Richard Powell, Mary Smith, Jacob Sekinger, Diamond Russell, Nicole Lim, Mylene Asmar-Rios, Yusef Museitif, Craig Mitchell, Tarik Whitham, Zachary Rutledge, Troy Porter, Andrea Newlands, Jami Ramsey, Mary Frances Curry, Nishay Holloman, Crystal Barket, Michelle Spear, Shelley Mahan, Taeleigra Greene, Zachary Eardley, Gen Moussa, Mary Ann Gottschlich	New Horizons Clinical Research	Cincinnati, OH
Sinikka L. Green, MD	Julie Hamilton, Alex Fuller, Jeanette Dickhaus, Colleen Jacobson, Triny Cooper, Michelle Jackson, Taylor Evans, Tabitha Judd, Kathryn Alexander, Megan Rosallo, Sikhongi Phungwayo, Robin Dotson, Dana Finley, Michael Vasquez, Cyndi Foster, Gregg Lucksinger, Sarah Smiley, Jayasree Krishnankutty, Ray Coon, Grishma Dhimmer, Melanie Wilkerson, Tatum Shawver, Mercedes Coffman, Devin Teal, Laura Crenshaw	Advanced Clinical Research	Cedar Park, TX
Carl P. Griffin, MD	William Schnitz, Andrea Romero, Kim Hamilton, Raymond Cornelison, Angela Genovese, Shelly Brunson, April Green, Lacey Dietz, Kim Calloway, Chris Hyatt, Destiny Heinzig-Cartwright, Chalimar Rojo, Sharee Wright, Kathi Shaw, Michael Pojezny, Avery Keller, Krystal Hightower, Dalia Tovar, Shanda Gower	Lynn Health Science Institute	Oklahoma City, OK
Milton Haber, MD	Maria Candelario, Martha Bunnell-Pollak, Lauren Wade, Jackie Ziegler, Deena Ramirez, Perla Avalos, Maria Drada, Jasmine Ali, Jessica McDowell, Kehinde Busari, Patricia Church, Ronald Meza, Marco Vela, Esteban Zurita, Chris Connolly, Ruben	Laguna Clinical Research Associates	Laredo, TX

Principal Investigator	Study Team	Institution	Location
	Del Bosque, Alisha Lutat, Chelsea Fleming, Brett Potthoff, Anita Suri, Cynthia Priester, Brenda Hernandez, Veronica Procasky, Eva Cerreta, Matt Honold, Melinda Rodriguez, Maria Regalado, Jordan Stauffer		
Greg Hachigian, MD	Michael Cancilla, Ricardo Castellanos, Angela Cuellar, Yaman Darmarathne, Shailla Faulker, Yana Gordeyeva, Michelle Hisey, Ashley Jungsten, Kristin Kiersey, Pawandeep Nagra, Nav Nagra-Kooner, Jazmin Nauta, Masaru Oshita, Kenneth Quick, Julie Raygoza, Amanny Sadek, Melisa Tinder, Jhoana Torres, Deborah Murray, Kristen Kiersey	Benchmark Research	Sacramento, CA
Laurie J. Han-Conrad, MD	Brandon Baldwin, Lucian Cappoli, Tenisha Garcia, Ella Grach, Brenda Grande, Nicolle Mendez, Natalie Moy, Matthew Musikanth, Karen Mylerberg, Brennan Opanasenko, Mark Pulera, Patti Sanchez-Emerly, Mireles Sarah, Todd Simmons, Denis Tarakjian	WR-Medical Center for Clinical Research	San Diego, CA
Wayne Lee Harper, MD	Toni Bland, Lori Bridges, Lucian Cappoli, Lisa Cohen, Leah Corts, Annie Craft, James Earnhardt, Lynn Eckert, Aubrey Farray, Laura Hoer, Matthew Hong, Chris Hoyle, Jenee Jiggetts, Brian Joseph, Bradley Killebrew, Kendra Lisee, Lucie Mangala, David Musante, Adnan Nasir, Amanda Olsen, Brennan Opanasenko, Marci Parks, Marion Peoples, Katherine Schuch, Judith Shand, Sabine Ucik, Douglas Wadeson, Barbara Wheeler	M3 Wake Research	Raleigh, NC
Ripley R. Hollister, MD	Jeremy Brown, Brandy Ball, Jeremy Brown, Valerie Dyster, Dalia Jeronimo, Shelby Pickle, Michael Pojezny, Melody Ronk, Kathi Shaw, Bobbi Shofner, Jami Wagner, Meghan York, Jill York	Lynn Institute of the Rockies	Colorado Springs, CO
Lisa A. Jackson, MD, MPH	Marilyn Nguyen, Maya Dunstan, Barbara Carste, Sarah Friend, Diana McFeters, Lynn Gross, Mohamed Ajenah, Jana Fitch, Audra Mccoy, David Skatula, Susan Lasicka, Kimberly Brinker, Karen Sherwin, Melissa Scheer, Paula Lins, Roger Calvert, Roxanne Erolin, Stella Lee, Vi Tran, Stephanie Pimental, Bruce Douglas, Lee Barr, Colin Fields, Erika Kiniry, Joe Choe, Janice Suyehira, Joyce Benoit, Michael Witte, Rebecca Lau	Kaiser Permanente Washington Health Research Institute	Seattle, WA
Spyros Andrews Kalams, MD	Greg Wilson, Kyle Rybczyk, Katie Crumbo, Carly Griffin, Latoya Hannah, Amy Kerrigan, Valerie Mitchell, Jenna Caserta, Mary Downey, Nicole Swindle, Shonda Sumner, Amber Massey, Trudy Sullivan, Rita Smith, Cindy Nochowicz, Eric Olson, Christian Warren, Josh Simmons, Dana King, Gwendolyn Rees, Matt Donio, Jesse Case, Keith Richardson, Jarissa Greenard	Vanderbilt University Medical Center	Nashville, TN
Colleen Kelley, MD, MPH	Valeria D. Cantos, Sheetal Kandiah, Carlos del Rio, Christina Bacher, Hannah Huston, Juliet Brown, Divya Bhamidipati, Nithin Gopalsamy, Brittany Lynn Speigel, Elizabeth (Betsy) Hall, Brandon Spratt, Kiran Dhillon, Caitlin Moran, Michael Chung, Felecia Wright, Marcia Peters, Rondell Jagggers, Vanessa Soliman, Ron Gaston, Christopher Foster, Sarah Wiatrek, Bezuayehu Mandefro, Pamela Weizel, Pamela Lankford-Turner, Anandi Sheth, John Gharbin, Catherine Abrams, Philip Powers, Paulina Rebolledo, Christin Root, Tiraje Lester, Sha Yi, Damien Swearing, Fred Ede, Isaac Perez, Kelly Likos, Meen Dhir, Aastha KC, Gabriela Georgial, Tucker Colvin, Nabeel Yar Khan, Valarie Hunter, D'Jamel Young, Felecia Atkinson	Emory University Emory University – Ponce de Leon Clinical Research Site	Atlanta, GA
Christina Kennelly, MD	Jacob Coleman, Brittany Bundeef, Melissa C. Hennessey, Kenneth Owen, Caroline Wilds Wilds, Jennifer Womack, Susan Martello, Chiedza Hooker, Robert Brownlee, Melissa James, Deborah Wesley-Farrington, Lori Whiteheart, Hala Webster, David Framm, Cortney Fretz, Gwyn Gibson, Susan Donahue, Kelly Woodell, Linda McCarty, Jim Vesely, Scott Chatterton, Andrew Ottesen, Enrico Belgrave, Krishna Shah, James Chester Alexander, Brittain Callahan	Javara	Charlotte, NC
Shishir Kumar Khetan, MD	Taja Adams, Tanya Alexander, Tanya Alexaner, Sydney Barmoy, Jake Bart, Kira Bell, Ira Berger, Jemario Blackwell, Priscilla Buahin, Bounphone Chanthavong, Juliana DeVito, Azure Erskine, Brandon Essink, Laura Falcone, Debra Gabrielson, Beau Garland, Barb Geiger, Tiana Oliver, Courtney Heisey, Sucharita Katikala, Andrew Kimball, Heather Lang, Jeanette Lee, Asefa Mekonnen, Devan Myers, Kimberly Nieves, Allison O'Brien, Oyebisi Olanrewaju, Nicole Osborn, Adunola Oshiyoye, Rahul Patel, Alan Pollack, April Poole, Collin Smith, Kathryn Stoddard, Chao Wang, Sean Whelan, Jonathan Whelan, Graciela Zapata, Nan Zhai	Meridian Clinical Research	Rockville, MD
Murray A. Kimmel, DO	Alexa Diec, Ann Riley, Bette Denmat, Bram Swarr, Christina Raidl, Dania Billman, Denise Dixon, Donald Dawson, Elaine Crudo, James Crowley, Katrina Carlson, Kaylie Worzick, Laura Worth, Lisbeth Gordon, Marion Oliver, Robert Holt, Simmy Pinto, Taylor Atkinson, Traci Mitchell, Lana Ghomrawi, Norma Rokoff	Optimal Research	Melbourne, FL
Judith L. Kirstein, MD	Jared Bradshaw, Krista Forster, Jeanette Dickhaus, Marcia Bernard, Erica Sanchez, Nikki Abels, Cynthia Kunakom, Vanessa Vandergoot, Jessica Fisher, Carol Remigio, Jourdan Manfred, Frederick Lloyd, Tiffany Williams, Clarisse Baudelaire, Lovette Cherelle, Nolan Mackey, Alan Valenzuela, Theodore Wyman, Alyssa Taber, Karen Myers, Craig Koch	Rancho Paseo Medical Group	Banning, CA
Michael J. Koren, MD	Shannon Trull, Amanda Elwood, Mary Strickland, Ivy Gulliermo, Chistopher Ganzhorn, Sonia Gerardo, Taylor Johnson, Victoria Kaposchansky, Cassie Lawler, Laura Little, Amanda Pratt, Sheldon Warren, Andrea West, Emery Noles, Nathaniel	Jacksonville Center for Clinical Research	Jacksonville, FL

Principal Investigator	Study Team	Institution	Location
	Grant, Jillian Agnew, Lori Alexander, Brenda Anderson, Deirdre Arrington, Sara Benner, Lisa Carl, Allison Crain, Nafisa Ishaku, Robert Nix, Sharon Smith, Amber Devries, Sandy Salceiro, Opara Chukwudi, Mikaela Karney-Trull, Ramil Castillo, David Graham, Gail Lowe, Alexander Hill, Carolyn Tran, Jeffrey Jacqmein, Darlene Bartilucci, Alpa Patel, Janet Garvey, Mitchell Rothstein, Kenneth Aung-Din, Margaret Gannaway, Arman Mughal, Sandra Fuit, Jolene Wolfer, Erin Schelhorn, Jacob Wolfer, Madison Martinez, Melissa Parks, Patricia Neal		
Karen L. Kotloff, MD	Matthew Laurens, Milagritos Tapia, Lisa Chrisley, Cheryl Young, Barbara Albert, Robin Barnes, Shernel Barrett, Andrea Berry, Melissa Billington, Shannon Bittner, Colleen Boyce, Faith Pa'Ahana Brown, James Campbell, Regina Carpenter, Jamonie Carter, Ginny Cummings, Brenda Dorsey, Jorge Flores, DeAnna Friedman-Klabanoff, Shirley George, Nancy Greenberg, Hassan Haji, Elizabeth Hammershaimb, Susan Holian, Leslie Howe, Myounghee Lee, Alyson Kwon, Kirsten Lyke, Alma Valle Maldonado, Jennifer Marron, Kaitlin Mason, Monica McArthur, Rosa McBryde, Sherry McCammon, Sandra Molina, Kathleen Neuzil, Daniele Nitkowski, Justin Ortiz, Rekha Rapaka, Mardi Reymann, Toni Robinson, Wanda Somrajit, Mark Travassos	University of Maryland, School of Medicine	Baltimore, MD
Mark E. Kutner, MD	Amanda Colina, Isett Caro, Frances Beltran, Jessie Downs, Jonathan Fernandez, Mariete Renden, Miraya Mujica-Alabaci, Susel Figueredo, Yanelis Dominguez, Jaime Blandon, Bryan Ruiz, Leidy Montoya, Edgardo Rodriguez, Jessie Downs, Jason Rothschild, Janett Acle, Yaime Martinez, Soraya Ricardo, Maria Hernandez Moran, Eloisa Guerra, Heidie Perez, Claudia Rodriguez, Victoria Moreno, Vanessa Hechavarria, Saray Carvajal, Daniel Lopez, Carlos Iviricu, Neiner Enriquez, Paola Garcia, Chris Hoyle, Marianela Carvajal, Janet Mendez, Edisleidy Mesa, Marco Ramirez, Dalila Del Valle, Jennifer Ortega, Yeni Hernandez, Jhobana Vargas, Carmen Amador, Juan Delgado, Maury Santos, Meredith Arguelles, Leyanis Coello, Vanessa Ansorena, Jorge Caso, Stacy Machado, Raydel Valdes, Giann Lightbourn, Dayami Davales, Alain Chang	Suncoast Research Group	Miami, FL
Mimi Van Der Leden, MD, PhD	Chrishea Harvey, Tricia Oyeyemi, Aicha Moutanni, Stephanie Melton, Peta-Gay Jackson Booth, Jennifer Yoon, Gloria Kim, Atanas Filev, Francis Uwandi, Meyling Lopez, Janice Spreitzer, Courtney Gennes, Xiangfei Cheng, Matthew Van Sickle, Nick Bart, Brianne Okunji, Frank Maloba	Optimal Research	Rockville, MD
Michael L. Levin, MD	Brennan Opanasenko, Yajaira Ramos, Shonda Lester, Rebecca Boucher, Shawn Harell, Shon Boucher, Patti Sanchez, Nina Scharbach, Alex Sanchez, Shyane Raniello, Wendy Guerra, Krystal Tyner, Kimberly Temple, Ruby Ortiz, Daniel Terreault, Amy Kill, Jade Odynski, Adolfo DeLeon, Debbie Carter, Eduardo Rodriguez, Julia Gass, Sara Esparza, Sierra Dansbee, Tammy Harrison, Marcy Kulic, Lucian Cappoli, Mora Kim, Matthew Fenner, Heather Jimenez, Shraddha Dubal, Julie Hussey	WR-Clinical Research Center of Nevada	Las Vegas, NV
Michael Lewis, MD	Nancy Mohler, Mai Pham, Ron Waldorf, Elham Ghadishah, Samantha Feril, Stella Lee, Dzuyen Nguyen, Ruoxiang Wang, Justine Velandria, Benjamin Dreskin, Joseph Yusin, Lauren Vigil, Sara Wong, Suchi Tiwari, Joseph Pisegna, Sunita Dergalust, Wayman Lee, Krissa Caroff	VA Greater Los Angeles Healthcare System	Los Angeles, CA
Gregg H. Lucksinger, MD	Jaleh Ostovar, Craig Koch, Danuel Hamlin, Kelly Chase, Jeanette Dickhaus, Edward Kerwin, Frederick Forde, Allison Alvord, Dawn Stewart, Dan Hamlin, Kevin Parks, Ryan Israelsen, Kary Kelly, Tiffany Smith, Melissa Myers, Ryan Rackley, Audrey Kuehl, Savannah Peterson, Hannah Hall, Jay Weisbart, Alison Dodenhoff, Emily Kelly	Velocity Clinical Research	Medford, OR
Mary Beth Manning, MD	Carol Salango, Alec Ireland, Lisa Hoagland, Jeanette Dickhaus, Toby Briskin, Joan Rothenberg, Michael Gaston, Sharita Tedder-Edwards, Denise Roadman, Megan Sokolowski, Tina Shickluna, Katherine Bielanski, Samantha Hood, Talia Chandler, Brianna Arman, Melinda DeLong, Naqib Ahmad, Karly Tarase, Jade Svoboda, Lisle Merriman, Melisa Sebera, Emma Landskroner, Amy Maroun, Brooke Glivar, Jennifer Gaston, Sarah Dzigiel, Cassandra Uminski, Karol Sabol, Devan Patel, Nick Zarbo, Briana Jackson, Brian Sharpe, Nicole Baitt, Kaitlyn Duffy, Gabrielle Jacobs, Ann Czuprun, Tracee Cash, Diamond Ivey, Kaitlyn Rubell	Rapid Medical Research	Cleveland, OH
Kristen Marks, MD	Grant Ellsworth, Tina Wang, Timothy Wilkin, Mary Vogler, Carrie Johnston, Marshall Glesby, Roy Gulick, Ole Vielemeyer, Rebecca Fry, Todd Stroberg, Caitlin Rhoades, Noah Goss, Shaun Barcavage, Valery Hughes, Jonathan Berardi, Caroline Greene, Sarah Galloway, Caique Mello, Ashley Machado, Mia Crowley, Monique Williams, Katherine Fee, Elizabeth DeJesus, Andrew Yu, Minkyung Lee, Susan Herder, Mary Ann Zweibel, Patrice Weller, Antonio Rivera-Lopez, Edward Kenny, Hetal May, Natella Fridman, Parul Shah, Ruby Lee, Venus Fernandez, Victoria Lesina, Celine Arar, Byron Bullough, Kinge-Ann Marcelin, Brian Mangano, Jessenia Fuentes, Jiamin Li, Genessi Rodriguez, Catherine Jerry, Nadi Islam, Liqun Cai, Wayne Burns, Akinbayo Caulcrick, Andrika Thomas, Barbara Batog, Guoan He, Sara Yoder, Tamara Crowder, Gianna Resso, Sophia Alvarez, Tahera Begum, Elizabeth Connolly, Roxanne Rosario, Paul Kim, Steven Wang, Vasilika Koci	Cornell Clinical Trials Units - Weill Cornell Chelsea and Uptown	New York, NY

Principal Investigator	Study Team	Institution	Location
Judith Martin, MD	Alejandro Hoberman, Timothy Shope, Gysella Muniz, Sonika Bhatnagar, Kumaravel Rajakumar, Anne-Marie Rick, Peri Unligil, Jennifer Nagg, Melissa Andrasko, Mary Ann Sieber, Jennifer Opal, Lalicia Roman, Spenser Kinsey, Michelle Burke, Matthew Lee, Dominic Kramer, Linette Milkovich, Emily Dougherty, Emily Camey, Shannon Mance, Nader Shaikh, Diana Kearney, Jamie Fries, Lisa Vavro, Shayla Goller	UPMC University Center	Pittsburgh, PA
John W. McGettigan, Jr., MD	Walter Patton, Jennifer Schnider, Riemeka Brakema, Heeten Desai, Mikell Brett Karsten, Patricia Jalomo, Cindy Finch Benoy, Karin Choquette, Jonlyn McGettigan, Yvonne De Los Reyes, Melissa Cozzens, Amanda Hermosillo, Cindy Montgomery, Susan Tarwid, Annette Elzy, Tianna Young, Saysamone Banks, Cristina Fernandez, Damaris Atondo, Zoe Sesma, Norma Barrientos, Maggie Tono, Kisha Adams, JoAnn Wilkins, Arianna Bermudez, Carol Sayer, Julie McDowell, Angelina Navarro, Mercedes Sullivan, Crystal Mata, Sheldon Gingrich, Aaliyah Sestiaga, Gia Longo	Quality of Life Medical & Research Centers	Tucson, AZ
Mark Montgomery McKenzie, MD	Tiffany Jewell, Zackery Harmon, Michael Elizabeth, Christy Sweet, Teresa Deese, Catherine Schon, Misti Earwood, Lou Cappoli, Brennan Opanasenko, Lisa Guider, Michelle Forgey, Justian Jarrett, Rachel Scott, Elizabeth Michael, Erica Osmundsen, Andrew Wood, Shelly Brooks, Gisela Heintz, Lilian Nukuna	WR-ClinSearch	Chattanooga, TN
Vicki E. Miller, MD	Sajjad Naqvi, Soofia Masood, Fredric Santiago, Sonia Guerrero, Subhash Koneru, Nirja Shah, Andrea Torres, Ramani Gali, Talha Baig, Heather Leary, Affah Ayub, Nayab Goher, Patti Tate, Reagen Reed, Muhammad Irfan, Amy Starr, Alefiyah Motiwala, Julia Kenny, Victoria Aguilar, Jessica Arguijo, Insiya Valika, Victoria Aguilar, Jagruti Patel, Anna Pena, Faryal Mahmood, Blanca Gomez, Nancy Torres, Kristyn Latil, Tarori Mark, Laura Djampou, Lindsey Kueng, Marianne Tadros, Mohammad Millwala, Monica Murray, Murtaza Marvi, Shivani Shah, Vanessa Gonzalez, Zohair Harianawala, Zainab Rizvi, Ambily Dileep, Jaquelyn Gonzales, Ragen Powell, Carolina Deandres, Syed Fahad Ali Kazmi, Sandra Natalia Perez, Shannon Amacker, Shiela Varghese	DM Clinical Research	Tomball, TX
Gowdhami Mohan, MD	Rodolfo Barrera, Emma Partin, Kelly White, Ashley Rochester, Charles Thompson, Stefanie Tyson, Ashten Sheriff, Alyssa-Kay Peay, Kayla Com, Barbara A. Richardson, Kristin Miller, Steven Clemons, Cameron King, Emma Partin, Gary Clemons, Brianna Starr, Danyel Johnson, Taylor Davis, Niki Tyson	VitaLink Research	Anderson, SC
Kathleen M. Mullane, DO, PharmD	David L. Pitrak, Cheryl Nuss, Karen Cornelius, Randee Estes, Amy Lockett, Michelle Moore, Judi Pi, Stephen Schrantz, Jill Stetkevych	University of Chicago	Chicago, IL
Joseph Lee Newberg, MD	Mary Reyes, Nicole Leahy, Victoria Andriulis, Herbert Whinna, Patricia James, Lana Ghomrawi, Carole Kempfer, Miriam Arroyo, Maria Castro, Anna Maddox, Reuben Martinez, Jacquilyn McCormick-Burks, Laura Pearlman, Rosalinda Vazquez, Shaheera Suleiman, Neha Atal, Rosalind Vazquez	Synexus Clinical Research	Chicago, IL
Richard M. Novak, MD	Regina Harden, Maria Schwarber, Michael Pacini, Rebeca Gansari, Margie Villarreal, Stephanie Martin, Michelle Lee, Richard Morrissy, , Taylor Ellis, Samuel Rene, Tara Cobbs, Claudia Preciado, Scott Borgetti, Maximo Brito, Olamide Jarrett, Mahesh Patel, Tracy Cable, Charity Ball, Maryann Holtcamp, Rodrigo Burgos, Sarah Michienzi, Emily Drwiega, Mikayla Johnson, Fischer Herald, Benjamin Ladner, Minseung Chu, Carolyn Dickens, Alfredo Mena Lora, Stockton Mayer, Andrea Wendrow, Habiba Sultana, Nanu Nunwar, David Chan, Marla Schwarber, Khandaker Anwar, Mahmood Ghassemi, Md Ruhul Amin, Doris Carroll, Rosa Valencia, Michelle Agnoli, Elena Linas, Samuel Rene, Liam Morrissy, Adrian Raygoza, Addis Mekonnen, Lisa Lindemann, Daniel Meslar, Karen Pacini, Corey Ringhisen, Amy Kennedy-Krage, Claudia Miller, Loma Sanchez McCann, Gizelle Alvarez, Nia Moragne-Oneal, Nusirat Williams, Ian Feather, Nikki Griffith, Wardrick Nealon, Renyech Powell, Nila Safaeian, Monica Gingell, Diana Bahena, Gerald Beck, Brad Farrington, Rod Reyes, Monica Wilson, Juline Wondrasek, Kimberly Shapiro, Shannon Whitted, Victoria Roehl, Braulio Carrasco, Michael Chen, Olivia Murray, Yasiel Lacalle, Tessa Eckley, Anna Schluckebier, Kevin Cao, Elise DeBruyn	University of Illinois at Chicago - Project WISH	Chicago, IL
Paul Joseph Nugent, DO	Leonard Singer, Jennifer Jones, April Smith, Georgettea Geuss, Lana Ghomrawi, Christine Bennett, Norma Blevins, Linda Brotherton, Michele Byrd, Krista Doss, Victoria Holden, Christine Hull, Jean Montgomery, Nancy Cipollone, Savannah Torline, Brandon Brown, Meagan Thomas, Katie Ziska, Dana Sias, Hannah Wagner	Synexus Clinical Research	Cincinnati, OH
Jeffrey Scott Overcash, MD	Hanh Chu, Kia Lee, Karla Zepeda, John Rodriguez, Adam Prince, Yashveer Dubbula, Elizabeth Tomatsu Michael Voskanian, Crystle Rajania, Stephanie Ramirez, Claudia Camacho, Lauren Arnett, Kecia Darbeau, Ashley Smith, Kimberly Quillin, Cesar Ramirez, Daniel Robitaille, Erica Sanchez, Allie Davis, Michael Waters, Pat Kappen, Valerie Horne, Thao Vuong, Andrew Dennis, Nikki Abels, Dominique Panis, Richard McQuaid, Whitley Harbison, Erika Trujillo, Andrea Garcia, Jose Jacob Esparza, Carlos Vera, Raquel Taitingfong, Cathy Meza, He Pu, Jackielynn Smith, Shandel Odom, Zahira Nieves, Ashleigh Lindsay, Ariana Nasatka, Jose Cazarez, Nora Martinez, Angela Hunt, Antonio Delgado, Linda Vega, Angela Anorve, Erica Martinelli, Melania Riordan, Sylvia Lindholm, Gina Ciezkowski, Grecia Perez, Jacob Pineda,	Velocity Clinical Research, San Diego	La Mesa, CA

Principal Investigator	Study Team	Institution	Location
	Nathan Tyler, Ranya Salem, Amara Yilmaz, Jessica Gonzales, Zabrina Ruiz, Laura Castillo, Yajaira Contreras, Angelica Guzman, Makenna Orel, Jeffery Alvarez, Gordon Bovee, Roxana Ramirez, Joan Esquivel		
James Todd Peterson, MD	Christopher Mickelson, Madeline Maldonado, Alison Charlton, Ashley Bragg, Sean Hansen, Emily Wilcox, Colby Bostock, Megan Henry, Pam Iwasaki, Bradley Young, Katelyn Walker, Joy Nguyen, Lindsey Bevan, Megan Grimmett, Madeline Grote, Heather Littell, Natalie Bee, Alexander Clark, Shana Eborn, Susan Edwards, Dan Henry, Heather Jackson, Gerald Kelly, Issac Pena-Renteria, Jacqueline Rohrer, Jack Taylor, Brooke Barrick, Ty Henry, Anna Dansie, Kenadie Hamblin	J. Lewis Research	Salt Lake City, UT
Paul Pickrell, MD	Susan Bonner, Blaire Graham, Staci Taggart, Hussain Malbari, Tiffany Lemuz, Ethan Shotton, Andrew Bell, Megan Malek, David Pampe, Carol Ann Linebarger, Michelle Peterson, Brandi Chalman, John Luna, Elizabeth Santellanes, Christina Martinez, Lisa Johnson, Lisa Savage, Melissa Winn, Wendi McKenzie, Eileen Euperio, Stefanie Mott, Paul Menefee, Katie Caballero, Darrell O'Brien, Morgan Schulle, Kate Jurek, Olivia Hapanowicz	Tekton Research, Inc.	Austin, TX
Terry L. Poling, MD	Meenakshi (Kavya) Natesan, Patricia Contreras, Denise Hole, Avi Woods, Jill Hiebert, Melissa Burton, Olivia Eagleson, Laura Holz, Terri Ford, Cindy Thome, Terry D Klein, Gregory Greer, Diandra Henriques, Tracy R Klein, Thomas C Klein, Christa Shue, Gina Young, Brenna Sprout	Alliance for Multispecialty Research	Wichita, KS
Bruce G. Rankin, DO	Jennifer Dittman, Lora Parahovnik, Crystal Paccione, Melissa Hodges, Katina Marchione, Matt Maxwell, Any Dominy, Diana Toney, Andrea Marrafino, Laura Isbell, Leandro Fernandez, Claxton Copeland, Michelle Tutt, Adam VanDeusen, Kevin Feldman, Clark Mason, Tifany Huertas, Over Seijas, Jennifer Cline, Christian Beierschmitt, Ryan Hobbick, Jessica Gilliam, Jeanette de Leon, Iman Mencia, Daniel Layish, Vienna Bauer, Shatonia Fields, Albert Garcia, Carrie Rycort, Tasha Brocato, Marshall Nash, Samantha Watts, Amy Houck-Dominy, Angela Hammerle, Teresa Logsdon, Erika Wierzbicki, Taylor Martin, Ranie Hutchins, Fadhel Alyunis, Gail Lavine, Jeffery Hood, Robert Duran, Michelle Jones, Ginny McClanahan, Heather Jackson, Leandra Fernandez, Douglas Winter, Antonio Rivera, Amber Vasquez, Thais Truffa, Daniel Campbell, Grace Newcomb, Elizabeth Orlando, Steven Shinn, John Hill, Christina Isbell, Dhaneshwar Oomrow, Alicia Cevera	Accel Research Sites	DeLand, FL
Michele Diane Reynolds, MD	Jennifer Bashour, Robert Schmidt, Cynthia Mayeux, Uvoka Huffman, Lisa Nicholson, Jacklyn Newton, Lynn Yauch, Cathy Monroe, Kathleen Carty, Angelica Banks, Taylor Werner, Pamela Echols, Pauline Jackson, Chana Hines, Lorine Cook, Cristina Puig, Patrick Brooks, Jennifer Ruiz, Deanna Bowman, Ladia Garcia	Synexus Clinical Research	Dallas, TX
Rambod Rouhbakhsh, MD, MBA	John Johnston, Richard Calderone, Tasha Stevenson, Tameka Fortune, Brandi Pace, Adreanna Pou, Jerrica Sullivan, Yolanda Lewis, April Rouse, Tiffany Jefferson, Elizabeth Danford, Jeff Repper, Mason Boutwell, Alexyia Washington, Krista Hirth, Meagan Grabel	MediSync Clinical Research Hattiesburg Clinic	Petal, MS
Nadine Roupheal, MD	Renata Dennis, Tigisty Girmay, Michelle Wiles, Sharon Curate-Ingram, Lauren Hewitt, Alexis Anonen, Mari Hart, Sarah Bechnak, Erin Carter, Lauren Nolan, Daniel Sans Graciaa, Geoffrey Kamau, Easton Beshears, Sy Tran, Mary Atha, Mary Bower, Ghina Alaaedine, Brandy Johnson, Jacob Usher, Eileen Osinski, Erin Scherer, C. Tae Stallworth, Stephanie Ramer, Rose Pope, Esther Park, Francine Dyer, Laura Clegg, Rebecca Gonzalez, Stacey Wheeler, Susan Rogers, Vy Ngo, Vanessa Soliman, Kristen Unterberger, Bernadine Panganiban, Christopher Huerta, Juton Winston, Ali Alvarez, Jianguo Xu, Colleen Kelley, Paulina Rebolledo, Nicholas Scanlon, Jessica Traenkner, Matthew Collins, Hollie Macenczak, Cassie Grimsely-Ackerley, Tiffany Lee, Amy Anderson, Michele Paine McCullough, Hannah Huston, Daniella Carter, Lisa Harewood, Srilatha Edupuganti, Varun Phadke, Mindee Adamson, Jeanne Allen, Debbie Bartenfeld, Lily Berz, Amy Cromwell, Sergio Cruz, Fred Ede, Monica Godfrey, Evan Gutter, Angelle Ijeoma, Sara Jo Johnson, Vinit Karmali, Dean Kleinhenz, Jennifer Kleinhenz, Alexandra Koumanelis, Maranda Leary, Tiraje Lester, Juliet Alise Morales, Shashi Nagar, Julia Paine, Dilshad Rafi Ahmed, Brittany Robinson, Amanda Rosner, Renee Silver, Trevor William Simon, Talib Sirajud-Deen, Damien Swearing, Maliya Tolbert, Pamela Turner, Chia Uziegbunam, Claire Wan, Dongli Wang, Erika Wimberly, Jean Winter, Joy Winters, Yong Xu, Sha Yi	Emory University - Hope Clinic	Decatur, GA
Richard Rupp, MD	Amber Stanford, Megan Berman, Laura Porterfield, Gerianne Casey, Hala Ghoson, Doreen Jones, Michael Willig, Cori Burkett, Robert Cox, Amy McMahan, Diane Barrett, Kristin Pollock	University of Texas Medical Branch	Galveston, TX
Jamshid Saleh, MD	Matthew Miles, Rafael Lupercio, Vicky Martin, Marla Clark, Matthew Pohlmeier, Ruba Zanaid, Veronica Blevins, Tara Ulberg, Carlyee Chambers, Marisol Corrales, Emily Crews, Mohamed Yassin, Sarah Sandberg, Frank Chen, Mandy Swanson	Paradigm Clinical Research Center	Redding, CA
John W. Sanders, MD, MPH	Stacy Harpe-Hall, Jesse Hopkins, Ann Schweppe, Jaymous Fayssoux, Kathryn Bender, James Peacock, Katharine Pearsall, Brandy Snyder, Deidre Knox, Megan Thorpe, Melissa Ellingson, Brittany Bundeuff, Lisa Ashworth, Meredith Hiatt, Ritu Rathee, Stacy Woodliff, Brian Strittmatter, Amanda Wright, Daisy DeWeese-Gatt,	Wake Forest University Health Sciences	Winston Salem, NC

Principal Investigator	Study Team	Institution	Location
	Caryn Morse, John Williamson, Samantha Wheeler, Lori Whiteheart, Susan Donahue, James Lovette, Kaitlyn Van Leuvan, Kelly Ledbetter, Scott Chatterton, Julio Nasim, Amie Sidberry, Ashley Davis, Carter Noecker, Chie Hooker, Johanna Breenan, Sam Cable, Anna Bowman, Stephanie Boothe, Shea Overcash		
Howard I. Schwartz, MD	Carlos Valladares, Jocelyn Morrera, Yulexis Amestoy, Tori Wallenburg, Thelma Beltran, Terry Piedra, Monica Garces, Alexandra Galvis, Wanda Delgado, Catherine Casas, Lesly Miguel Sosa, Vivian Rosales, Jose Fernando Henriquez, Mikael Yaniz, Beatriz Rivera, Peter Ventre, Gabriella Huyke, Maria Companioni, Jessie De Vega, Brianna Gamez, Stephanie Diaz, James Jean-Mary, Americo Padilla, Nikita Notise, Yorlina Luquetta, Monifa Wilson-Morris, Kenia Gutierrez, Roilan Garcia, Karla Pentzke, Leyda Valentin, Lazara Novas, Marlein Camacho, Jazmin Henfield, Laymis Alvarez, Myriam Rosado, Maxine Bryant, Maria Pinero, Laura Raucci, Francisco Ramirez, Angelic Gamez, Mailin Perez, Yasmin Baddour, Hary Leon Joseph, Yaquelin De la Cruz, Dunia Torres, Rosaidaliz Carreira, Chanella Garcia, Surisaday Mederos, Jose Muniz, Karendra Plotka, Sara Gomez, Maria Soto, Cathy Cruz, Nelia Sanchez-Crespo, Jennifer Schwartz, Barbara Corral, Matthew Muniz, Dayana Deltejo, Ana Castro, Reem Hassan	Research Centers of America	Hollywood, FL
Nathan Segall, MD	Michelle Sowell, Nancy Levine, Erynn McKinley, Hannah Smith, Karen Hickson, Elizabeth West, Patrizia Greene, Jon Finley, Mildred Stull, Susan Jones, Jennifer LeBrun, Pamela Talbott, Kwanda Whatley, Jeffrey Jones, Michelle Binns, Donna Toepfer, Cynthia Steele, Grace Newville, Gillian Waite, Cynthia Pinckney, Karen Yangapatty, Kiara Tyner, Kimberly Cobb, Kourtney Richardson	Clinical Research Atlanta	Stockbridge, GA
William Seger, MD	Kimberly Pullen, Jean Seignon, Anthony Kim, Mohammed Antwi, Allison Green, Lizzy Seger, Elizabeth Boydston, Abdur Rafay Qadri, Deborah Devlin, Tasha Todd, Oluwatosin Akingbala, Alma Guel, Tisha Davis, Melody Dufrene, Samantha Loudermilk, Virginia Loudermilk, Crystal Starr, John Villegas, Ben Seger, Katherine Hollie	Benchmark Research	Fort Worth, TX
Neil Parmanand Sheth, MD	Kenneth Stell, David Beckett, Enitt Gonzalez, Donna McGunigal, Amanda Bums, Nancy Wood, Shelley Miceli, Christina Avila, Rebecca Baker, Laura Vigliotti, Sarah Kading, Samer Salama	Synexus Clinical Research	Glendale, AZ
William B. Smith, MD	Richard L Gibson, Jennifer Winbigler, Elizabeth Parker, Madison Watts, Suzann Cloninger, Talya Thomas	Alliance for Multispecialty Research	Knoxville, TN
Joel Solis, MD	Martha Carmen Medina, Xavier Morales, Hank Heller, Blake Torrence, Joanna Gurrola-Mahoney, Cynthia Bueno, Heather Holloway, Irving Salinas, Joel Perez, Paola Garcia, Erica Canales, Blanca Urbina, Brancisilio Gutierrez, Carolina Cantu, Chelsea Vargas, Cindy Vasquez, Cody McIntire, Gabriela Gutierrez, Hugo Sosa, Irvin Munoz, Jessica Estrada, Jonna Lopez, Kaegan Knox, Mirella Melendez, Natalia Valle, Natalie Echavarría, Nicole Litton, Amber Victor, Nancy Torrence, Madhu Shreya, Mathew Maran, Asfak Alam, Westly Keating, Tara Green, Devora Torrence, Gerardo Sedas, Shruti Konda, Prem Jangam, Mario Echavarría, Alejandro Silva, Anne McNulty, Daniel Contreras, Daniel Gomez, Edgar Garcia, Elizabeth Weber, Luis Lopez, Samuel Ramirez, Kayla Lopez, Pedro Penalo, Angel Salinas, Jaime Solis, Shannon Moyer, Aryana Ibarra, Guadalupe Gurrola, Jenna Anastasiades, Uchechi Ehiemua, Sara Solorzano	Centex Studies, Inc.	McAllen, TX
Stephen A. Spector, MD	Amaran Moodley, Jill Blumenthal, Baharin Abdullah, Christina Addington, Juan Carlos Alcantar, Deyna Arellano, Bernadette Cale, Brendan Costello, Tammelita Cotton-Pineda, Fanny Delebecque, Karen Deutsch, Aram Dimayuga, Son Do, Yasmeen Eshshaki, Aileen Everhart, Cindy Ewing, Veronica Figueroa, Medardo Gaytan, Crystal Groom, Carolyn Hernandez, Heather Huitema, Benjamin Hull, Sylvia Isaac, Jaclyn Jaskowiak, Cindy Knott, Leander Lazaro, Thuan Le, Megan Loughran, Michelle Madey, Rosalva Martha-Patten, Colleen McLellan, Jeff Ledford-Mills, Asami Mimura, Patty Moraes, Jennifer Morales, Jessica Nasca, Phirum Nguyen, Marielys Padilla-Martinez, Dennis Perpetua, Mike Pizza, Shannon Ransom, Emily Rizo, Carlos Rojas, Thaine Ross, Marie Sagrado, Eugene Sato, Lisa Stangl, Ji Sun, Nancy Tang, Mina Trivedi, Rodney Trout, Donna Voss, Lindsey Woronicz	University of California, San Diego	La Jolla, CA
Cynthia Becher Strout, MD	Rica Santiago, Yvonne Davis, Patty Howenstine, Alison Bondell, Jaime Robertson, Anissa Moussa, Geronimo Feria Garzon, Sierra Bennett, Marlena Petrie	Coastal Carolina Research Center	Mount Pleasant, SC
Shobha Swaminathan, MD	Amesika Nyaku, Tilly Varughese, Rondalya Deshields, Michelle L DallaPiazza, Elise Lewis, Jennifer Punsal, Mario Portilla, Malithi Desilva, Christina Daliani, Susana Rivera, Aidan Ziobro, Andressa Rebellatto, Brian Murloy, Christina Ninan, Ernest Pianim, Eunice Wang, Merit Henen, Muhammad Usman, Rebecca Kim, Shiao Wang, Gener Eric Cruz, Bethany Birago, Joyell Arscott, Dina Meawad, Christie Lyn Costanza, Francesca Escaleira, Zoraida Cruz-Barahona, Jared Khan, Valeria Cadoret, Jamir Tuten, Travis Love, Eric Asencio, Sukhwinder Singh	Rutgers New Jersey Medical School	Newark, NJ

Principal Investigator	Study Team	Institution	Location
Ramy Joseph Toma, MD	Olivia Graves, Josiah Robinson, Patricia Hammonds, Lana Ghomrawi, Kara Quinnelly, Shaun O'Conor, Michael Lambe, Rachell Stewart, William Kirby, Pink Folmar, Rachel Culbreth, Heidi Leblanc, Julie McDaniel, Rian Montgomery, Andrea Woodle, Samantha Williams, Hunter Russell, Shereen Lowe, Maureen Mayer, Hollis Ryan, Elaine Reese	Synexus Clinical Research	Birmingham, AL
Timothy P. Vachris, MD	Mark Hutchens, Stephen Daniels, Margaret Wells, Sandra Clancy, Rebecca Martinez, Jessica Buot, Merissa Daugherty, Julie Hamilton, Kimberly Hernandez, Ashli Alejandro, Amy Collins, Monique Gawlik, Patricia Johnson, Maria Moreno, Ashley Washington, Tina Rountree, Daniel Dore, Ravi Davuluri, Ashlee Brunaugh, Jorge Martinez, James Hermon, Vianai Carreno, Mia Rountree, Colleen Coelho	Optimal Research	Austin, TX
Keith William Vrbicky, MD	Charles Harper, Chelsie Nutsch, Wendell Lewis III, Cathy Laflan, Linden DeBoer, Kayla Andal, Misty Appeldorn, Jenniger Grebe, Russell Herstein, Catherine King, Samantha Wieseler, Alisha Kiepke, Christy Lee, Kelsey Kelley, Kelli James, Ashley Frisch, Courtney Green, Taysa Hingst, Jeni Hoppe, Kimber Breeden, Debra Gabrielson, Ginny McNew	Meridian Clinical Research	Norfolk, NE
Larkin T. Wadsworth III, MD	Ashley Dale, Christy Schultz, Rebecca Munsch, Anya Penly, Liz Garner, Stephanie Tesson, George Chermiawski, Angie Kean, Dan Reed, Courtney Kubiak, Maureen Dempsey, Heather Chermiawski, Breanna Galibert, Kristin Branson, Laura Hartuppee, Karen Knapp, Horacio Marafioti, Lyly Dang, Jennifer Berry, Lauren Clement, Megan Dandurand	Sundance Clinical Research	St. Louis, MO
Jordan L. Whatley, MD	Patricia Whatley, Christopher Dedon, Anika Payne, Amie Shannon, Kristen Losavio, Nicole Harrell, Mary Margaret Dobson, Lindsey Hall, Chaney Bennett, Crystal Rowell, Mimi Dimmick, Amy Thomassie, Kimber Breeden, Cody LaFleur, Makaylea Truitt, Taryn Collett, Emily Best, Alexandra Caillouet,	Meridian Clinical Research	Baton Rouge, LA
Judith White, MD	Amy Edridge, Chelsea Montalvo, Eugenia Clark, Lisa Russell, Zahra Somji, Lesli Leimer, Robert Meyer, Christine Murphy, Prity Patel, Sejal Patel, Ruben Moliere, Samantha Merveillard, Yarnick Mirjah, Bryn Walls, Joey Cruz, Aaron Cooper, Jessica Bienaime, Ashley Gilcrist, Alisa Petit, Tyler Knightly, Kimberly Stokes, Christina Rosario, Talhia Matos, Ilona Boggs, Nicholas Weber, Felix Busot, Linda Colon, Heather Gillenwater, Cristina Kaplun, Melissa Caputi, Shayna Siplin, Daminee Shah, Samuel Martin, Alexis Waldorf, Vihar Upadhyay, Adolfo Henriquez, Saskia Singh, Maria Roberts, John Caporelli, Shirley Salvador, Quevina Scarver, Vanessa Garcia, Taylor Moore, Jayasen Singh, Curshinda Galvin-Burch, Mary Kesner, Jasmin Gil, Shay Gray, Steven Monsegur, Michele Steinmetz, Michael Lambe, Heather Powell, Sandra Torres, Shaban Katbeh, Taylor Wilson	Synexus Clinical Research	Orlando, FL
Priyantha N. Wijewardane, MD	Natalie Johnson, Martha Evans, Sondra Wright, Richard Pellegrino, Lastida Burns, Natasha Williams, Haylee Rowe, Kayla Graham, Amanda Horn, Eric Bravo, Jeffrey Thessing, A. Michele Maxwell, Amy Cooper, Lauren Evans, Tonya Cato, Haylee Tucker, Lesa Gann, Hannah Jones, Amanda May, Tiffany Walker, A. LeiAn Diaz, Laura Khalil, Lydia Purcell, Timothy Campbell, Charlotte Garcia-Velez, Andrea Scarborough, Beatrice A. Miller, Keith Bracy, Aujania Thompson, Cassandra Johnson, Krishana Day, Freddie Hicks, Jamie Pettus	Baptist Health Center for Clinical Research	Little Rock, AR
Barton G. Williams, MD	Flo Abbott, Nicole Burton, Alice Cipollini, Madison Croucher, Philip Dattilo, Erin Harrelson, Kelsey Heston, James Ingram, William H Jones, Karla Lane, Brandy Lowman, Evan Lucas, Megan Marles, Morgan Mathis, Angie Northcott, Clyda Pasquantonio, Alyssa Valente, Ciara Winders, Stephanie Graham	Trial Management Associates	Wilmington, NC
Marcus J. Zervos, MD	Paul Kilgore, Mayur Ramesh, Jelena Verkler, Pardeep Pabla, Andrew Clark, Katrina Williams, Dee Dee Wang, Beverley Duthie, Samia Arshad, Alandra White, Anna Kern, Ashley Mattern, Bilqis Mosed, Dana Parke, Doreen Dankerlui, Dragana Spasevska, Hanah Woods, Helina Misikir, Howard Klausner, Janay Scott, Jessica Heinonen, John Zervos, Joseph Miller, Kate Zenlea, Kristin Eis, Marissa Vasquez, Maurice Slaughter, Meaghan Flynn, Michael Garcia, Michelle Sankah, Nina Paeilli, Philip Benson, Robert Devore, Stevanya Baho, Tony Eljallad, Tyler Prentiss, Yaman Ahmed, Sharon Mathys, Linda Kaljee, Jeffrey Van Laere, Claudia Hanni, Hassan Zafar, Mona Desai, Gina Maki, Mary Perri, Dora Vager, Shannon Thomas, Autumn Robinson, Isis Hamilton, Sonia Eliya, Jehan Jazrawi, Biljana Popovic, Sharon Zahul, Joshua Ruzzin, John Laguo, Ali Mathena, Bobby Cook Jr., Marlene Hesler, Rochelle Fleming, Terria Minniefield, John Simons, Sherese Henderson, Ashley Hopkins, Rebecca McFarlane, Raeshell Carson, Jonathan Williams, Katherine Reyes, Erica Herc, Indira Brar, Mayur Ramesh, John McKinnon, Lacquis Duncan, Tim Asmar, Margaret Beyer, Kaleem Chaudhry, Madison Lee, Jo-Ann Rammal, Karthik Sridasyam, Siddesh Veer, Angelique Buluran, Kimberlyn Lott, Jeremiah Rooker, Alayna Wilder, Kathleen Wilson, Allison Weinmann, Hassan Mourtada	Henry Ford Health System	Detroit, MI

United States Government (USG)/Coronavirus Prevention Network (CoVPN) Biostatistics Team
(PubMed listed, and ordered alphabetically by institution affiliation)

Affiliation	Team Members
Biomedical Advanced Research and Development Authority (BARDA), Washington, DC	Di Lu, James Zhou
Department of Biostatistics and Bioinformatics, Rollins School of Public Health, Emory University	David Benkeser
Vaccine and Infectious Disease Division, Fred Hutchinson Cancer Research Center, Seattle, WA	Jessica Andriesen, Bhavesh Borate, Lindsay N. Carpp, Andrew Fiore-Gartland, Youyi Fong*, Peter B. Gilbert*, Ying Huang*, Yunda Huang, Ellis Hughes, Ollivier Hyrien, Holly E. Janes*, Michal Juraska, Yiwen Lu, April K. Randhawa, Brian Simpkins, Brian D. Williamson, Lars W.P. van der Laan, Chenchen Yu
Biostatistics Research Branch, NIAID, NIH, Bethesda, MD	Michael P. Fay, Dean Follmann, Martha Nason
Division of Biostatistics, School of Public Health, University of California, Berkeley, CA	Nima S. Hejazi
Department of Biostatistics, University of Washington, Seattle, WA	Marco Carone, Kendrick Li, Wenbo Zhang
Department of Statistics, University of Washington, Seattle, WA	Alex Luedtke
Department of Population Health Sciences, Weill Cornell Medical College, New York, New York	Iván Díaz

*YF, PBG, YH, and HEJ are also affiliated with the Department of Biostatistics, University of Washington, Seattle, WA. PBG is also affiliated with the Public Health Sciences Division, Fred Hutchinson Cancer Research Center, Seattle, WA.

Trial design and COVID-19 endpoint evaluated for correlates

From July 27 2020 to October 23 2020, 30 415 participants were randomized (1:1 ratio) to receive two injections of mRNA-1273 (100 µg) or placebo, one at Day 1 and one at Day 29 (6). (We use “Day 1”, “Day 29”, and “Day 57” to denote the Day 1, 29, and 57 study visits, respectively). Correlates were evaluated against the protocol-specified primary endpoint, hereafter “COVID-19”: first occurrence of acute symptomatic COVID-19 with virologically-confirmed SARS-CoV-2 infection in participants with no evidence of previous SARS-CoV-2 infection (6). Correlates analyses included COVID-19 endpoints diagnosed starting 7 days post antibody marker measurement through completion of the blinded phase of follow-up (fig. S3). COVID-19 endpoints less than 7 days post antibody measurement were not included because the antibody levels may have been influenced by natural SARS-CoV-2 infection, complicating the interpretation of immune correlates. The data cutoff date was March 26, 2021.

Laboratory methods

Solid-phase electrochemiluminescence S-binding IgG immunoassay (ECLIA)

Serum IgG binding antibodies to spike and to RBD were quantitated using a validated solid-phase electrochemiluminescence S-binding IgG immunoassay. The ECLIA assay enables simultaneous quantitative detection of IgG antibodies to three distinct SARS-CoV-2 antigens in human serum. For this validated assay, custom MSD SECTOR® plates were precoated by Meso

Scale Discovery (MSD; Rockville, Maryland) with SARS-CoV-2 spike (S-2P), receptor binding domain (RBD) protein, Nucleocapsid (N) protein and a Bovine Serum Albumin (BSA) control in each well in a specific spot-designation for each antigen. The assay was performed with a Beckman Coulter Biomek based automation integration platform including the Biotek 405TS Plate Washer. Serum samples were heat-inactivated for 30 minutes at 56°C prior to assay. Plates were blocked for 60 minutes at room temperature (RT) with MSD blocker A solution without shaking. Plates were washed and MSD reference standard (calibrator), QC test sample (pool of COVID-19 convalescent sera) and human serum test samples were added to the precoated wells in duplicates in an 8-point dilution series. Reference standard was added in triplicates. MSD Control sera (low, medium and high) were added undiluted in triplicates as per validated assay format. Additional assay controls might be added in triplicates. Samples were incubated at RT for 4 hours with shaking on a Titramax Plate shaker (Heidolph) at 1500 rpm. SARS-CoV-2 specific antibodies present in the sera or controls bound to the coated antigens. Plates were washed to remove unbound antibodies. Antibodies bound to the SARS-CoV-2 viral proteins were detected using an MSD SULFO-TAG™ anti-human IgG detection antibody incubated for 60 minutes at RT and with shaking. Plates were washed and a read solution (MSD GOLD™ read buffer) containing electrochemiluminescence (ECL) substrate was applied to the wells, and the plate was entered into the MSD MESO Sector S 600 detection system. An electric current was applied to the plates and areas of well surface which form antigen-anti human IgG antibody SULFO-TAG™ complex emitted light in the presence of the ECL substrate.

The MSD MESO Sector S 600 detection system quantitates the amount of light emitted and reports the ECL unit response as a result for each test sample, control sample and reference standard of each plate. Analysis was performed with the MSD Discovery Workbench software, Version 4.0. Calculated ECLIA parameters to measure binding antibody activities include interpolated concentrations or assigned arbitrary units (AU/mL) read from the standard curve.

Neutralization assay

Serum neutralizing antibodies were measured in a validated pseudovirus-based assay as a function of reductions in luciferase reporter gene expression after a single round of infection with SARS-CoV-2.D614G spike-pseudotyped virus in 293T/ACE2 cells (293T cell line stably overexpressing the human ACE2 cell surface receptor protein, obtained from Drs. Mike Farzan and Huihui Mu at Scripps) as detailed in Shen et al. (39). Briefly, spike-pseudotyped virus was prepared by transfection in 293T cells (human embryonic kidney cells in origin; obtained from American Type Culture Collection, cat. no. CRL-11268) using a lentivirus backbone vector, a spike-expression plasmid, a TMPRSS2 expression plasmid and a firefly Luc reporter plasmid. A pre-titrated dose of pseudovirus was incubated with eight serial 5-fold dilutions of serum samples (1:10 start dilution) in duplicate in 96-well flat-bottom poly-L-lysine-coated culture plates (Corning, cat. no. 354516) for 1 hr at 37° C prior to adding 293T/ACE2 cells. One set of eight wells received cells + virus (virus control) and another set of eight wells received cells only (background control), corresponding to technical replicates. Luminescence was measured after 66-72 hr of incubation using Promega 1X lysis buffer (Promega, cat. no. E1531) and Bright-Glo luciferase reagent (Promega, cat. no. E2650). Neutralization titers are the inhibitory dilution of serum samples at which relative luminescence units (RLUs) were reduced by either 50% (ID50)

or 80% (ID80) compared to virus control wells after subtraction of background RLUs. Serum samples were heat-inactivated for 30 min at 56°C prior to assay.

Ethics

The Institutional IRB approval number for the use of human sera in the neutralization assay as described here is Pro00105358 (DUHS Institutional Review Board, 2424 Erwin Rd, Durham, NC, 919.668.5111, Federalwide Assurance No: FWA 00009025 Suite 405).

Bridging of binding antibody assay readouts and neutralizing antibody assay readouts to the WHO International Standard for anti-SARS-CoV-2 immunoglobulin

All serological assay readouts assessed as immune correlates were first expressed in assay values relative to the WHO International Standard for anti-SARS-CoV-2 immunoglobulin (40): spike bAbs and RBD bAbs were converted to Binding Antibody Units per ml (BAU/ml) and ID50 and ID80 nAb titers were calibrated to International Units/ml (IU/ml), yielding calibrated ID50 and ID80 titers expressed in units IU50/ml and IU80/ml, respectively (40, 41). Further details are provided below.

Conversion of AU/ml binding antibody readouts to BAU/ml. Recently the arbitrary units were bridged to the WHO International Standard (41) and a conversion factor was calculated and confirmed (see the Statistical Analysis Plan). Parallelism was established for all three antigens between the MSD provided reference standard and the WHO provided international standard. Concentration assignments were performed and then confirmed both at MSD and as part of a multi-site confirmation study. Sample results reported here have been converted to binding antibody units (BAU) per ml.

Calibration of ID50 and ID80 neutralization titers to International Units/ml (IU50/ml and IU80/ml). Results from the neutralization assay are reported as calibrated ID50 and calibrated ID80 titers, expressed in International Units/ml (IU50/ml and IU80/ml, respectively). The calibration was conducted for the First WHO International Standard for Anti-SARS-CoV-2 Immunoglobulin (20/136) in the SARS-CoV-2 spike-pseudotyped virus neutralization assay in 293T/ACE2 cells. The reagent is intended to be used in part to normalize neutralization titers across multiple SARS-CoV-2 neutralization assays (SOP CFAR02-A0026 “Measuring Neutralizing Antibodies Against SARS-CoV2 Using Pseudotyped Virus and 293T/ACE2 Cells” from the Duke Montefiori lab). The calibration work was performed by the “Neutralizing Antibody Core” Laboratory in the Surgical Oncology Research Facility, under the GCLP oversight of the Quality Assurance for Duke Vaccine Immunogenicity Programs (QADVIP).

Reagent description. In December 2020, the WHO released a well-characterized international standard for the purpose of improving comparability of results among different assays in different laboratories and reducing interlaboratory variability of anti-SARS-CoV-2 antibody assays (40). As described in the user instructions provided by the National Institute for Biological Standards and Controls (NIBSC): “The First WHO International Standard for anti-SARS-CoV-2 immunoglobulin is the freeze-dried equivalent of 0.25 mL of pooled plasma obtained from eleven individuals recovered from SARS-CoV-2 infection. The preparation was evaluated in a WHO International Collaborative study. The intended use of the International Standard is for the calibration and harmonization of serological assays detecting anti-SARS-

CoV-2 neutralizing antibodies. The preparation can also be used as an internal reference reagent for the harmonization of binding antibody assays. The preparation has been solvent-detergent treated to minimize the risk of the presence of enveloped viruses” (41).

Reagent preparation and storage. The reagent was shipped as a lyophilized powder by the NIBSC on December 23, 2020 and was received at Duke on January 4, 2021. A second shipment of the lyophilized reagent was received from the NIBSC on March 15, 2021. The reagent was stored at -80°C upon arrival. Each vial of lyophilized reagent was reconstituted with 0.25 mL of sterile distilled water (Invitrogen, Cat No. 10977015, Ultra-pure DNase, RNase free, Lot 2186762, Exp 30-Aug-2022) as described in the instruction packet (41) and stored at 4°C until use (no longer than 4 weeks).

Protocol and assay results. Neutralization assays were conducted in accordance with SOP CFAR02-A0026 “Measuring Neutralizing Antibodies Against SARS-CoV2 Using Pseudotyped Virus and 293T/ACE2 Cells” using the spike pseudotyped virus CoV-2 VRC7480.D614G.1[CMVΔR8.2]/293T/17. The assays were performed between January 5, 2021 and April 16, 2021 by four operators. All assays used either a 1:20 or 1:30 start dilution and a 5-fold dilution series for a total of 8 dilutions. One vial of the standard was reconstituted on January 5 and assayed once on each of 10 plates in a single setting by a single operator (EY) on January 5, 2021; the plates were read on January 8, 2021 (Exp ID EY18-134). These 10 assay results were described in Duke-02-MVR-COVID0001.2. In response to FDA/CBER recommendations (MF 026862, comments dated March 1, 2021), additional assays were performed over different operators and days to yield more precise estimates of the calibration factors. Additional vials of the reagent were reconstituted on March 20, 2021 and assayed in quadruplicate by two operators on two days, corresponding to technical replicates. A third operator assayed the reconstituted standard in quadruplicate on 3 days. All assays were set up within 24 days of reconstitution. The WHO assigned an arbitrary unitage of 250 IU/ampoule (1000 IU/mL) for neutralizing activity. For calibration purposes, ID50 and ID80 titers may be converted to IU50s and IU80s, respectively, by dividing 1000 IU/mL by either the mean, median or geometric mean ID50 and ID80 titer as a dilution factor. Thus, the calibration factor for mean ID50 is $1000 \div 4135 = 0.242$. The calibration factor for mean ID80 is $1000 \div 666 = 1.502$. The calibration factor for median ID50 is $1000 \div 2422 = 0.413$. The calibration factor for median ID80 is $1000 \div 489 = 2.045$. The calibration factor for geometric mean ID50 is $1000 \div 3047 = 0.328$. The calibration factor for geometric mean ID80 is $1000 \div 567 = 1.764$. The calibration factors are summarized below:

Summary values for WHO anti-SARS-CoV-2 IgG (20/136)

Virus: SARS-CoV-2 D614G Variant		Calibration Factor
Arithmetic mean ID50	4135	0.242
Arithmetic mean ID80	666	1.502
Median ID50	2422	0.413
Median ID80	489	2.045
Geometric Mean ID50	3047	0.328
Geometric Mean ID80	567	1.764

The three types of calibration factors (based on arithmetic mean, median, and geometric mean) were compared head-to-head on validation data from Day 29 and Day 57 ID50 and ID80 values from 30 recipients of the mRNA-1273 vaccine, with the common samples conducted by both the Duke Montefiori neutralization assay used for the COVE trial immune correlates study and the Monogram PhenoSense neutralization assays. The results showed that using arithmetic mean of the WHO IS sample for calibration yielded the highest agreement between the calibrated vaccine responses from the two labs, based on the concordance correlation coefficient (manuscript in preparation). Based on this validation experiment, the arithmetic mean calibration factors were selected for use in reporting results in terms of ID50 and ID80 (expressed in IU50/ml and IU80/ml, respectively).

Statistical methods

All data analyses were pre-specified in the Statistical Analysis Plan (SAP), available in the Supplementary Material. Two separate correlates analyses were done, which assessed the antibody markers measured at Day 29 or at Day 57 as correlates. These time points were selected for antibody measurement in both being scheduled 28 days post previous dose, and Day 57 was presumed to be when antibodies approximately peak and have wide inter-vaccinee variability.

Case-cohort sets included in correlates analyses

Through a case-cohort sampling design, participants were randomly sampled for antibody marker measurement at Day 1, 29, 57 (42). Without replacement stratified sampling was used, with 24 strata defined by randomization arm cross-classified by baseline SARS-CoV-2 positivity, protocol randomization strata (age below 65 years at risk, age below 65 years not at risk, age above 65 years), and minority status. “At risk” refers to participants believed to be at increased risk of severe COVID-19 illness and comprised six self-reported health/comorbidities, as in Baden et al (6). “Minority” includes Blacks or African Americans, Hispanics or Latinos, American Indians or Alaska Natives, Native Hawaiians, and other Pacific Islanders. Non-Minority includes all other races with observed race (Asian, Multiracial, White, Other) and observed ethnicity Not Hispanic or Latino. The sampling design oversampled baseline negative vaccine recipients and minorities, to improve power and ensure characterization of immunogenicity in minorities (see the SAP for details). In addition, the antibody markers were measured at Day 1, 29, 57 in all vaccine recipients with a breakthrough COVID-19 endpoint. Data analyses restricted to participants with no immunologic or virologic evidence of prior COVID-19 (negative nasopharyngeal swab test and/or anti-nucleocapsid binding antibodies below the limit of detection or the lower limit of quantification at Day 1; see table S3 for assay limits), as in Baden et al. (6), and per-protocol, i.e. received both doses without major protocol violations (see footnote 3 of fig. S2); we refer to these qualifying participants as baseline negative per-protocol participants. The “immunogenicity subcohort” is the subset of the randomly sampled participants who have antibody marker data at Day 1, 29, and 57 (N = 1010 vaccine recipients, N = 137 placebo recipients), which is almost 100% of sampled participants (fig. S1).

Correlates analyses for each marker time point were based on segregating vaccine recipients into non-cases vs. vaccine breakthrough cases, where the two analyses used the same set of non-cases: the subset of the immunogenicity subcohort who were baseline negative per-protocol and never had any evidence of SARS-CoV-2 infection (N=1005 vaccine recipients). The vaccine breakthrough case sets differed, defined based on “intercurrent endpoints” that start 7 days post Day 29 through 6 days post Day 57 and “post Day 57 endpoints” that start 7 days post Day 57 (fig. S3). Day 29 marker analyses included all intercurrent endpoints and all post Day 57 endpoints with antibody data at Day 1 and 29 (N=46 cases), and Day 57 marker analyses included all post Day 57 endpoints with antibody data at Day 1, 29, and 57 (N=36 cases) (fig. S1). The “Day 29 case-cohort set” included in Day 29 marker analyses comprised baseline negative per-protocol vaccine recipients in the immunogenicity subcohort plus the qualifying baseline negative per-protocol vaccine breakthrough cases, and the “Day 57 case-cohort set” included in Day 57 marker analyses was the same except intercurrent endpoints were excluded (table S2). The correlates analyses included follow-up through to the last pre-unblinding vaccine breakthrough endpoint post Day 29 and post Day 57, which were 126 and 100 days, respectively.

For each antibody marker, values below the assay limit of detection (LOD) were set to LOD/2, and values above the upper limit of quantitation (ULOQ) were set to ULOQ. Positive response for each marker is defined in Fig. 1 and table S3. Positive response rates were estimated by an IPS-weighted average, with 95% confidence interval (CI) calculated with an IPS-weighted Clopper-Pearson method. Differences in response rates with 95% CIs were calculated by the Wilson-Score method without continuity correction (43). Geometric mean concentration (GMC) or titer (GMT) and their ratios between cases vs. non-cases were estimated with 95% CIs based on the t-distribution with IPS weighting.

Covariate-adjustment

All correlates analyses adjusted for baseline variables prognostic for COVID-19: at risk status, membership in a community of color (all persons other than White Non-Hispanic), and the logit of predicted COVID-19 risk score built from machine learning of placebo arm participants (supplementary text S1).

Correlates of risk in vaccine recipients

For each marker, IPS-weighted Cox regression was applied to estimate the covariate-adjusted hazard ratio of COVID-19 across marker tertiles or per 10-fold increase in the quantitative marker level with 95% CIs and Wald-based p-values. The Cox model fits were used to estimate marker-conditional cumulative incidence of COVID-19 in the population of per-protocol baseline negative vaccine recipients, with 95% CIs computed using the bootstrap. The Cox models were fit using the *survey* R package (44). Additional analyses estimated the same quantity with a generalized additive model with degrees of freedom selected by generalized cross-validation (45), and by nonparametric targeted minimum loss-based threshold regression (46).

Correlates of protection: controlled vaccine efficacy and mediation

Vaccine efficacy by marker level was estimated by a causal inference approach implemented using the same IPS-weighted Cox regression described above for the vaccine arm, combined with unweighted Cox regression for the entire baseline SARS-CoV-2 negative per-protocol placebo arm (details in SAP Section 12.1.1). The analysis of the placebo arm ignored

antibody marker data given that all values were negative / undetectable given the absence of exposure to SARS-CoV-2 antigens (28) (see SAP). A sensitivity analysis was conducted to assess robustness of the results to unmeasured confounding of the effect of the antibody marker on COVID-19 (supplementary text S2 and SAP Section 12.1.2) (28). In addition, for each antibody marker with at least 10% of vaccinated participants with value the same as for placebo recipients, i.e., negative for IgG markers or undetectable for neutralization markers, the proportion of vaccine efficacy mediated by the antibody marker was estimated (30). (Availability of sufficient overlap in the vaccine and placebo arms is technically required for feasibility of median analysis, as detailed in the SAP.)

Hypothesis testing

All p-values were two-sided. For each set of hypothesis tests for Day 29 and Day 57 marker correlates of risk separately, Westfall-Young multiplicity adjustment (47) was applied to obtain false-discovery rate adjusted p-values and family-wise error rate adjusted p-values.

Calibration of ID50 and ID80 titers between the Duke neutralization assay on COVE trial samples and the Monogram PhenoSense neutralization assay performed on AstraZeneca COV002 samples

Using the WHO First Anti-SARS CoV-2 Immunoglobulin International Standard (20/136): 1000 IU/mL, PhenoSense SARS CoV-2 nAb titers can be converted to IU50/ml or IU80/ml by multiplying the nAb titer (ID50 or ID80) by the appropriate conversion factor, where conversion factors were estimated both for the D614 pseudovirus vaccine strain and for the D614G pseudovirus mutation strain. For each strain, conversion factors were calculated using the mean, geometric mean and median based on 24 replicate tests of the 20/136 standard (6 replicates per day x 4 days). Based on the validation data noted above the arithmetic mean conversion factor was used. For the D614 strain, the conversion factors for ID50 and ID80 were 0.1428 and 0.4585, respectively. For the D614G strain, the conversion factors for ID50 and ID80 were 0.0653 and 0.2281, respectively. In the main article, these conversion factors were first applied as follows: the ID50 values reported in Table 2 of Feng et al. (19) (COV002 immune correlates results) corresponding to 70% and 90% estimated vaccine efficacy were multiplied by 0.1428, where the D614 strain factor was used because the AZD12222 performed the Monogram PhenoSense pseudovirus neutralization assay on participant samples using the D614 strain. Specifically, the ID50 values 57, 183, 982, 303 reported in Table 2 of Feng et al. were each multiplied by 0.1428 to obtain ID50 values (in IU50/ml) 8, 26, 140, 43, respectively; these values are reported in the main article.

Sensitivity analysis comparing correlate of protection results between COV002 and COVE

The neutralization assays employed for COV002 and COVE used the D614 and D614G pseudovirus, respectively, such that this comparison is affected by any difference in neutralization sensitivity of these two strains. Therefore, we also performed a sensitivity analysis that assumes that D614G is more sensitive to neutralization by vaccine recipient sera than D614. The multiplicative factor defining more sensitive was taken to be $(0.1428/0.0653) = 2.19$, the ratio of conversion factors (D614 vs. D614G) calculated in the Monogram study that defined the conversion factors. This factor was applied to each ID50 value from the AZD12222 study, which means that each AZD12222 ID50 value on its original scale was multiplied by $0.1428 * 2.19 = 0.31$. Therefore, in this sensitivity analysis, the ID50 values 57, 183, 982, 303

reported in Table 2 of Feng et al. were each multiplied by 0.31 to obtain the ID50 (in IU50/ml) values 18, 57, 307, 95, respectively. According to this sensitivity analysis, estimated AZD1222 vaccine efficacy in COV002 was 70% and 90% at ID50 titer of 18 ($< \text{LOD} = 2.42, 57$) and 307 (95, NC) IU50/ml, respectively.

Software and data quality assurance

The analysis was implemented in R version 4.0.3; code was verified using mock data.

Research reproducibility approach

All analyses were done reproducibly based on R scripts hosted at the Github code repository, which are publicly available with application to a mock COVE trial data set. The code is available at: <https://zenodo.org/record/5593130#.YXLhQ0X3bDs> (38).

Table S1. Demographics and clinical characteristics of baseline SARS-CoV-2 negative per-protocol trial participants in the immunogenicity subcohort and thus have Day 1, 29, 57 antibody marker data.

Characteristics	Vaccine (N = 1010)	Placebo (N = 137)	Total (N = 1147)
Age			
Age < 65	670 (66.3%)	91 (66.4%)	761 (66.3%)
Age ≥ 65	340 (33.7%)	46 (33.6%)	386 (33.7%)
Mean (Range)	54.6 (18.0, 87.0)	53.4 (19.0, 85.0)	54.4 (18.0, 87.0)
BMI			
Mean ± SD	30.9 ± 7.6	31.3 ± 9.0	30.9 ± 7.8
Risk for Severe COVID-19			
At-risk	396 (39.2%)	57 (41.6%)	453 (39.5%)
Not at-risk	614 (60.8%)	80 (58.4%)	694 (60.5%)
Age, Risk for Severe COVID-19			
Age < 65 At-risk	291 (28.8%)	40 (29.2%)	331 (28.9%)
Age < 65 Not at-risk	379 (37.5%)	51 (37.2%)	430 (37.5%)
Age ≥ 65	340 (33.7%)	46 (33.6%)	386 (33.7%)
Sex Assigned at Birth			
Female	476 (47.1%)	63 (46.0%)	539 (47.0%)
Male	534 (52.9%)	74 (54.0%)	608 (53.0%)
Hispanic or Latino Ethnicity			
Hispanic or Latino	322 (31.9%)	44 (32.1%)	366 (31.9%)
Not Hispanic or Latino	685 (67.8%)	93 (67.9%)	778 (67.8%)
Not reported and unknown	3 (0.3%)	0 (0.0%)	3 (0.3%)
Race			
White	735 (72.8%)	99 (72.3%)	834 (72.7%)
Black or African American	182 (18.0%)	24 (17.5%)	206 (18.0%)
Asian	25 (2.5%)	6 (4.4%)	31 (2.7%)
American Indian or Alaska Native	17 (1.7%)	2 (1.5%)	19 (1.7%)
Native Hawaiian or Other Pacific Islander	5 (0.5%)	0 (0.0%)	5 (0.4%)
Multiracial	12 (1.2%)	4 (2.9%)	16 (1.4%)
Other	25 (2.5%)	2 (1.5%)	27 (2.4%)
Not reported and unknown	9 (0.9%)	0 (0.0%)	9 (0.8%)
White Non-Hispanic	468 (46.3%)	61 (44.5%)	529 (46.1%)
Communities of Color	542 (53.7%)	76 (55.5%)	618 (53.9%)

This table summarizes the baseline SARS-CoV-2 negative per-protocol immunogenicity subcohort, which was randomly sampled within 12 strata defined by enrollment characteristics: Assigned treatment arm × Baseline SARS-CoV-2 naïve vs. non-naïve status (defined by serostatus and NAAT testing) × Randomization strata (Age < 65 and at-risk, Age < 65 and not at-risk, Age ≥ 65) × Minority status (Minority vs. Non-minority) defined by White Non-Hispanic vs. all others [same as in (6)]. “At Risk” refers to participants believed to be at increased risk of severe COVID-19 illness and comprised six self-reported health/comorbidities, as in (6). “Minority” includes Blacks or African Americans, Hispanics or Latinos, American Indians or Alaska Natives, Native Hawaiians, and other Pacific Islanders. Non-Minority includes all other races with observed race (Asian, Multiracial, White, Other) and observed ethnicity Not Hispanic or Latino. Numbers and percentages are based on inverse probability of sampling weighting.

Table S2. Sample sizes of baseline SARS-CoV-2 negative per-protocol vaccine recipients included in immune correlates analyses, by baseline sampling strata and case/non-case strata.

Day 29 marker case-cohort set = Baseline negative per-protocol vaccine recipients included in Day 29 marker correlates analyses (in the immunogenicity subcohort and/or an intercurrent case or a post Day 57 case)

Day 57 marker case-cohort set = Baseline negative per-protocol vaccine recipients included in Day 57 marker correlates analyses (in the immunogenicity subcohort and/or a post Day 57 case)

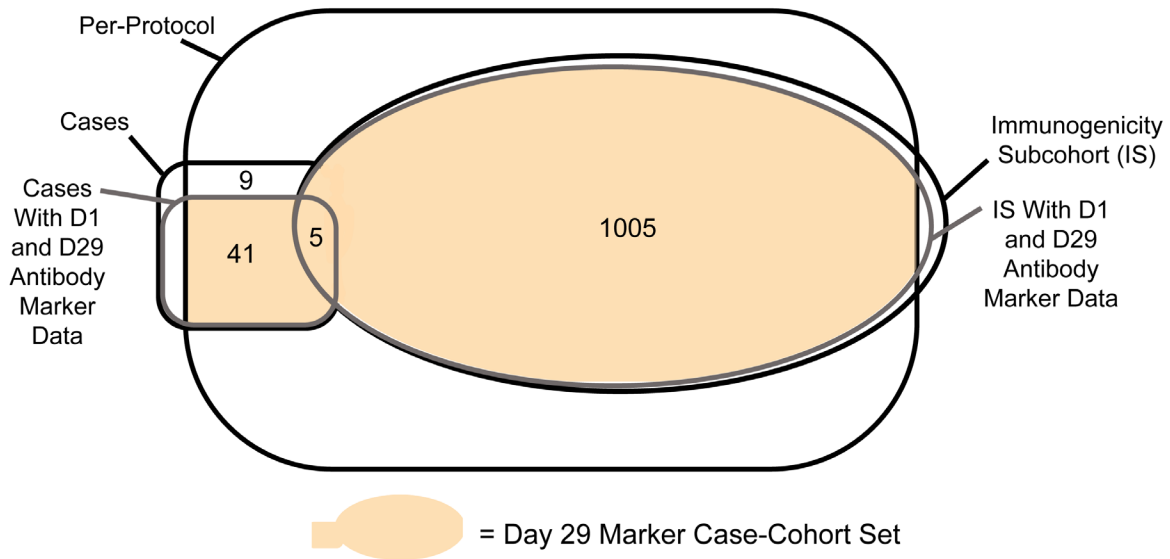
	Baseline Sampling Strata ¹ of SARS-CoV-2 Negative Per-Protocol Vaccine Recipients Included in Correlates Analyses						Total
	1	2	3	4	5	6	
Intercurrent Cases	0	2	0	0	4	4	10
Post Day 57 Cases	1	4	2	8	5	16	36
Breakthrough cases included in Day 29 marker correlates analyses	1	6	2	8	9	20	46
Breakthrough cases included in Day 57 marker correlates analyses	1	4	2	8	5	16	36
Non-Cases in Immunogenicity Subcohort	171	168	143	146	188	189	1005

¹Demographic covariate strata: 1. Age ≥ 65 Minority; 2. Age ≥ 65 Non-Minority; 3. Age < 65 At-risk Minority; 4. Age < 65 At-risk Non-Minority; 5. Age < 65 Not At-risk Minority; 6. Age < 65 Not At-risk Non-Minority. Minority includes Blacks or African Americans, Hispanics or Latinos, American Indians or Alaska Natives, Native Hawaiians, and other Pacific Islanders. Non-Minority includes all other races with observed race (Asian, Multiracial, White, Other) and observed ethnicity Not Hispanic or Latino. Participants not classifiable as Minority or Non-Minority because of unknown, unreported, or missing information were not included.

Cases for Day 29 marker correlates analyses are baseline SARS-CoV-2 negative per-protocol vaccine recipients with the symptomatic infection COVID-19 primary endpoint diagnosed starting 7 days after Day 29 through the end of the blinded phase. Cases for Day 57 marker correlates analyses are baseline SARS-CoV-2 negative per-protocol vaccine recipients with the symptomatic infection COVID-19 primary endpoint diagnosed starting 7 days after Day 57 through the end of the blinded phase. Non-cases are baseline SARS-CoV-2 negative per-protocol participants sampled into the immunogenicity subcohort with no COVID-19 endpoint through the end of the blinded phase and no evidence of SARS-CoV-2 infection up to six days post Day 57.

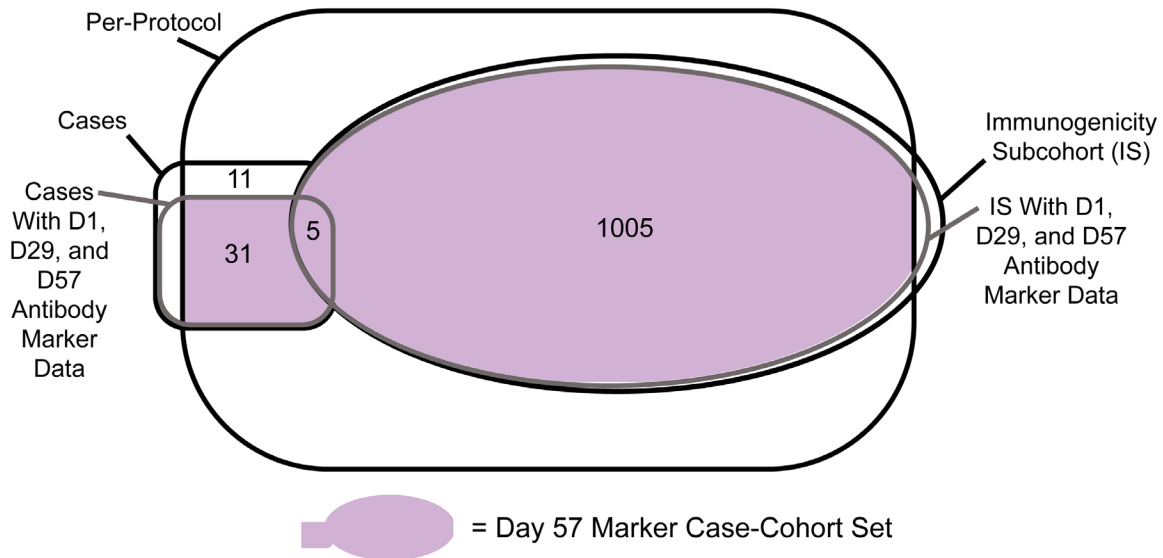
A. For Day 29 Marker Correlates Analyses:

Among Baseline SARS-CoV-2 Negative Vaccine Recipients:



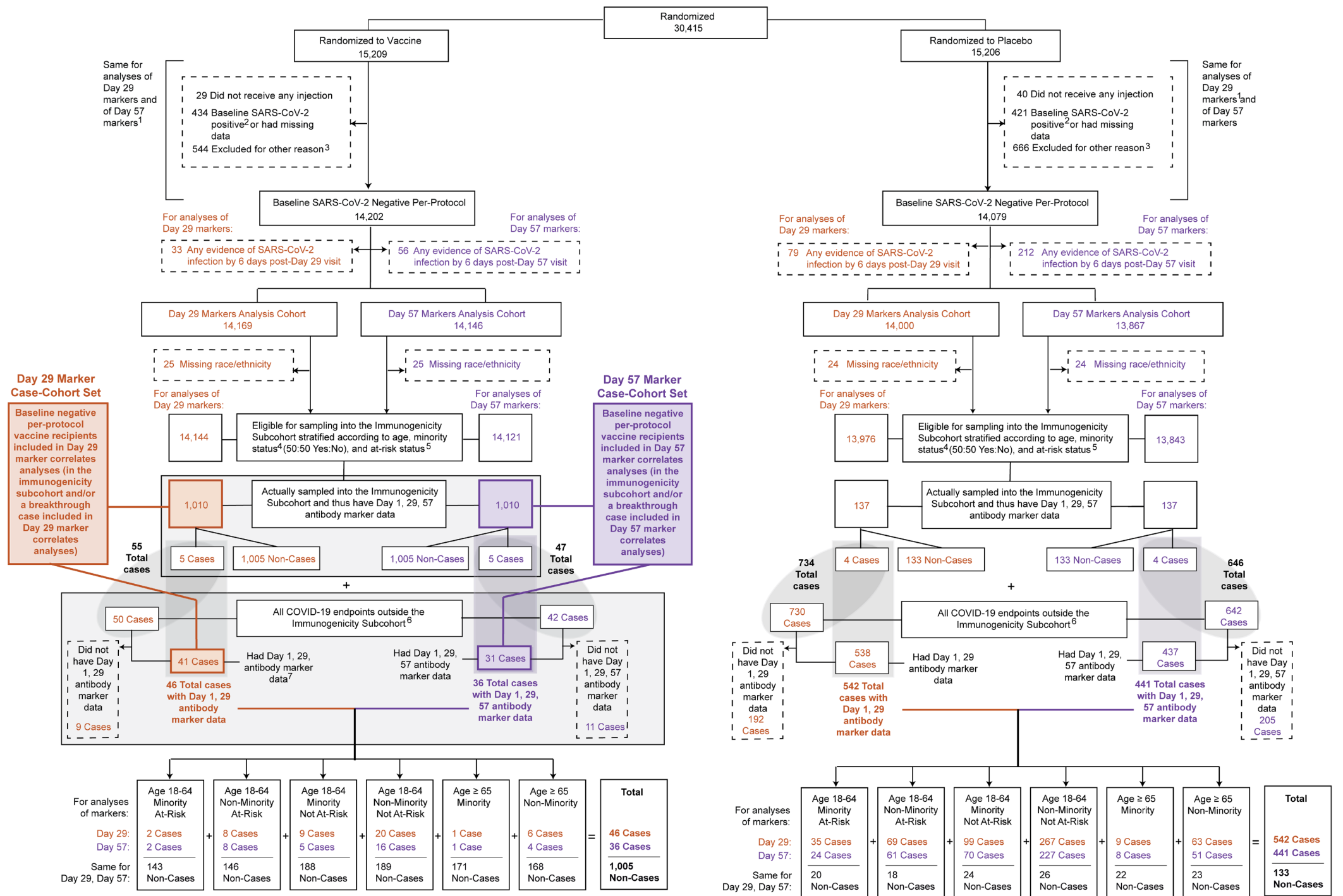
B. For Day 57 Marker Correlates Analyses*:

Among Baseline SARS-CoV-2 Negative Vaccine Recipients:



*The Venn diagram in panel B is completely nested within the Venn diagram in panel A.

Fig. S1. (A) Day 29 marker case-cohort set and (B) Day 57 marker case-cohort set.



1 If a participant had multiple reasons for exclusion from the Per-Protocol Set, they were only counted in the earliest-listed reason.

2 Baseline SARS-CoV-2 positive is defined as immunologic or virologic evidence of prior COVID-19 (i.e. a positive nasopharyngeal swab and/or binding antibodies against SARS-CoV-2 nucleocapsid above the limit of detection or above the lower limit of quantification) at Day 1 before the first dose of investigational product (same definition as in Baden et al. 2021).

3 The other reasons for exclusion were: did not receive second dose; received incorrect vaccine; received dose 2 out of window; other major protocol deviations; were living with HIV; adjudicated COVID-19 cases up to Day 29 visit (dose 2 date).

4 Minority includes Blacks or African Americans, Hispanics or Latinos, American Indians or Alaska Natives, Native Hawaiians, and other Pacific Islanders. Non-Minority includes all other races with observed race (Asian, Multiracial, White, Other) and observed ethnicity Not Hispanic or Latino.

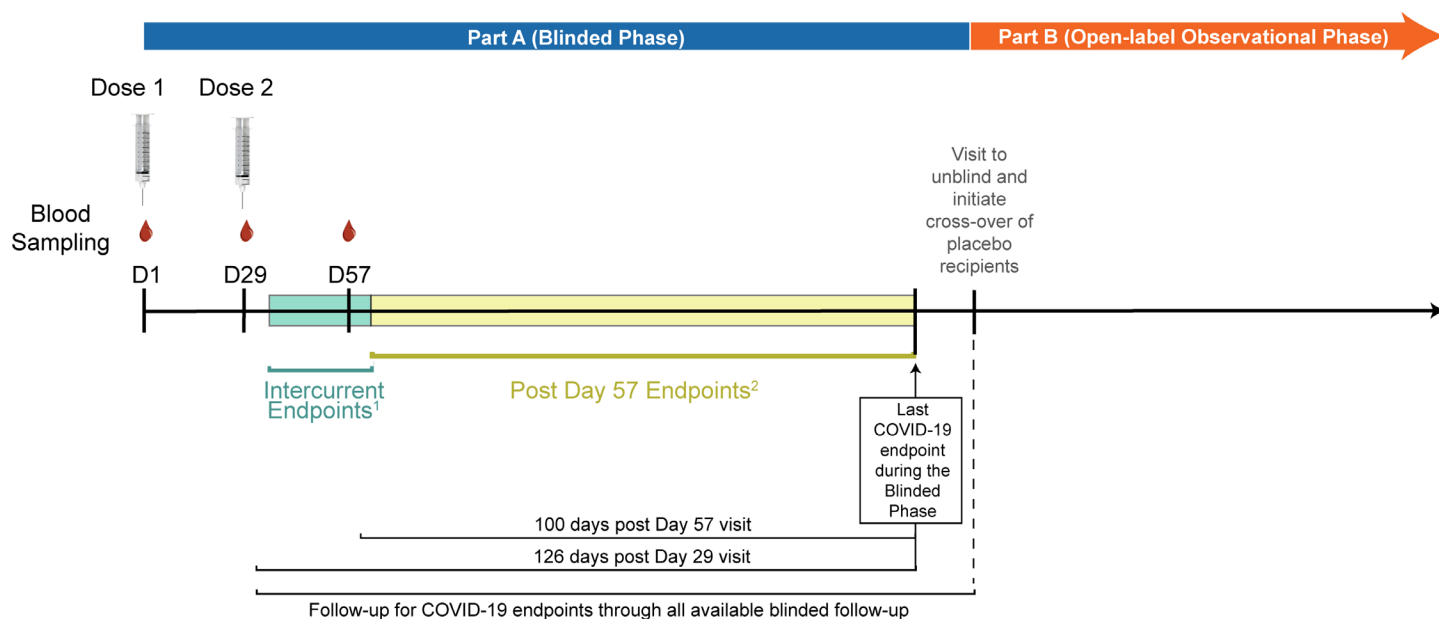
5 Participants 18-64 were categorized as "At-Risk" (of severe COVID-19 illness) if they had at least one of the following risk factors: chronic lung disease (e.g., emphysema, chronic bronchitis, idiopathic pulmonary fibrosis, cystic fibrosis, or moderate-to-severe asthma); cardiac disease (e.g., heart failure, congenital coronary artery disease, cardiomyopathies, or pulmonary hypertension); severe obesity (BMI ≥ 40); diabetes (type 1, type 2, or gestational); liver disease; or HIV infection (same as in Baden et al. 2021).

6 Correlates analyses of Day 29 markers start counting COVID-19 endpoints at 7 days post Day 29 visit, and correlates analyses of Day 57 markers start counting COVID-19 endpoints at 7 days post Day 57 visit.

7 For Day 29 marker correlates analyses, intercurrent cases may not have Day 57 antibody data, as Day 57 antibody data are not used.

Fig. S2. Flowchart of study participants from enrollment to the Day 29 and Day 57 case-cohort sets of baseline SARS-CoV-2 negative per-protocol participants. Antibody data from the placebo arm are not used in correlates analyses, given no variability in values; they were only used to verify low false positive rates of the immunoassays.

For Baseline Negative Per-Protocol recipients of two doses of mRNA-1273:



¹Intercurrent Endpoints: ≥ 7 days post Day 29 visit through 6 days post Day 57 visit; used in Day 29 marker correlates analyses only

²Post Day 57 Endpoints: ≥ 7 days post Day 57 visit through the end of the Blinded Phase (last COVID-19 endpoint in the Blinded Phase occurred at 126 days Post Day 29 visit); used in Day 29 and in Day 57 marker correlates analyses

Counting of Intercurrent Endpoints started ≥ 7 days post Day 29 visit to help ensure that the endpoint did not occur before Day 29 antibody measurement; counting of Post Day 57 Endpoints started ≥ 7 days post Day 57 visit to help ensure that the endpoint did not occur before Day 57 antibody measurement.

Fig. S3. Phases of the COVE trial, timing of mRNA-1273 doses and blood sampling, and the two time periods for diagnosis of COVID-19 endpoints (“Intercurrent” and “Post Day 57”). The schematic applies to baseline SARS-CoV-2 negative per-protocol recipients of two doses of mRNA-1273. During Part A (Blinded Phase) of the trial, participants were blinded to treatment assignment. After issuance of the Emergency Use Authorization from the US FDA on Dec 18, 2020, the trial entered Part B (Open-Label Observational Phase), where participants could choose to be unblinded; those assigned to placebo could opt to receive two doses of mRNA-1273 vaccine.

Table S3. Meso-Discovery (MSD) and pseudovirus neutralization assay limits of the four antibody markers evaluated as immune correlates.

Reported units	MSD Binding Assay (VRC)			PsV nAb (Duke)	
	BAU/ml*			IU50/ml (ID50); IU80/ml (ID80)**	
	Spike	RBD	N	ID50	ID80
Positivity Cutoff	10.8424	14.0858	23.5	2.42	15.02
LOD	0.3076	1.5936	0.09	2.42	15.02
LLOQ	1.7968	3.43	4.49	4.477	21.4786
ULOQ	10,155.95	16,269	575	10919	15368

*AU/ml units converted to BAU/ml units for all data analysis.

**Original titers calibrated to the WHO anti-SARS-CoV-2 immunoglobulin International Standard (NIBSC code: 20/136) for all data analyses (41). ID50 = ID50 titer in IU50/ml; ID80 = ID80 titer in IU80/ml.

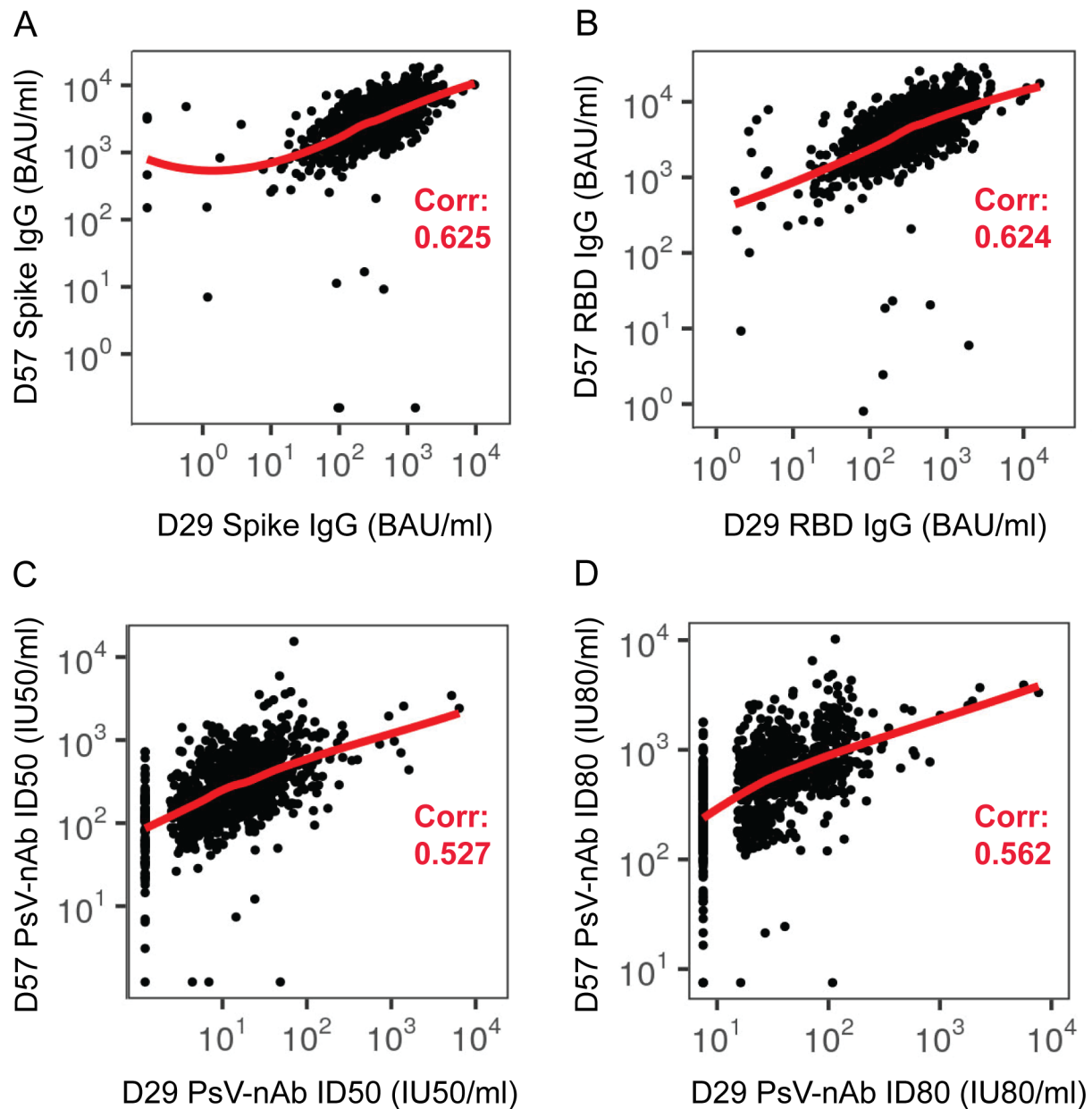


Fig. S4. For each antibody marker, correlations of Day 29 levels with Day 57 levels in baseline SARS-CoV-2 negative per-protocol vaccine recipients in the immunogenicity subcohort. Corr = baseline variable adjusted IPS-weighted Spearman rank correlation. PsV, pseudovirus.

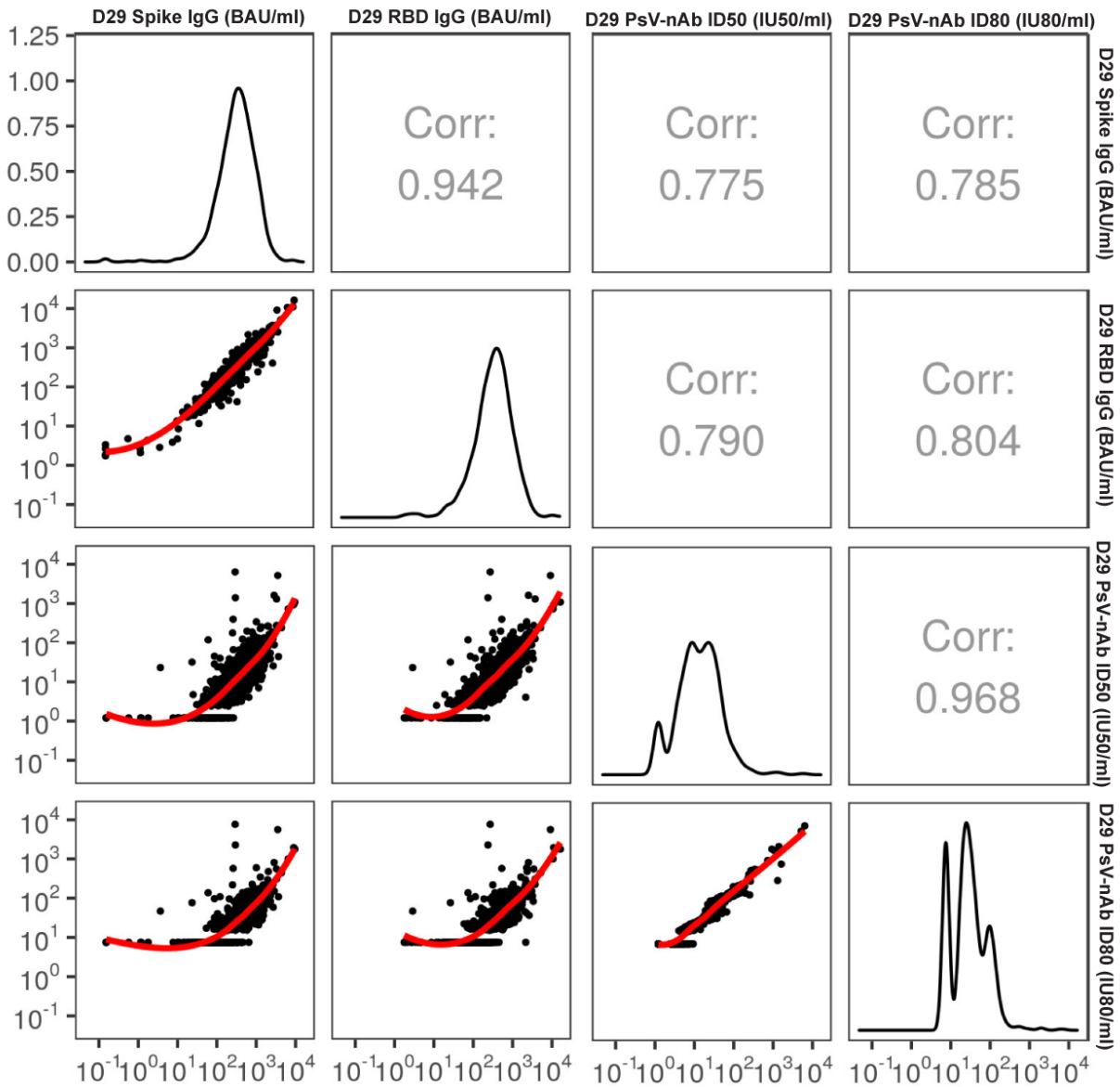


Fig. S5. Correlations of Day 29 antibody markers in baseline SARS-CoV-2 negative per-protocol vaccine recipients in the immunogenicity subcohort. Corr = baseline variable adjusted Spearman rank correlation. PsV, pseudovirus.

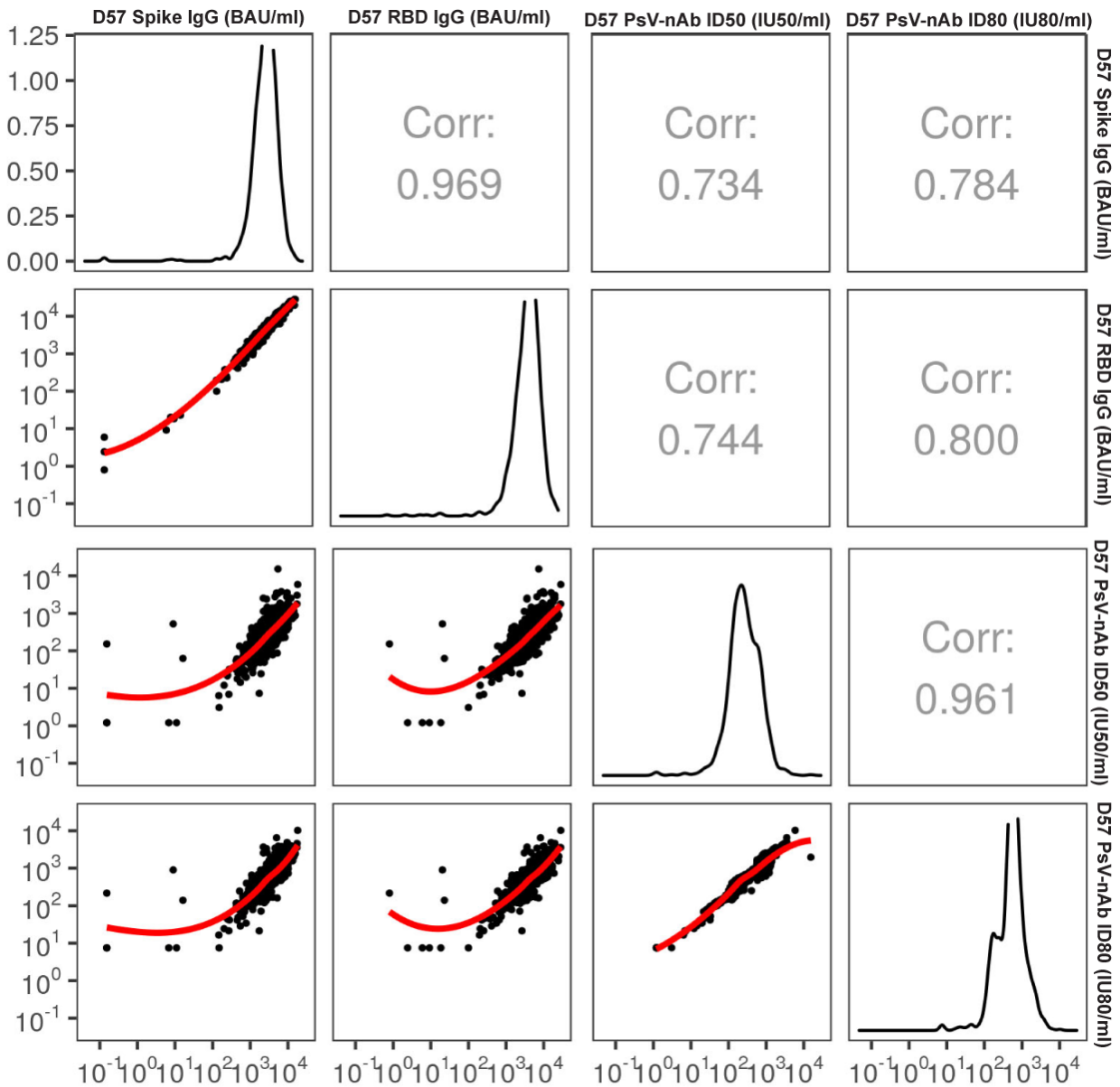


Fig. S6. Correlations of Day 57 antibody markers in baseline SARS-CoV-2 negative per-protocol vaccine recipients in the immunogenicity subcohort. Corr = baseline variable adjusted Spearman rank correlation. PsV, pseudovirus.

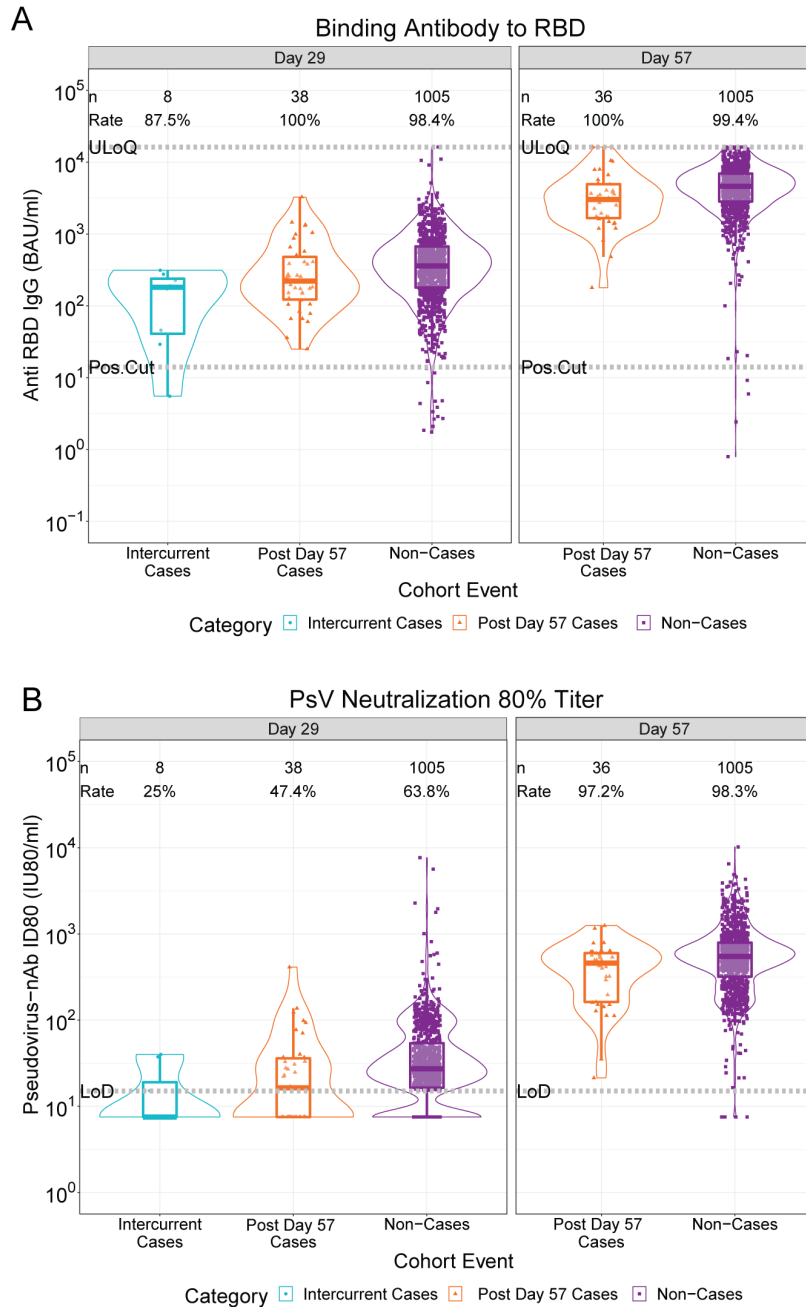


Fig. S7. A) Anti-RBD IgG concentration and B) pseudovirus neutralization ID80 titer by COVID-19 outcome status. Data points are from baseline SARS-CoV-2 negative per-protocol vaccine recipients in the Day 29 marker or Day 57 marker case-cohort sets. Pos.Cut, Positivity cut-off. LoD, limit of detection. ULoQ, upper limit of quantitation; ULOQ = 15,368 for ID80 (above all data points). Post Day 57 cases are COVID-19 endpoints starting 7 days post Day 57; Intercurrent cases are COVID-19 endpoints starting 7 days post Day 29 through 6 days post Day 57.

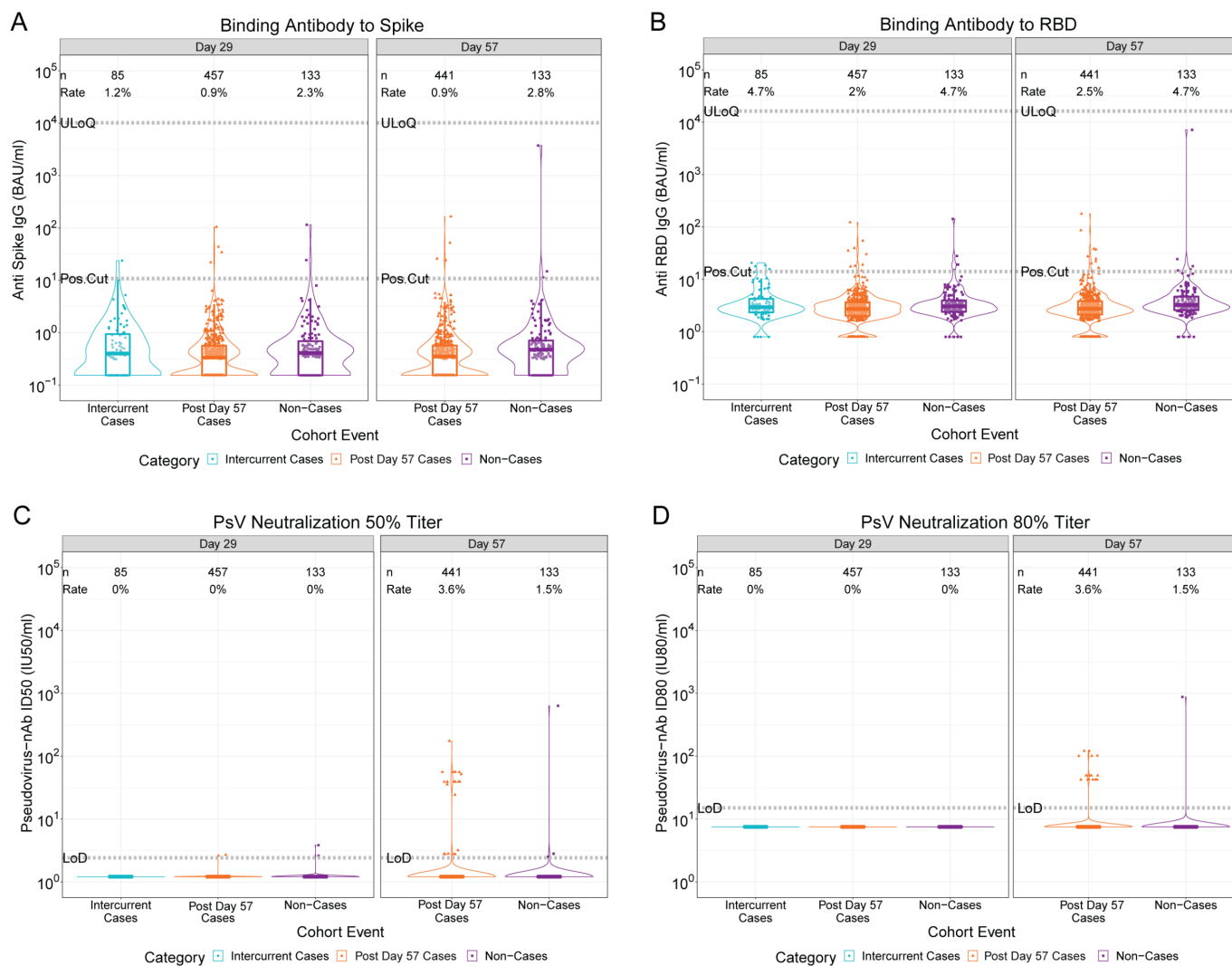


Fig. S8. Marker values (spike IgG, RBD IgG, ID50, ID80) by COVID-19 outcome status in placebo recipients. Data points are from baseline SARS-CoV-2 negative per-protocol placebo recipients in the Day 29 marker or Day 57 marker case-cohort set. Positive response rates are computed with Inverse Probability Sampling (IPS) weighting. Pos.Cut, Positivity cut-off. LoD, limit of detection. ULoQ, upper limit of quantitation.

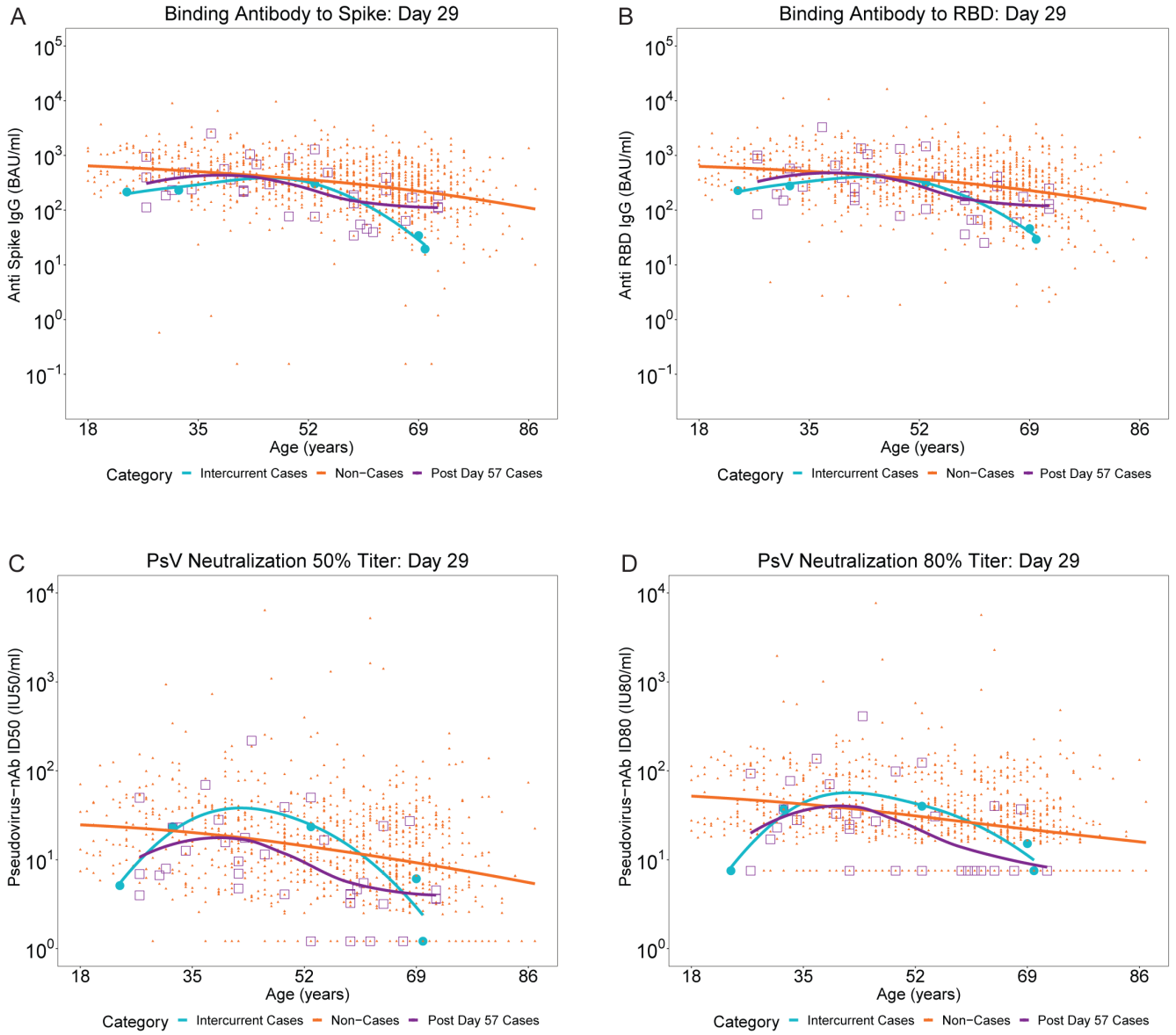


Fig. S9. Day 29 marker data points from baseline SARS-CoV-2 negative per-protocol vaccine recipients in the Day 29 marker case-cohort set. Non-cases are represented by orange dots, intercurrent cases by large blue circles, and post Day 57 cases by large purple squares.

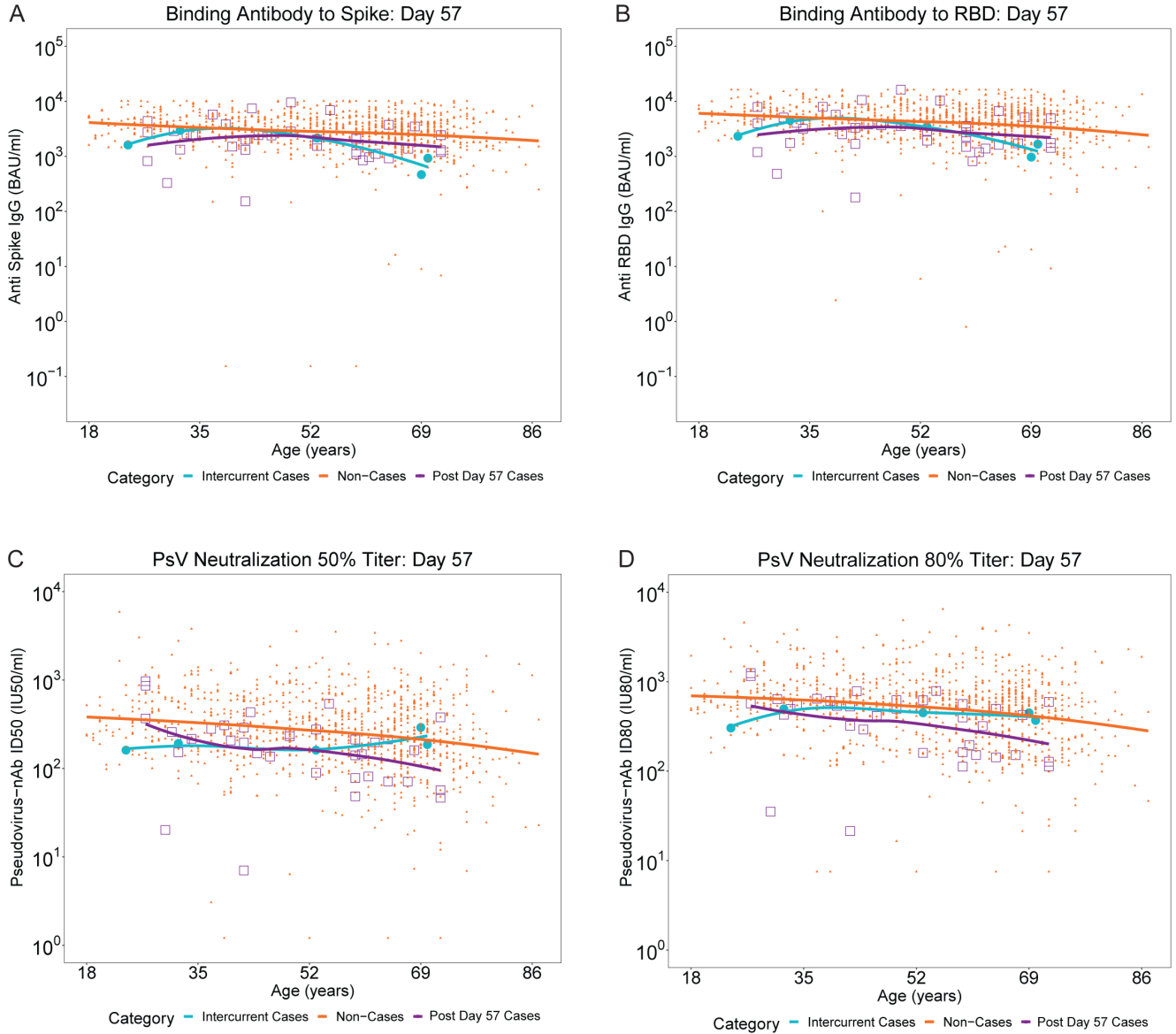


Fig. S10. Day 57 marker data points from baseline SARS-CoV-2 negative per-protocol vaccine recipients in the Day 57 marker case-cohort set. Non-cases are represented by orange dots, intercurrent cases by large blue circles, and post Day 57 cases by large purple squares.

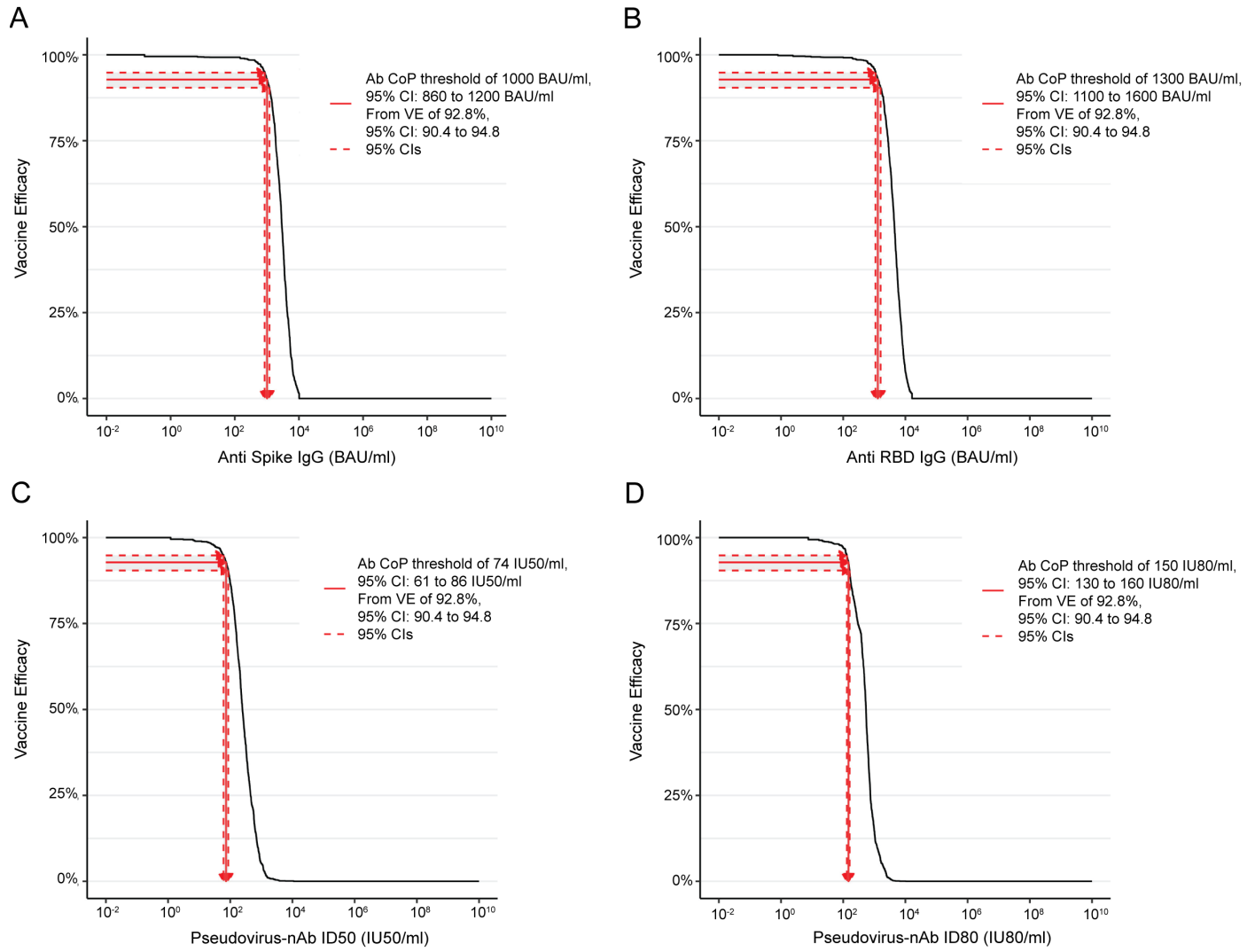


Fig. S11. Inverse probability sampling (IPS)-weighted empirical reverse cumulative distribution function curves for each Day 57 marker (spike IgG, RBD IgG, ID50, ID80) and application of the Siber (2007) method (27) for estimating a threshold of perfect vs. no protection.

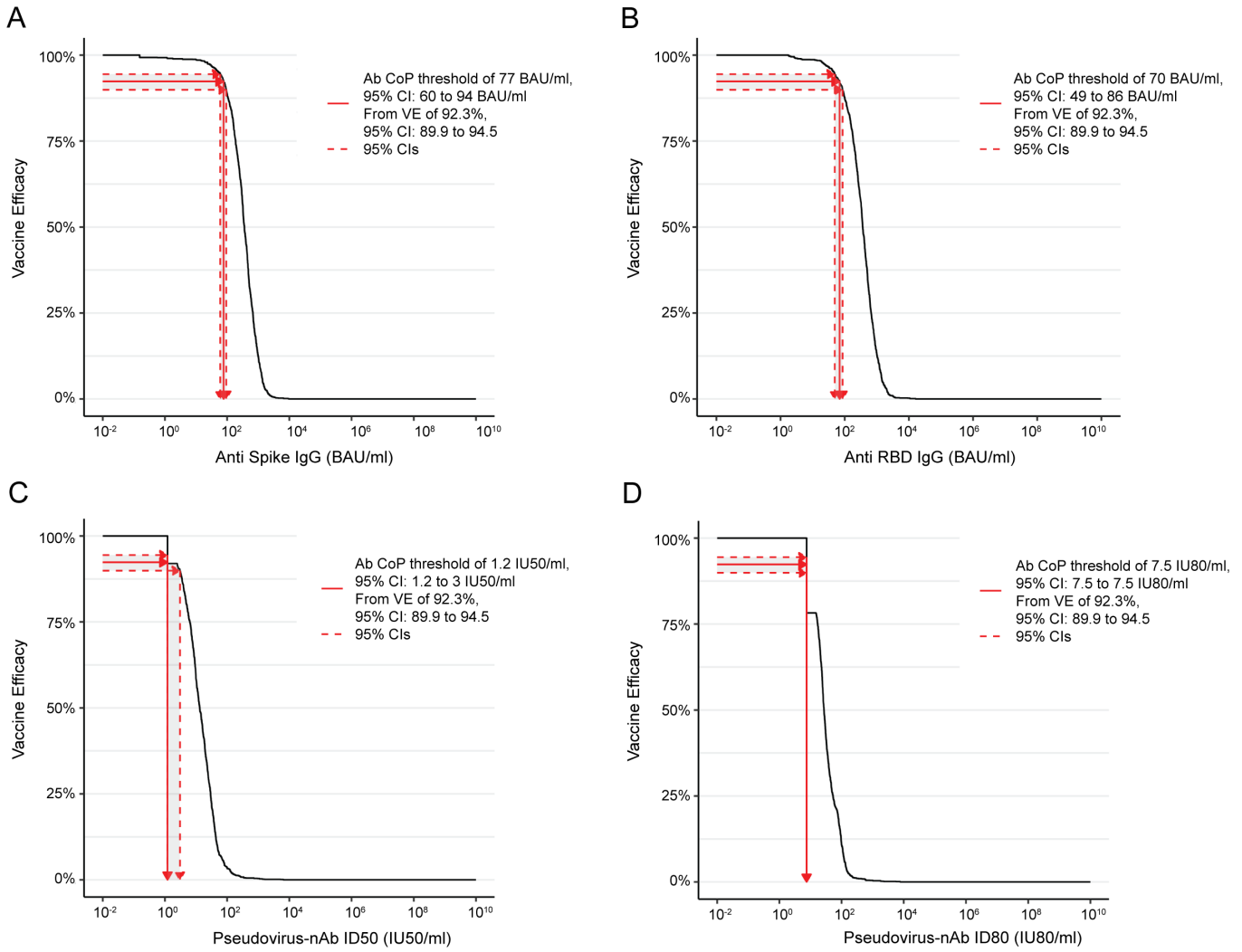


Fig. S12. Inverse probability sampling (IPS)-weighted empirical reverse cumulative distribution function curves for each Day 29 marker (spike IgG, RBD IgG, ID50, ID80) and application of the Siber (2007) method (27) for estimating a threshold of perfect vs. no protection.

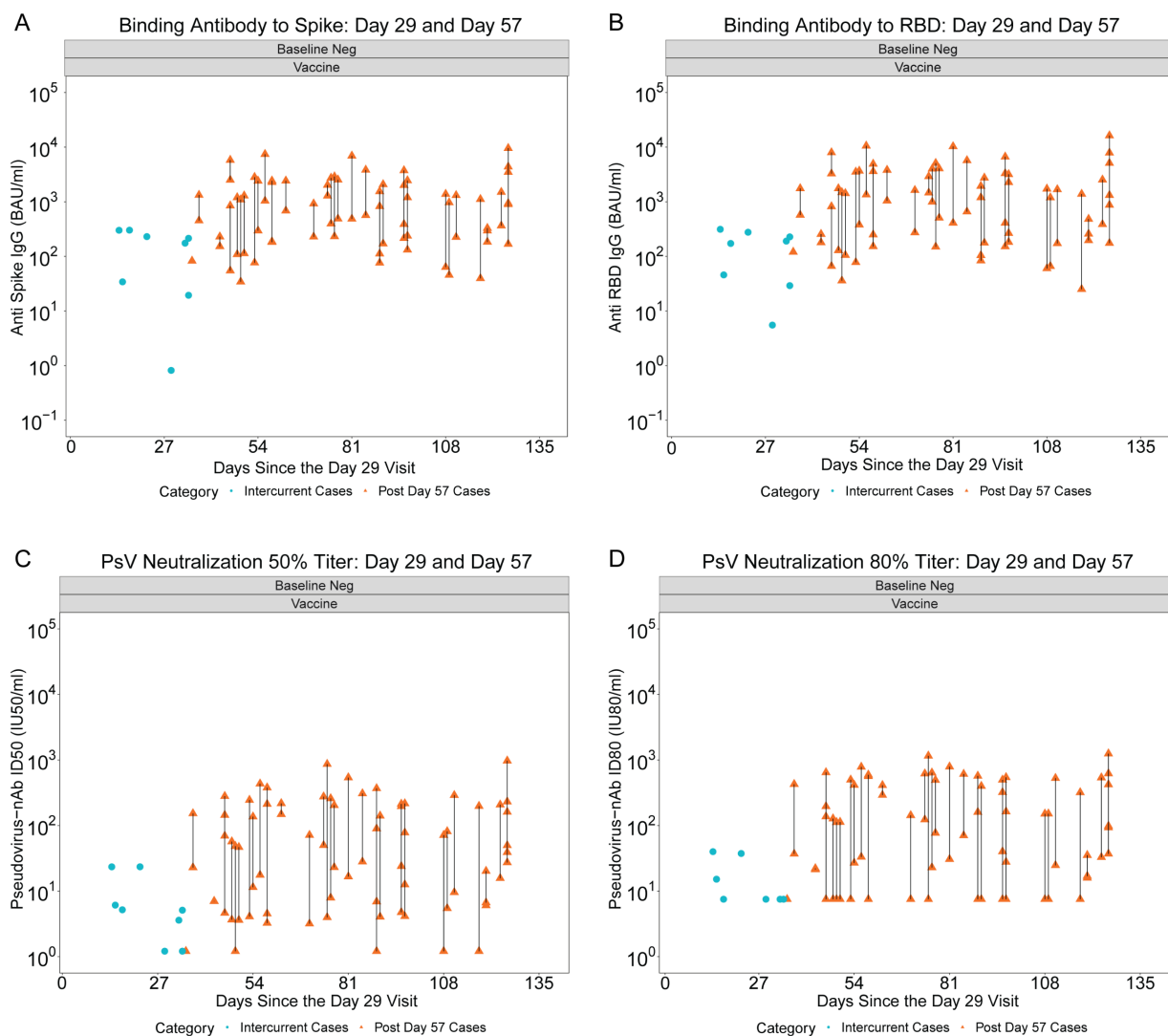
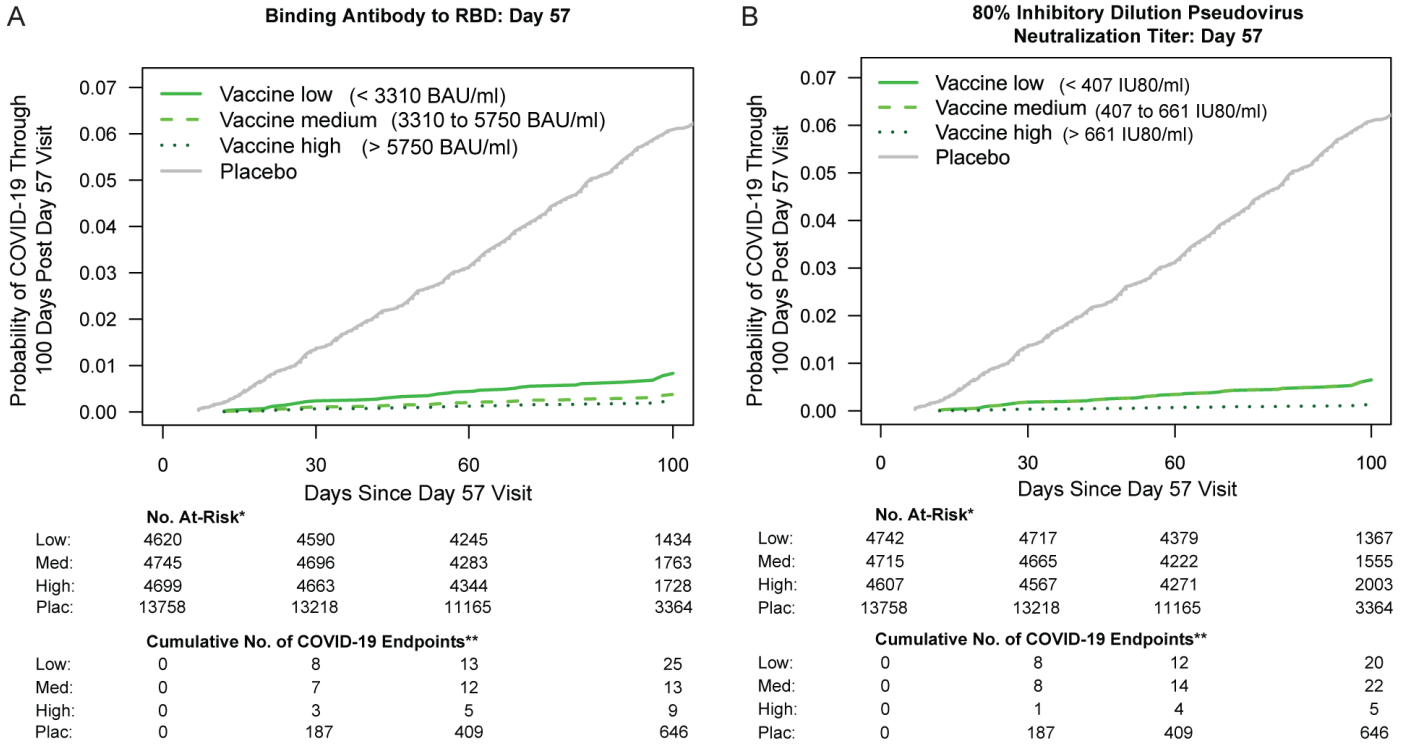


Fig. S13. Day 29 and Day 57 antibody markers (spike IgG, RBD IgG, ID50, ID80) vs. number of days from Day 29 visit until COVID-19 primary endpoint diagnosis for per-protocol baseline SARS-CoV-2 negative vaccine recipient breakthrough cases. Blue circles are Day 29 marker values for Intercurrent Cases. Orange triangles are Day 29, Day 57 marker values for Post Day 57 cases, with paired marker values from the same participant joined by a vertical line segment, with Day 57 marker value always the top triangle.



*No. At-Risk = estimated number in the population for analysis: baseline negative per-protocol vaccine recipients not experiencing the COVID-19 endpoint through 6 days post Day 57 visit.
 **Cumulative No. of COVID-19 Endpoints = estimated cumulative number of this cohort with a COVID-19 endpoint.

Fig. S14: Covariate-adjusted cumulative incidence of COVID-19 by Low, Medium, High tertile of Day 57 IgG concentration or pseudovirus neutralization titer. (A) Anti-RBD IgG concentration; (B) ID80 titer.

Supplementary Text S1

Baseline covariates adjusted for in immune correlates analyses, including the baseline COVID-19 risk score

In addition to adjusting for the at-risk indicator (a stratification factor used in the COVE trial randomization) and the indicator of membership in community of color, all correlates analyses adjust for a baseline COVID-19 risk score that was developed through machine learning of the baseline SARS-CoV-2 negative per-protocol placebo arm data in the COVE trial. This supplementary text summarizes the COVID-19 risk score, with the Statistical Analysis Plan providing additional details.

Table S4 lists the input variables that were included in the machine learning to build a model predicting the COVID-19 endpoint, where cases are COVID-19 endpoints starting 7 days post Day 57 visit and non-cases are participants with follow-up beyond 7 days post Day 57 visit and that never registered a COVID-19 endpoint. The risk score is defined as the logit of the predicted COVID-19 outcome probability from the predictive regression model, estimated using the ensemble algorithm superlearner (i.e. stacking), where this logit predicted outcome is scaled to have empirical mean zero and empirical standard deviation one.

Table S4. Individual baseline variables input into the Superlearner model for predicting occurrence of COVID-19 in baseline SARS-CoV-2 negative per-protocol placebo recipients.¹

Variable Name	Definition	Total missing values
MinorityInd	Baseline covariate minority status	0/14079 (0.0%)
EthnicityHispanic	(1=minority, 0=non-minority)	0/14079 (0.0%)
	Indicator ethnicity = Hispanic (0 = Non-Hispanic)	
EthnicityNotreported	Indicator ethnicity = Not reported (0 = Non-Hispanic)	0/14079 (0.0%)
EthnicityUnknown	Indicator ethnicity = Unknown (0 = Non-Hispanic)	0/14079 (0.0%)
Black	Indicator race = Black (0 = White)	0/14079 (0.0%)
Asian	Indicator race = Asian (0 = White)	0/14079 (0.0%)
NatAmer	Indicator race = American Indian or Alaska Native (0 =	0/14079 (0.0%)
	=	
PacIsl	White)	0/14079 (0.0%)
	Indicator race = Native Hawaiian or Other Pacific	
Multiracial	Islander (0 = White)	0/14079 (0.0%)
	Indicator race = Multiracial (0 = White)	
Other	Indicator race = Other (0 = White)	0/14079 (0.0%)
Notreported	Indicator race = Not reported (0 = White)	0/14079 (0.0%)
Unknown	Indicator race = unknown (0 = White)	0/14079 (0.0%)
HighRiskInd	Baseline covariate high risk pre-existing condition	0/14079 (0.0%)
Sex	(1=yes, 0=no)	0/14079 (0.0%)
	Sex assigned at birth (1=female, 0=male)	
Age	Age at enrollment in years, between 18 and 85	0/14079 (0.0%)
BMI	BMI at enrollment (kg/m ²)	79/14079 (0.6%)

¹The per-protocol group for immune correlates analysis is slightly different than that for the primary vaccine efficacy analysis (6), due in part to a data cutoff for the primary vaccine efficacy analysis of November 25, 2020 (6) vs a data cutoff for the immune correlates analysis of March 26, 2021, and also in part due to the inclusion of participants with HIV in the per-protocol set for vaccine efficacy analysis (6) vs. the exclusion of participants with HIV from the per-protocol set for the immune correlates analysis

The following details were used in the implementation of superlearner of the baseline SARS-CoV-2 negative per-protocol placebo arm:

- All of the selected learners (i.e., regression methods for classifying whether a participant has a COVID-19 outcome or not) were coded into the SuperLearner R package available on CRAN, and the analysis was done using this R package.
- Each quantitative and ordinal variable was pre-scaled to have empirical mean 0 and standard deviation 1.
- 5-fold cross-validation was used with no more than $\max(20, \text{floor}(np/20))$ input variables included in each model, where np is the number of evaluable placebo arm cases.
- High-correlation variable screening was used, not allowing any pair of input variables to have Spearman rank correlation $r > 0.9$.
- Two levels of cross-validation (CV) were used. The outer level computed CV-AUC over 5-fold cross-validation, and the inner level used 5-fold CV.
- Results for comparing classification accuracy of different models were based on point and 95% confidence interval estimates of cross-validated area under the ROC curve (CV-AUC) (48, 49). Results are presented as forest plots of point and 95% confidence interval estimates similar to those used in Figure 3B of Neidich et al. (50) and in Figure 2 of Magaret, Benkeser, and Williamson et al. (51). CV-AUC was estimated using the *vimp* R package (52) available on CRAN.

Table S5 lists the learning algorithms that were applied to estimate the conditional probability of the COVID-19 outcome based on the input variables listed in **table S4**. Some of the algorithms are non-data-adaptive type learning algorithms, such as parametric regression models (e.g., generalized linear models [glms]), which are simple and stable. Data-adaptive type algorithms are also included, for increasing flexibility of modeling and reducing the risk of model misspecification: SL.randomForest, SL.gam, SL.polymars, and SL.xgboost. All of the selected learners are coded into the SuperLearner R package.

Table S5. Learning algorithm-screen combinations (14 in total) used as input to the Superlearner model in baseline negative per-protocol placebo recipients.

Learner	Screen*
SL.mean	All
SL.glm	all glmnet univar_logistic_pval highcor_random
SL.glm.interaction	glmnet univar_logistic_pval highcor_random
SL.glmnet	All
SL.gam	glmnet univar_logistic_pval highcor_random
SL.xgboost	All
SL.ranger.imp	All

*Screen details:

all: includes all variables

glmnet: includes variables with non-zero coefficients in the standard implementation of SL.glmnet that optimizes the lasso tuning parameter via cross-validation

univar_logistic_pval: Wald test 2-sided p-value in a logistic regression model < 0.10

highcor_random: if pairs of quantitative variables with Spearman rank correlation > 0.90 , select one of the variables at random

Table S6 shows the weights that the Superlearner ensemble model applied to each of the individual prediction algorithms in the modeling of the placebo arm.

Table S6. Weights assigned by Superlearner to each individual learner in the COVID-19 prediction modeling of the placebo arm

Learner	Screen	Weight
SL.gam	screen_highcor_random	0.369
SL.gam	screen_univariate_logistic_pval	0.291
SL.ranger.imp	screen_all	0.165
SL.mean	screen_all	0.112
SL.xgboost	screen_all	0.062
SL.glm	screen_all	0.000
SL.glmnet	screen_all	0.000
SL.glm	screen_glmnet	0.000
SL.glm	screen_univariate_logistic_pval	0.000
SL.glm	screen_highcor_random	0.000
SL.glm.interaction	screen_glmnet	0.000
SL.glm.interaction	screen_univariate_logistic_pval	0.000
SL.glm.interaction	screen_highcor_random	0.000
SL.gam	screen_glmnet	0.000

To inform about which individual input variables were most important for the risk score, **table S7** shows the predictors used in the learners that were assigned positive weight by the Superlearner model, with multiple metrics reported that can be used for ranking variable importance. BMI and age were ranked as the two most important variables for predicting COVID-19.

Table S7. Predictors in learners assigned positive weight by Superlearner in the COVID-19 prediction modeling of the placebo arm.

Learner	Screen	Weight	Predictors	Coefficient	Odds		Importance	Feature	Gain	Cover	Frequency
					Ratio						
SL.gam	screen_highcor_random	0.369	(Intercept)	-3.109	0.045		NA	NA	NA	NA	NA
SL.gam	screen_highcor_random	0.369	s(Age,2)	-0.280	0.756		NA	NA	NA	NA	NA
SL.gam	screen_highcor_random	0.369	s(BMI,2)	0.174	1.190		NA	NA	NA	NA	NA
SL.gam	screen_highcor_random	0.369	MinorityInd	-0.042	0.959		NA	NA	NA	NA	NA
SL.gam	screen_highcor_random	0.369	EthnicityHispanic	0.027	1.028		NA	NA	NA	NA	NA
SL.gam	screen_highcor_random	0.369	EthnicityNotreported	-0.046	0.955		NA	NA	NA	NA	NA
SL.gam	screen_highcor_random	0.369	EthnicityUnknown	-0.056	0.945		NA	NA	NA	NA	NA
SL.gam	screen_highcor_random	0.369	Black	-0.250	0.779		NA	NA	NA	NA	NA
SL.gam	screen_highcor_random	0.369	Asian	-0.047	0.954		NA	NA	NA	NA	NA
SL.gam	screen_highcor_random	0.369	NatAmer	-0.059	0.943		NA	NA	NA	NA	NA
SL.gam	screen_highcor_random	0.369	PacIsl	-0.442	0.643		NA	NA	NA	NA	NA
SL.gam	screen_highcor_random	0.369	Multiracial	-0.143	0.866		NA	NA	NA	NA	NA
SL.gam	screen_highcor_random	0.369	Other	0.018	1.018		NA	NA	NA	NA	NA
SL.gam	screen_highcor_random	0.369	Notreported	0.033	1.034		NA	NA	NA	NA	NA
SL.gam	screen_highcor_random	0.369	Unknown	0.029	1.030		NA	NA	NA	NA	NA
SL.gam	screen_highcor_random	0.369	HighRiskInd	0.007	1.007		NA	NA	NA	NA	NA
SL.gam	screen_highcor_random	0.369	Sex	0.054	1.056		NA	NA	NA	NA	NA
SL.gam	screen_univariate_logistic_pval	0.291	(Intercept)	-3.084	0.046		NA	NA	NA	NA	NA
SL.gam	screen_univariate_logistic_pval	0.291	s(Age,2)	-0.274	0.761		NA	NA	NA	NA	NA
SL.gam	screen_univariate_logistic_pval	0.291	s(BMI,2)	0.183	1.201		NA	NA	NA	NA	NA
SL.gam	screen_univariate_logistic_pval	0.291	EthnicityHispanic	0.010	1.010		NA	NA	NA	NA	NA
SL.gam	screen_univariate_logistic_pval	0.291	Black	-0.268	0.765		NA	NA	NA	NA	NA
SL.gam	screen_univariate_logistic_pval	0.291	Multiracial	-0.150	0.861		NA	NA	NA	NA	NA
SL.ranger.imp	screen_all	0.165	MinorityInd	NA	NA	3.296	NA	NA	NA	NA	NA
SL.ranger.imp	screen_all	0.165	EthnicityHispanic	NA	NA	3.844	NA	NA	NA	NA	NA
SL.ranger.imp	screen_all	0.165	EthnicityNotreported	NA	NA	1.069	NA	NA	NA	NA	NA
SL.ranger.imp	screen_all	0.165	EthnicityUnknown	NA	NA	0.433	NA	NA	NA	NA	NA
SL.ranger.imp	screen_all	0.165	Black	NA	NA	2.608	NA	NA	NA	NA	NA
SL.ranger.imp	screen_all	0.165	Asian	NA	NA	2.318	NA	NA	NA	NA	NA
SL.ranger.imp	screen_all	0.165	NatAmer	NA	NA	0.971	NA	NA	NA	NA	NA
SL.ranger.imp	screen_all	0.165	PacIsl	NA	NA	0.133	NA	NA	NA	NA	NA
SL.ranger.imp	screen_all	0.165	Multiracial	NA	NA	1.394	NA	NA	NA	NA	NA

SL.ranger.imp	screen_all	0.165	Other	NA	NA	2.155	NA	NA	NA	NA
SL.ranger.imp	screen_all	0.165	Notreported	NA	NA	1.390	NA	NA	NA	NA
SL.ranger.imp	screen_all	0.165	Unknown	NA	NA	1.682	NA	NA	NA	NA
SL.ranger.imp	screen_all	0.165	HighRiskInd	NA	NA	4.380	NA	NA	NA	NA
SL.ranger.imp	screen_all	0.165	Sex	NA	NA	6.329	NA	NA	NA	NA
SL.ranger.imp	screen_all	0.165	Age	NA	NA	50.511	NA	NA	NA	NA
SL.ranger.imp	screen_all	0.165	BMI	NA	NA	109.263	NA	NA	NA	NA
SL.xgboost	screen_all	0.062	NA	NA	NA	NA	BMI	0.664	0.796	0.75
SL.xgboost	screen_all	0.062	NA	NA	NA	NA	Age	0.238	0.153	0.17
SL.xgboost	screen_all	0.062	NA	NA	NA	NA	Sex	0.025	0.006	0.01
SL.xgboost	screen_all	0.062	NA	NA	NA	NA	Black	0.022	0.018	0.01
SL.xgboost	screen_all	0.062	NA	NA	NA	NA	MinorityInd	0.018	0.009	0.01
SL.xgboost	screen_all	0.062	NA	NA	NA	NA	HighRiskInd	0.014	0.006	0.01
SL.xgboost	screen_all	0.062	NA	NA	NA	NA	EthnicityHispanic	0.011	0.004	0.00
SL.xgboost	screen_all	0.062	NA	NA	NA	NA	Multiracial	0.007	0.004	0.00
SL.xgboost	screen_all	0.062	NA	NA	NA	NA	Asian	0.001	0.003	0.00
SL.xgboost	screen_all	0.062	NA	NA	NA	NA	Other	0.000	0.001	0.00

Figure S15 Panel A shows the cross-validated receiver operating characteristic curve for the 2 top-performing learners, Superlearner, and the Discrete Superlearner models classifying COVID-19 outcome status in baseline SARS-CoV-2 negative per-protocol placebo recipients, with predictive performance summarized by cross-validated area under the receiver operating characteristic curve (CV-AUC). The point estimate of CV-AUC for the Superlearner was 0.612 with 95% CI 0.591, 0.633.

Figure S15 Panel B shows the receiver operating characteristic curve for the Superlearner model built from baseline SARS-CoV-2 negative per-protocol placebo recipients applied to baseline SARS-CoV-2 negative per-protocol vaccine recipients, for which the point estimate of AUC for classifying COVID-19 outcome status was 0.614.

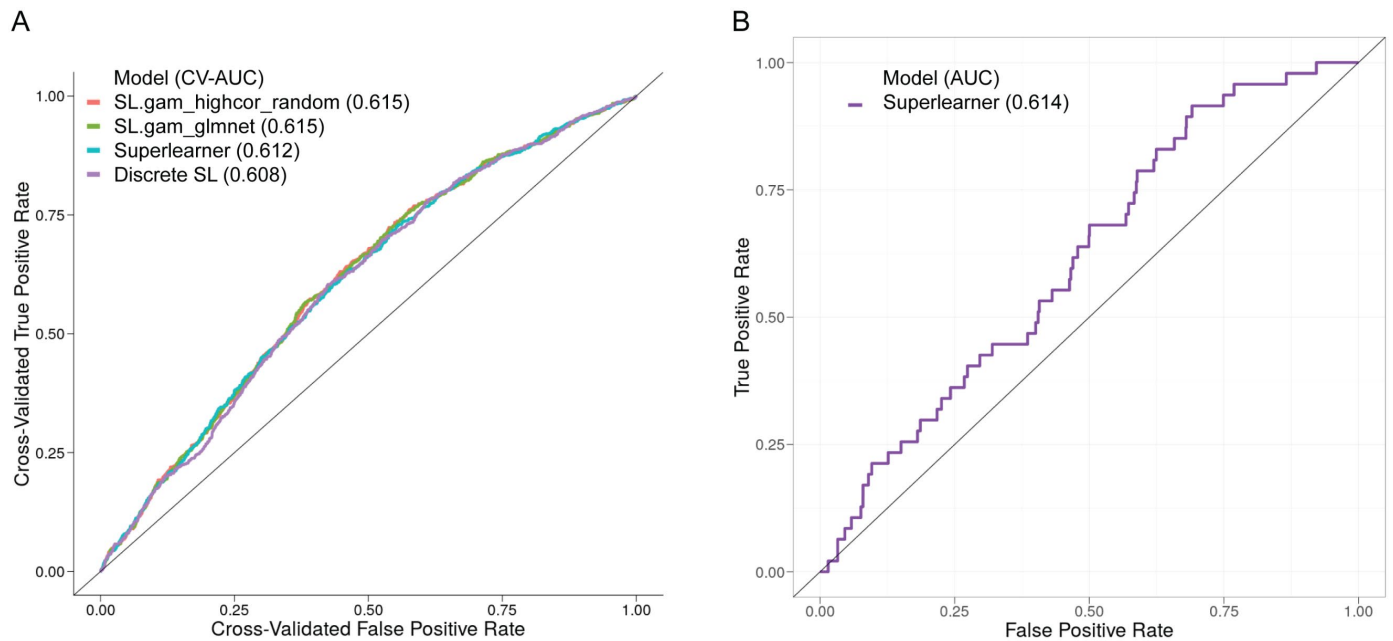


Fig. S15. (A) Cross-validated receiver operating characteristic curve for the two top-performing learners, Superlearner, and the Discrete Superlearner models classifying COVID-19 outcome occurrence in baseline SARS-CoV-2 negative per-protocol placebo recipients, with cross-validated area under the curve (CV-AUC) summarizing classification performance. (B) Receiver operating characteristic curve for the Superlearner upon applying the model built from placebo recipients to baseline SARS-CoV-2 negative per-protocol vaccine recipients, with AUC in parentheses summarizing classification performance.

Figure S16 shows Superlearner model predicted probabilities of the COVID-19 endpoint starting 7 days post Day 57 visit by case vs. non-case status, for baseline SARS-CoV-2 negative per-protocol vaccine recipients in the Day 57 marker case-cohort set.

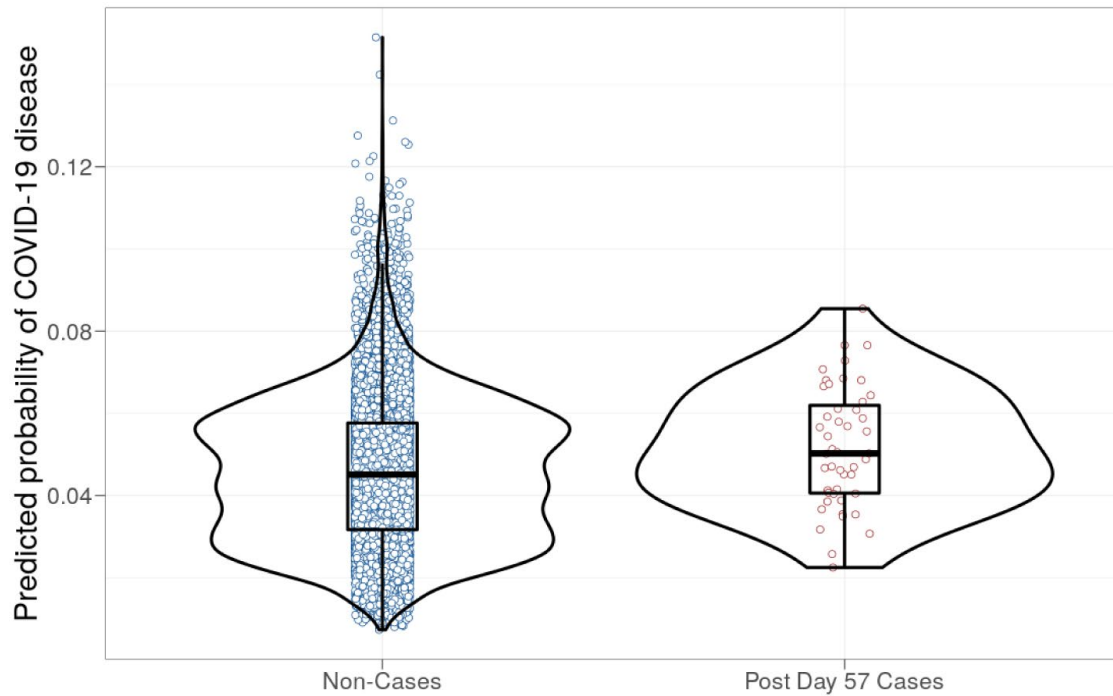


Fig. S16. Superlearner model predicted probabilities of the COVID-19 endpoint starting 7 days post Day 57 visit by case vs. non-case (i.e., control) status, for baseline SARS-CoV-2 negative per-protocol vaccine recipients in the Day 57 marker case-cohort set.

A

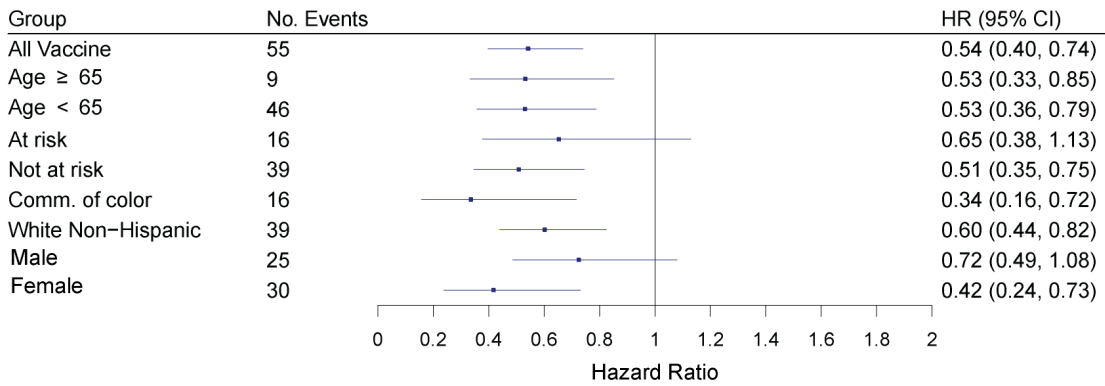
Immunologic Marker	No. cases / No. at-risk*	HR per 10-fold incr. Pt. Est.	95% CI	P-value (2-sided)	FDR- adjusted p-value**	FWER- adjusted p-value
COVE						
Anti Spike IgG (BAU/ml)	55/14,141	0.54	(0.40,0.74)	<0.001	<0.001	<0.001
Anti RBD IgG (BAU/ml)	55/14,141	0.46	(0.30,0.70)	<0.001	0.001	0.001
PsV-nAb ID50 (IU50/ml)	55/14,141	0.33	(0.17,0.65)	0.001	0.003	0.002
PsV-nAb ID80 (IU80/ml)	55/14,141	0.19	(0.07,0.56)	0.003	0.004	0.003

*No. at-risk = estimated number in the population for analysis: baseline negative per-protocol vaccine recipients not experiencing the COVID-19 endpoint through 6 days post Day 29 visit; No. cases = estimated number of this cohort with an observed COVID-19 endpoint starting 7 days post Day 29 visit. The count 55 differs from 46 (Figure 1, Table 1) because the 55 includes all vaccine breakthrough cases including the 9 without Day 1, 29, 57 antibody marker data.

** FDR (false discovery rate)-adjusted p-values and FWER (family-wise error rate)-adjusted p-values are computed over the set of p-values both for quantitative markers and categorical markers (Low, Medium, High) using the Westfall and Young permutation method (10,000 replicates).

B

Binding Antibody to Spike: Day 29



C

50% Inhibitory Dilution Pseudovirus Neutralization Titer: Day 29

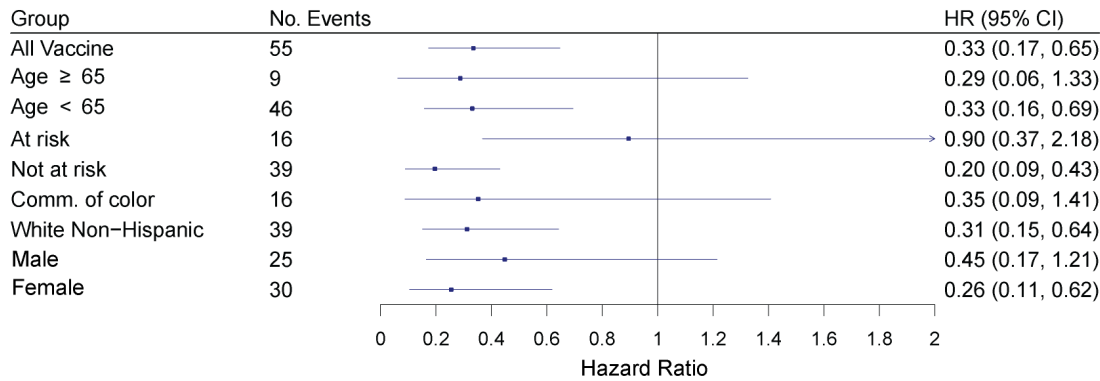
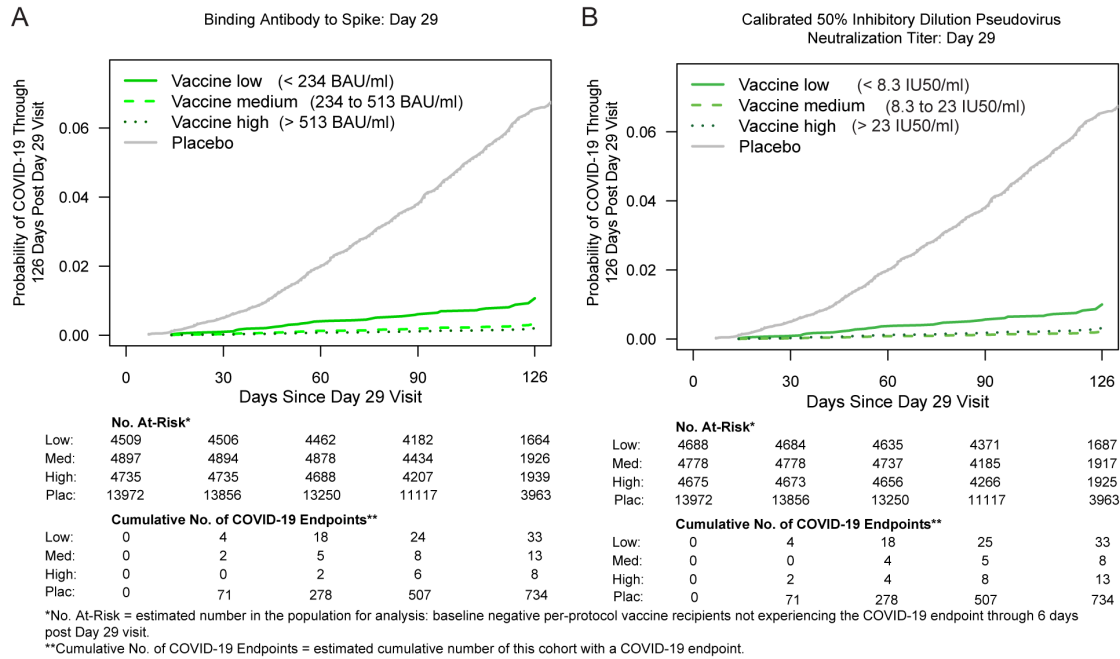


Fig. S17. Covariate-adjusted hazard ratios of COVID-19 per 10-fold increase in each Day 29 antibody marker in baseline SARS-CoV-2 negative per-protocol vaccine recipients overall and in subgroups. (A) Inferences for IgG (spike, RBD) and (ID50, ID80); (B) Forest plots for anti-spike IgG concentration; (C) Forest plots for ID50. Community of color is the complement of White Non-Hispanic (different from Minority because missing values are included in Community of color).



C

COVE Immunologic Marker	Tertile [†]	No. cases / No. at-risk [‡]	Attack rate	Haz. Ratio Pt. Est.	95% CI	P-value (2-sided)	Overall P-value	FDR-adjusted p-value [†]	FWER-adjusted p-value [†]
Anti Spike IgG (BAU/ml)	Low	33/4,509	0.0073	1	N/A	N/A	<0.001	<0.001	<0.001
	Medium	13/4,897	0.0027	0.31	(0.15, 0.65)	0.002			
	High	8/4,735	0.0017	0.19	(0.08, 0.44)	<0.001			
Anti RBD IgG (BAU/ml)	Low	30/4,559	0.0066	1	N/A	N/A	0.002	0.004	0.003
	Medium	14/4,803	0.0029	0.40	(0.19, 0.84)	0.016			
	High	11/4,779	0.0023	0.28	(0.13, 0.60)	0.001			
Pseudovirus-nAb ID50 (IU50/ml)	Low	33/4,688	0.0070	1	N/A	N/A	<0.001	0.001	0.001
	Medium	8/4,778	0.0017	0.22	(0.09, 0.53)	<0.001			
	High	13/4,675	0.0028	0.32	(0.15, 0.69)	0.003			
Pseudovirus-nAb ID80 (IU80/ml)	Low	31/4,709	0.0066	1	N/A	N/A	0.001	0.003	0.002
	Medium	16/4,827	0.0033	0.44	(0.21, 0.90)	0.025			
	High	8/4,604	0.0017	0.22	(0.09, 0.51)	<0.001			
Placebo		734/13,972	0.0525						

Baseline covariates adjusted for: baseline risk score, At Risk status, Community of color status.
Maximum failure event time 126 days post Day 29 visit.

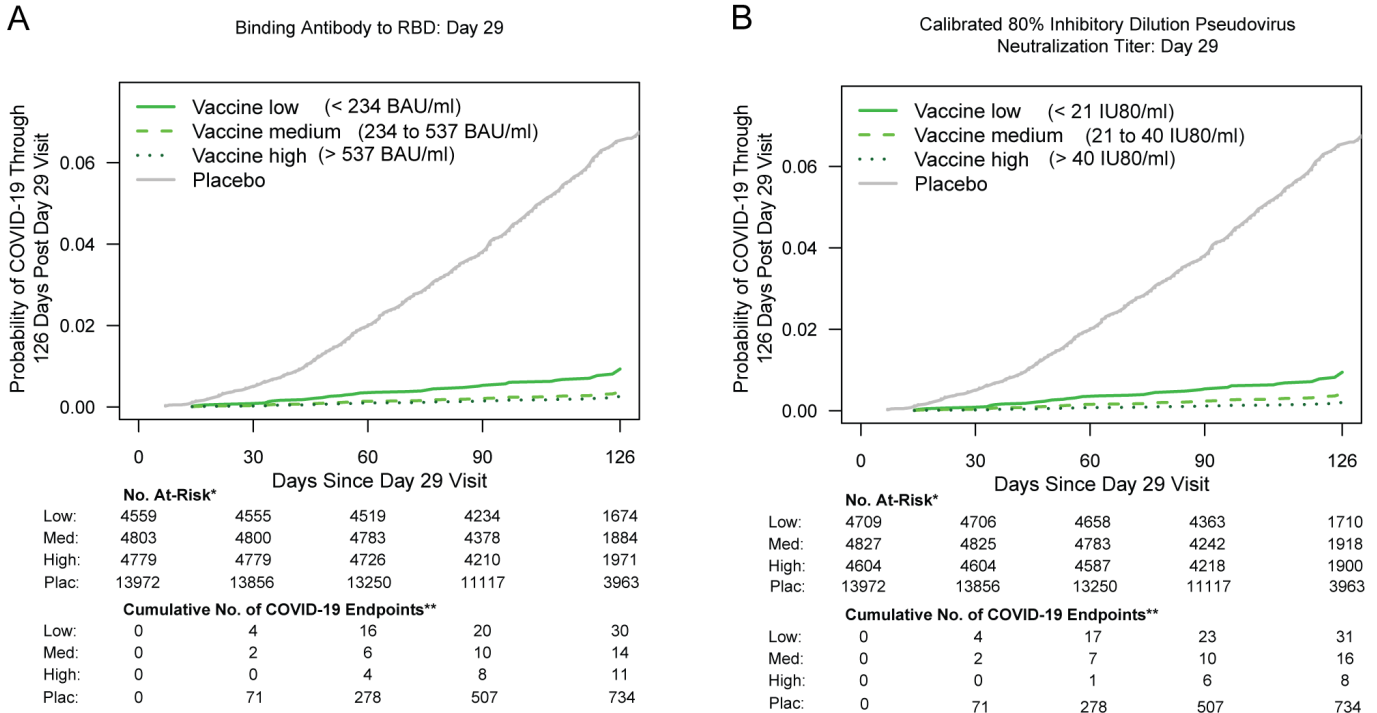
[†]Tertiles:

Spike IgG: Low is < 234 BAU/ml, Medium is 234 to 513 BAU/ml, High is > 513 BAU/ml.
RBD IgG: Low is < 234 BAU/ml, Medium is 234 to 537 BAU/ml, High is > 537 BAU/ml.
ID50: Low is < 8.3 IU50/ml, Medium is 8.3 to 23 IU50/ml, High is > 23 IU50/ml.
ID80: Low is < 21 IU80/ml, Medium is 21 to 40 IU80/ml, High is > 40 IU80/ml.

[‡]No. at-risk = estimated number in the population for analysis; baseline negative per-protocol vaccine recipients not experiencing the COVID-19 endpoint through 6 days post Day 29 visit; No. cases = estimated number of this cohort with an observed COVID-19 endpoint. The total count (55) across all tertiles for each marker differs from 46 (Figure 1, Table 1), because the 55 includes all vaccine breakthrough cases including the 9 without Day 1, 29, 57 antibody marker data.

[†]FDR (false discovery rate)-adjusted p-values and FWER (family-wise error rate)-adjusted p-values are computed over the set of p-values both for quantitative markers and categorical markers (Low, Medium, High) using the Westfall and Young permutation method (10,000 replicates).

Figure S18. Covariate-adjusted cumulative incidence of COVID-19 by Low, Medium, High tertile of Day 29 IgG concentration or pseudovirus neutralization titer in baseline SARS-CoV-2 negative per-protocol participants. (A) Anti-spike IgG concentration; (B) ID50 titer; (C) IgG (spike, RBD) and (ID50, ID80). The overall p-value is from a generalized Wald test for whether the COVID-19 hazard differed across Low, Medium, and High subgroups.



*No. At-Risk = estimated number in the population for analysis: baseline negative per-protocol vaccine recipients not experiencing the COVID-19 endpoint through 6 days post Day 29 visit.
 **Cumulative No. of COVID-19 Endpoints = estimated cumulative number of this cohort with a COVID-19 endpoint.

Figure S19: Covariate-adjusted cumulative incidence of COVID-19 by Low, Medium, High tertile of Day 29 IgG concentration or pseudovirus neutralization titer. (A) Anti-RBD IgG concentration; (B) ID80 titer.

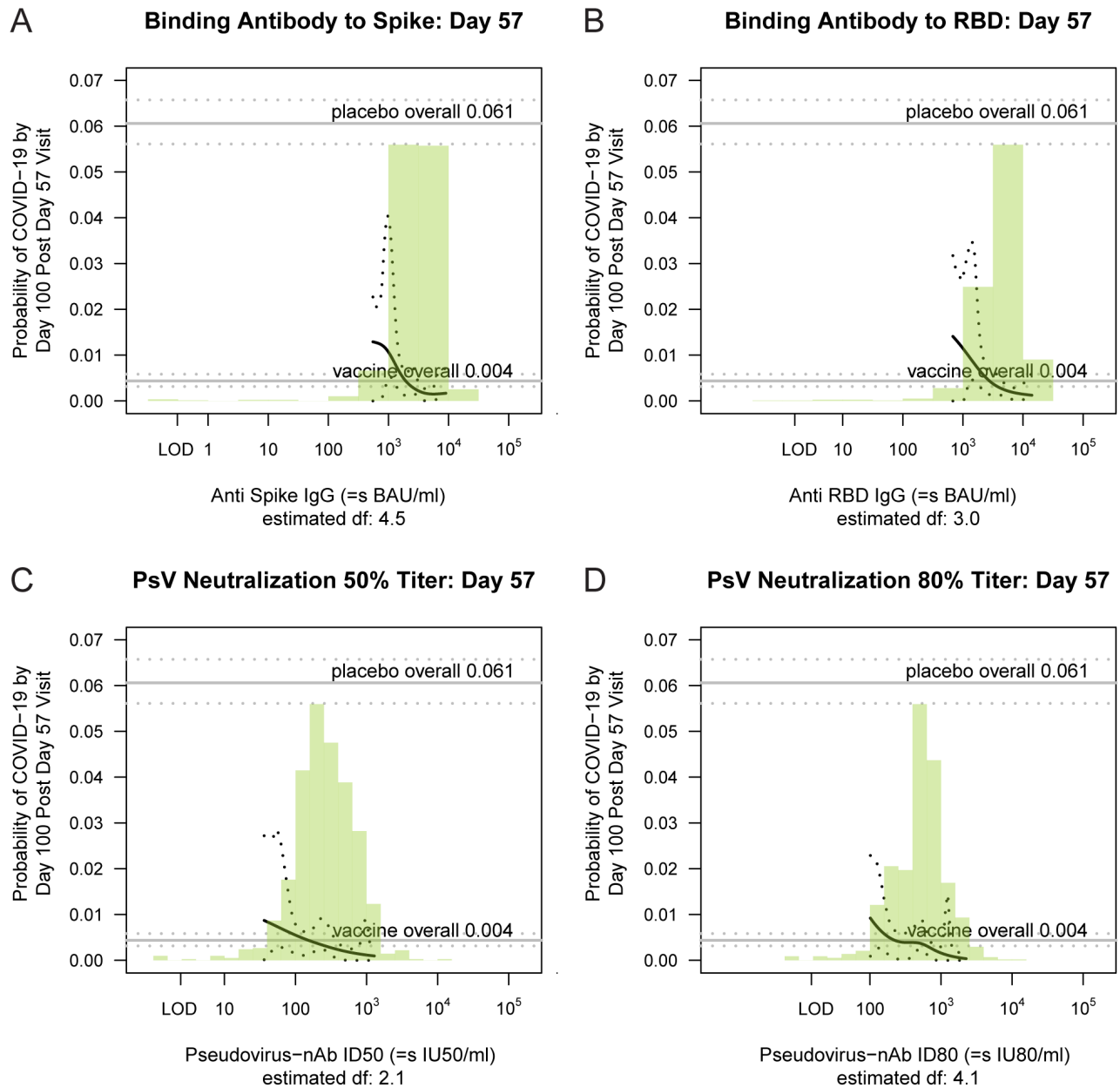


Fig. S20. Covariate-adjusted risk of COVID-19 by the level of each Day 57 marker (spike IgG, RBD IgG, ID50, ID80), estimated with a generalized additive model, in baseline SARS-CoV-2 negative per-protocol vaccine recipients.

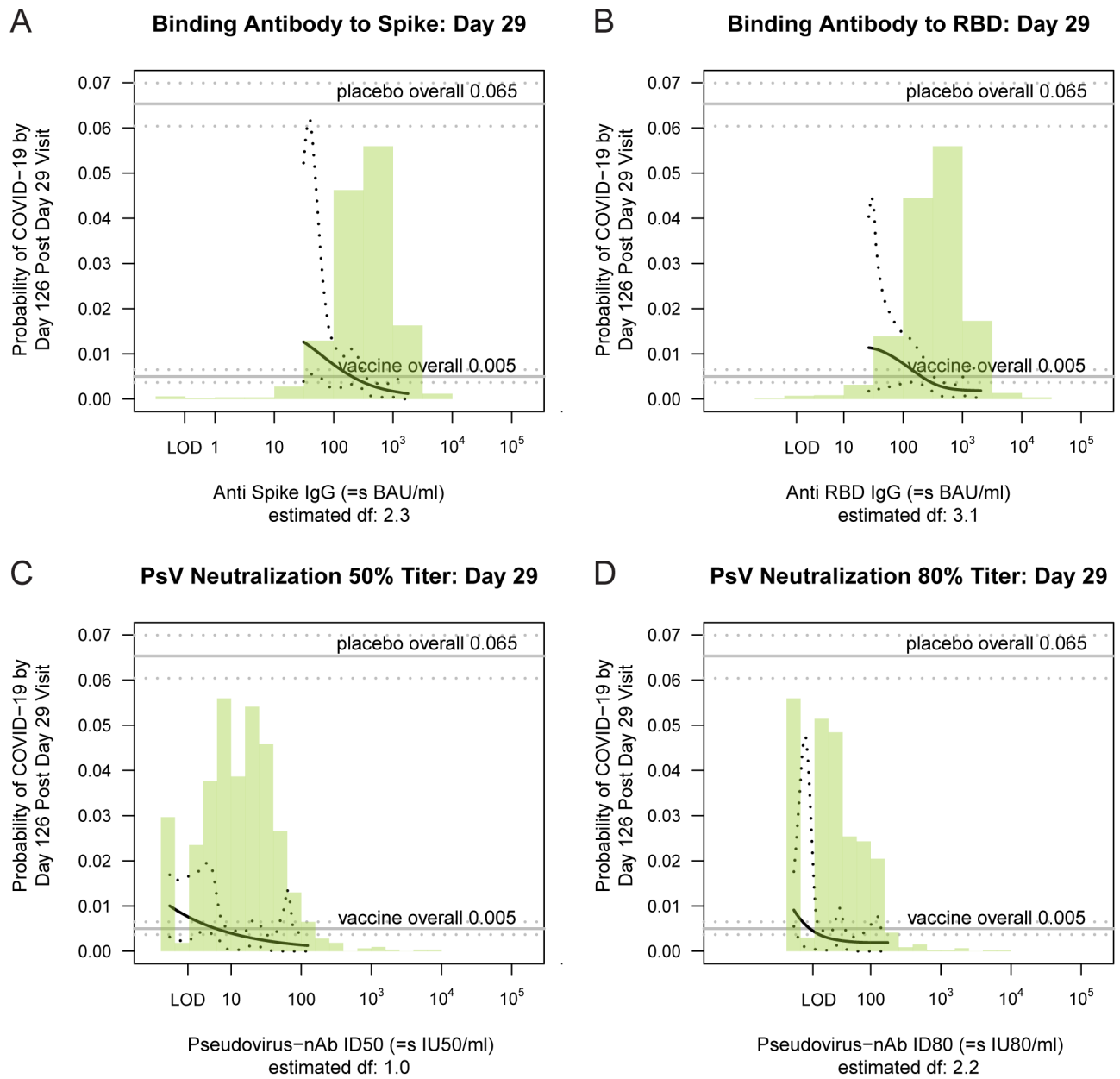


Fig. S21. Covariate-adjusted risk of COVID-19 by the level of each Day 29 marker (spike IgG, RBD IgG, ID50, ID80), estimated with a generalized additive model, in baseline SARS-CoV-2 negative per-protocol vaccine recipients.

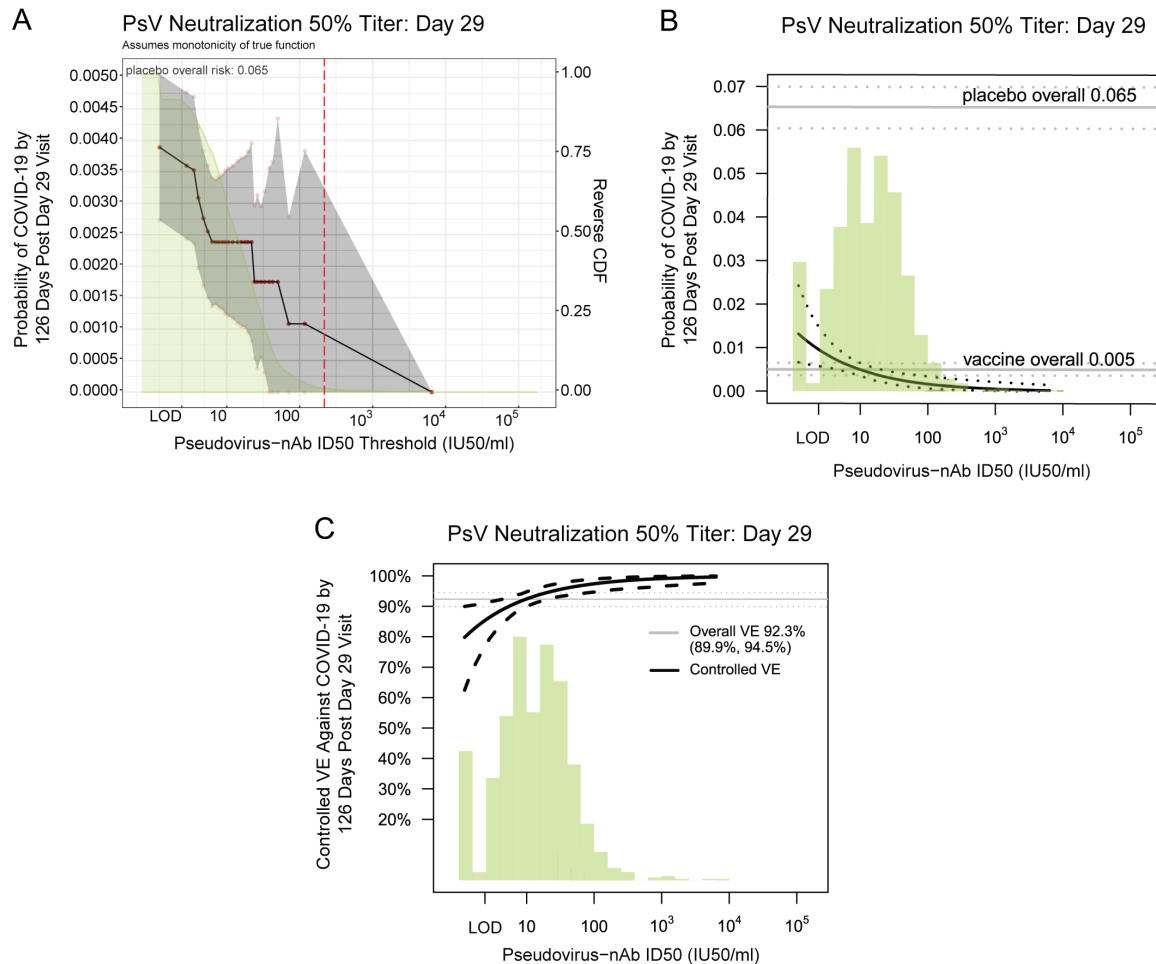


Fig. S22. Further analyses of Day 29 ID50 level as a correlate of risk and as a correlate of protection. (A) Covariate-adjusted cumulative incidence of COVID-19 by 126 days post Day 29 by vaccinated baseline SARS-CoV-2 negative per-protocol subgroups defined by Day 29 ID50 level above a threshold, with reverse cumulative distribution function (CDF) of Day 29 ID50 level overlaid in green. The red dots are point estimates at 35 threshold values equally spaced over quantiles of the observed marker values, linearly interpolated by solid black lines; the gray shaded area is pointwise 95% confidence intervals (CIs). The upper boundary of the green shaded area is the estimate of the reverse cumulative distribution function (CDF) of Day 29 ID50 level in baseline SARS-CoV-2 negative per-protocol vaccine recipients. The vertical red dashed line is the Day 29 ID50 threshold above which no post Day 29 COVID endpoints occurred. (B) Covariate-adjusted cumulative incidence of COVID-19 by 126 days post Day 29 by Day 29 ID50 level. The dotted black lines indicate bootstrap point-wise 95% CIs. The upper and lower horizontal gray lines are the overall cumulative incidence of COVID-19 from 7 to 126 days post Day 29 in placebo and vaccine recipients, respectively. (C) Vaccine efficacy (solid black line) by Day 29 ID50 level, estimated using the method of Gilbert, Fong, and Carone (28). The dashed black lines indicate bootstrap point-wise 95% CIs. The horizontal gray line is the overall vaccine efficacy from 7 to 126 days post Day 29, with the dotted gray lines indicating the 95% CIs (this number 92.3% differs from the 94.1% reported in (6), which was based on counting COVID-19 endpoints starting 14 days post Day 29). In (B) and (C), the green histograms are an estimate of the density of Day 29 ID50 level in baseline negative per-protocol vaccine recipients. LOD, limit of detection. Baseline covariates adjusted for: baseline risk score, at risk status, community of color status.

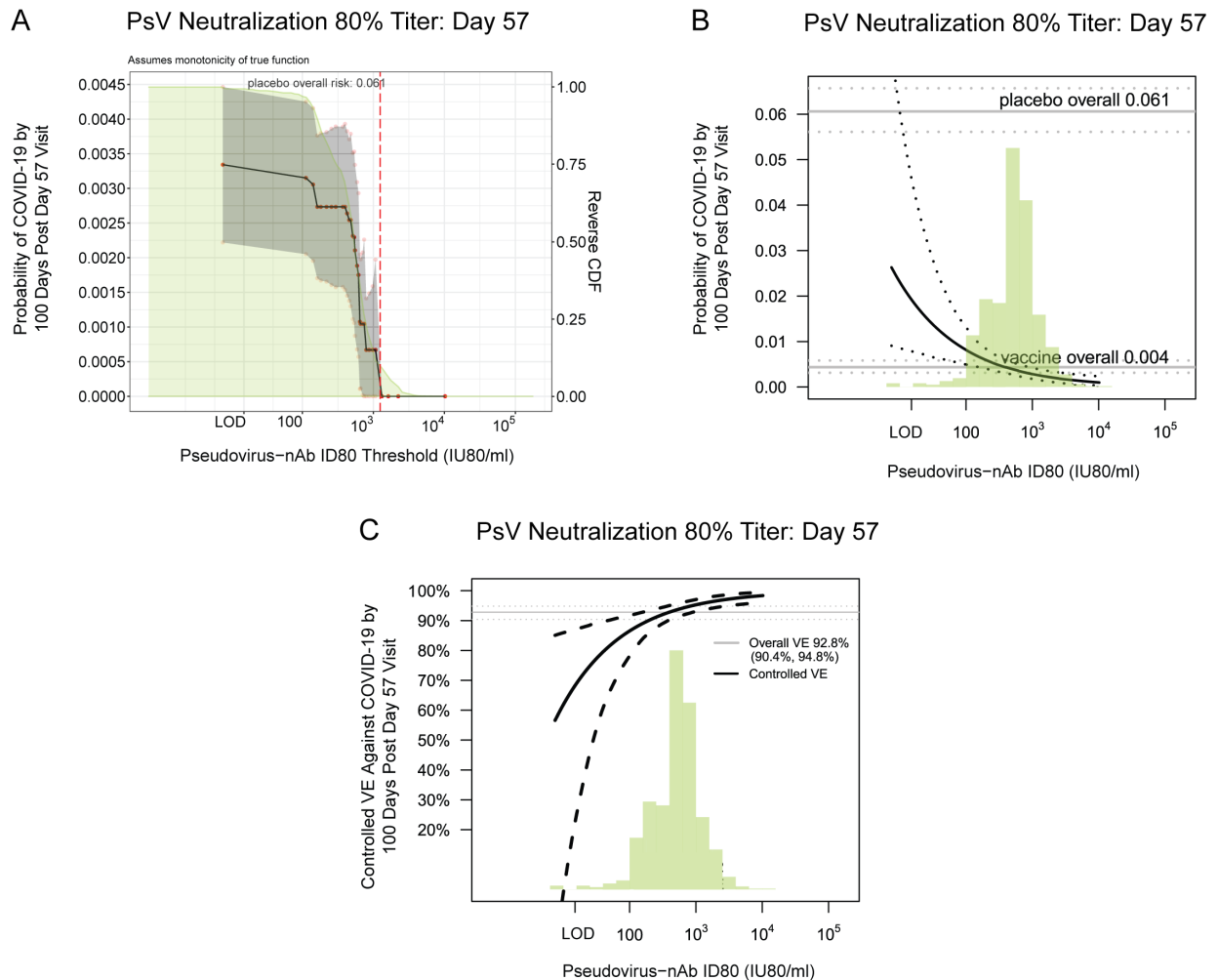


Fig. S23. Further analyses of Day 57 ID80 level as a correlate of risk and analysis as a correlate of protection. (A) Covariate-adjusted cumulative incidence of COVID-19 by 100 days post Day 57 by vaccinated baseline SARS-CoV-2 negative per-protocol subgroups defined by Day 57 ID80 level above a threshold, with reverse cumulative distribution function (CDF) of Day 57 ID80 level overlaid in green. The red dots are point estimates at 35 threshold values equally spaced over quantiles of the observed marker values, linearly interpolated by solid black lines; the gray shaded area is pointwise 95% confidence intervals (CIs). The upper boundary of the green shaded area is the estimate of the reverse cumulative distribution function (CDF) of Day 57 ID80 level in baseline SARS-CoV-2 negative per-protocol vaccine recipients. The vertical red dashed line is the Day 57 ID80 threshold above which no post Day 57 COVID endpoints occurred. (B) Covariate-adjusted cumulative incidence of COVID-19 by 100 days post Day 57 by Day 57 ID80 level. The dotted black lines indicate bootstrap point-wise 95% CIs. The upper and lower horizontal gray lines are the overall cumulative incidence of COVID-19 from 7 to 100 days post Day 57 in placebo and vaccine recipients, respectively. (C) Vaccine efficacy (solid black line) by Day 57 ID80 level, estimated using the method of Gilbert, Fong, and Carone (28). The dashed black lines indicate bootstrap point-wise 95% CIs. The horizontal gray line is the overall vaccine efficacy from 7 to 100 days post Day 57, with the dotted gray lines indicating the 95% CIs (this number 92.8% differs from the 94.1% reported in (6), which was based on counting COVID-19 endpoints starting 14 days post Day 29). In (B) and (C), the green histograms are an estimate of the density of Day 57 ID80 level in baseline negative per-protocol vaccine recipients. LOD, limit of detection. Baseline covariates adjusted for: baseline risk score, at risk status, community of color status.

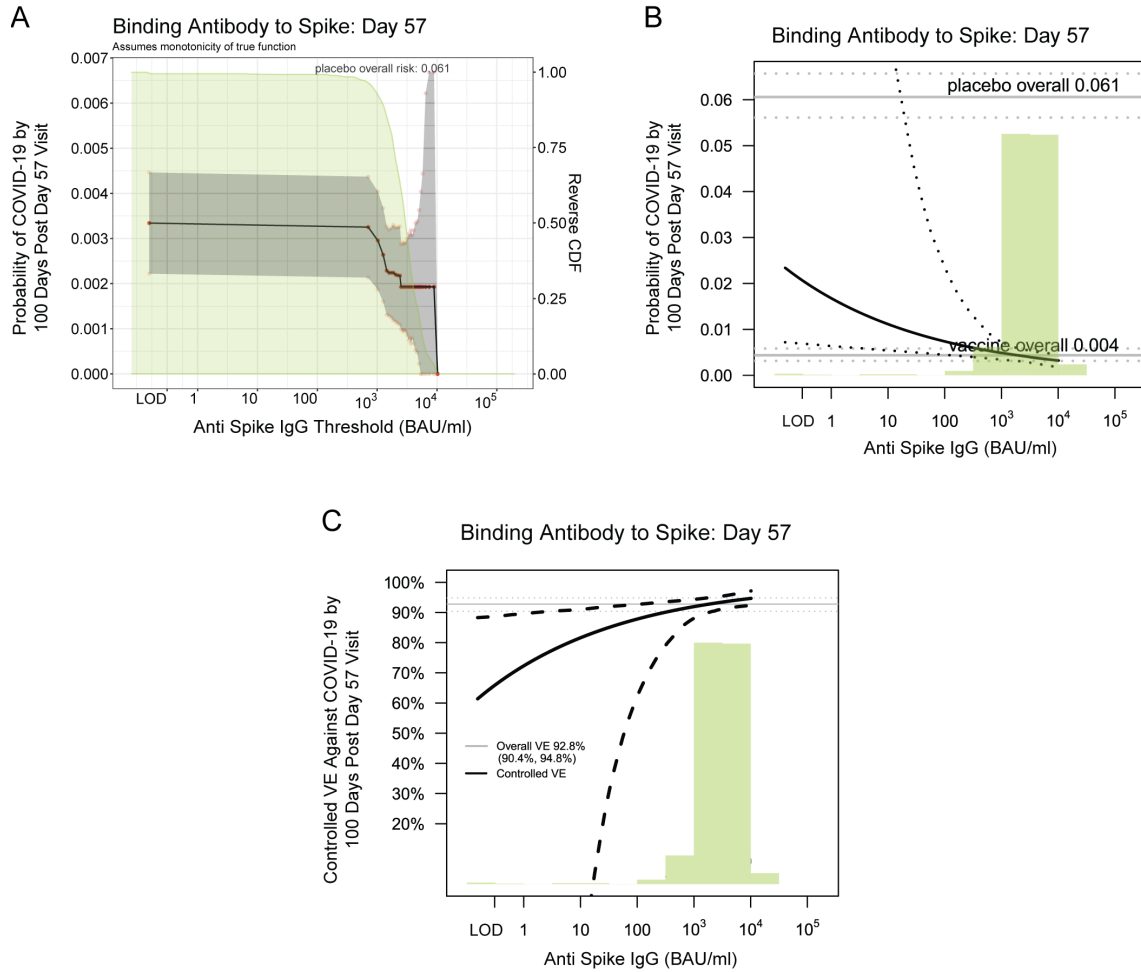


Fig. S24. Further analyses of Day 57 anti-spike IgG level as a correlate of risk and as a correlate of protection. (A) Covariate-adjusted cumulative incidence of COVID-19 by 100 days post Day 57 by vaccinated baseline SARS-CoV-2 negative per-protocol subgroups defined by Day 57 anti-spike IgG level above a threshold, with reverse cumulative distribution function (CDF) of Day 57 anti-spike IgG level overlaid in green. The red dots are point estimates at 35 threshold values equally spaced over quantiles of the observed marker values, linearly interpolated by solid black lines; the gray shaded area is pointwise 95% confidence intervals (CIs). The upper boundary of the green shaded area is the estimate of the reverse cumulative distribution function (CDF) of Day 57 anti-spike IgG level in baseline SARS-CoV-2 negative per-protocol vaccine recipients. The vertical red dashed line is the Day 57 anti-spike IgG threshold above which no post Day 57 COVID endpoints occurred. (B) Covariate-adjusted cumulative incidence of COVID-19 by 100 days post Day 57 by Day 57 anti-spike IgG level. The dotted black lines indicate bootstrap point-wise 95% CIs. The upper and lower horizontal gray lines are the overall cumulative incidence of COVID-19 from 7 to 100 days post Day 57 in placebo and vaccine recipients, respectively. (C) Vaccine efficacy (solid black line) by Day 57 anti-spike IgG level, estimated using the method of Gilbert, Fong, and Carone (28). The dashed black lines indicate bootstrap point-wise 95% CIs. The horizontal gray line is the overall vaccine efficacy from 7 to 100 days post Day 57, with the dotted gray lines indicating the 95% CIs (this number 92.8% differs from the 94.1% reported in (6), which was based on counting COVID-19 endpoints starting 14 days post Day 29). In (B) and (C), the green histograms are an estimate of the density of Day 57 anti-spike IgG level in baseline negative per-protocol vaccine recipients. LOD, limit of detection. Baseline covariates adjusted for: baseline risk score, at risk status, community of color status.

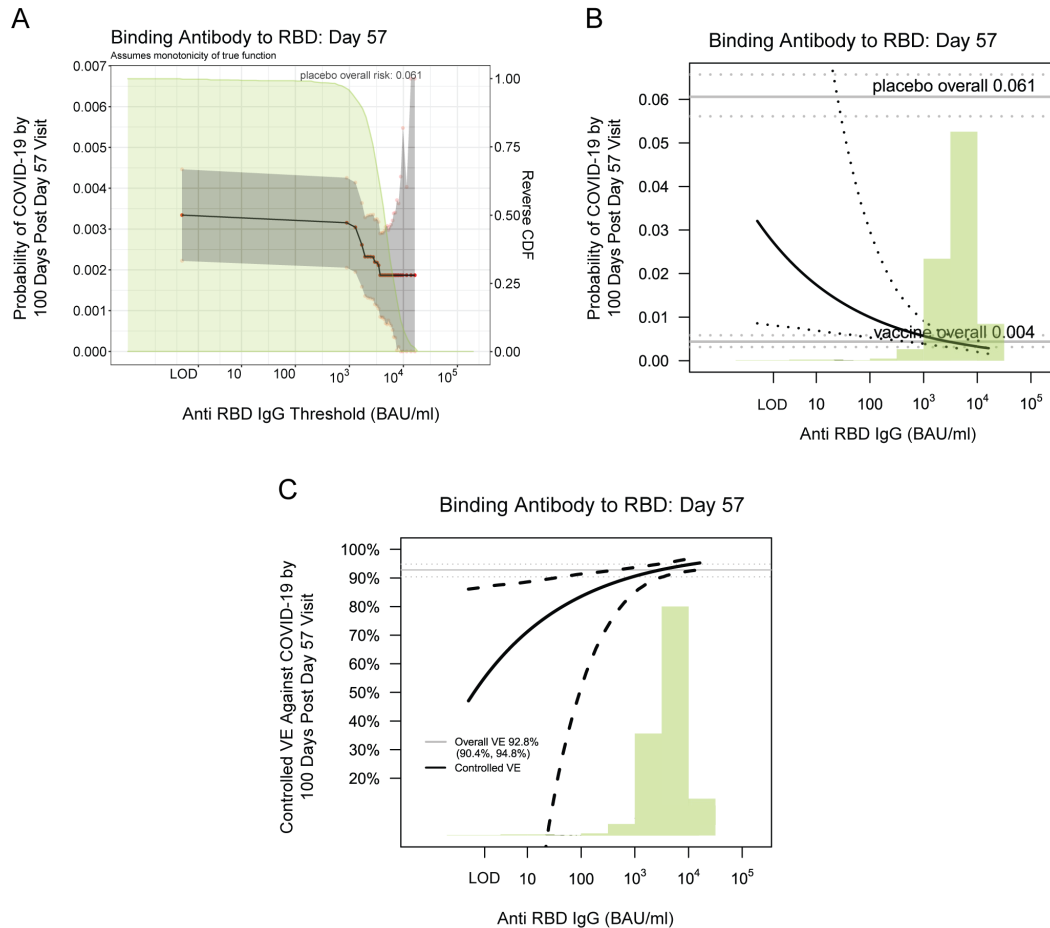


Fig. S25. Further analyses of Day 57 anti-RBD IgG level as a correlate of risk and as a correlate of protection. (A) Covariate-adjusted cumulative incidence of COVID-19 by 100 days post Day 57 by vaccinated baseline SARS-CoV-2 negative per-protocol subgroups defined by Day 57 anti-RBD IgG level above a threshold, with reverse cumulative distribution function (CDF) of Day 57 anti-RBD IgG level overlaid in green. The red dots are point estimates at 35 threshold values equally spaced over quantiles of the observed marker values, linearly interpolated by solid black lines; the gray shaded area is pointwise 95% confidence intervals (CIs). The upper boundary of the green shaded area is the estimate of the reverse cumulative distribution function (CDF) of Day 57 anti-RBD IgG level in baseline SARS-CoV-2 negative per-protocol vaccine recipients. The vertical red dashed line is the Day 57 anti-RBD IgG threshold above which no post Day 57 COVID endpoints occurred. (B) Covariate-adjusted cumulative incidence of COVID-19 by 100 days post Day 57 by Day 57 anti-RBD IgG level. The dotted black lines indicate bootstrap point-wise 95% CIs. The upper and lower horizontal gray lines are the overall cumulative incidence of COVID-19 from 7 to 100 days post Day 57 in placebo and vaccine recipients, respectively. (C) Vaccine efficacy (solid black line) by Day 57 anti-RBD IgG level, estimated using the method of Gilbert, Fong, and Carone (28). The dashed black lines indicate bootstrap point-wise 95% CIs. The horizontal gray line is the overall vaccine efficacy from 7 to 100 days post Day 57, with the dotted gray lines indicating the 95% CIs (this number 92.8% differs from the 94.1% reported in (6), which was based on counting COVID-19 endpoints starting 14 days post Day 29). In (B) and (C), the green histograms are an estimate of the density of Day 57 anti-RBD IgG level in baseline negative per-protocol vaccine recipients. LOD, limit of detection. Baseline covariates adjusted for: baseline risk score, at risk status, community of color status.

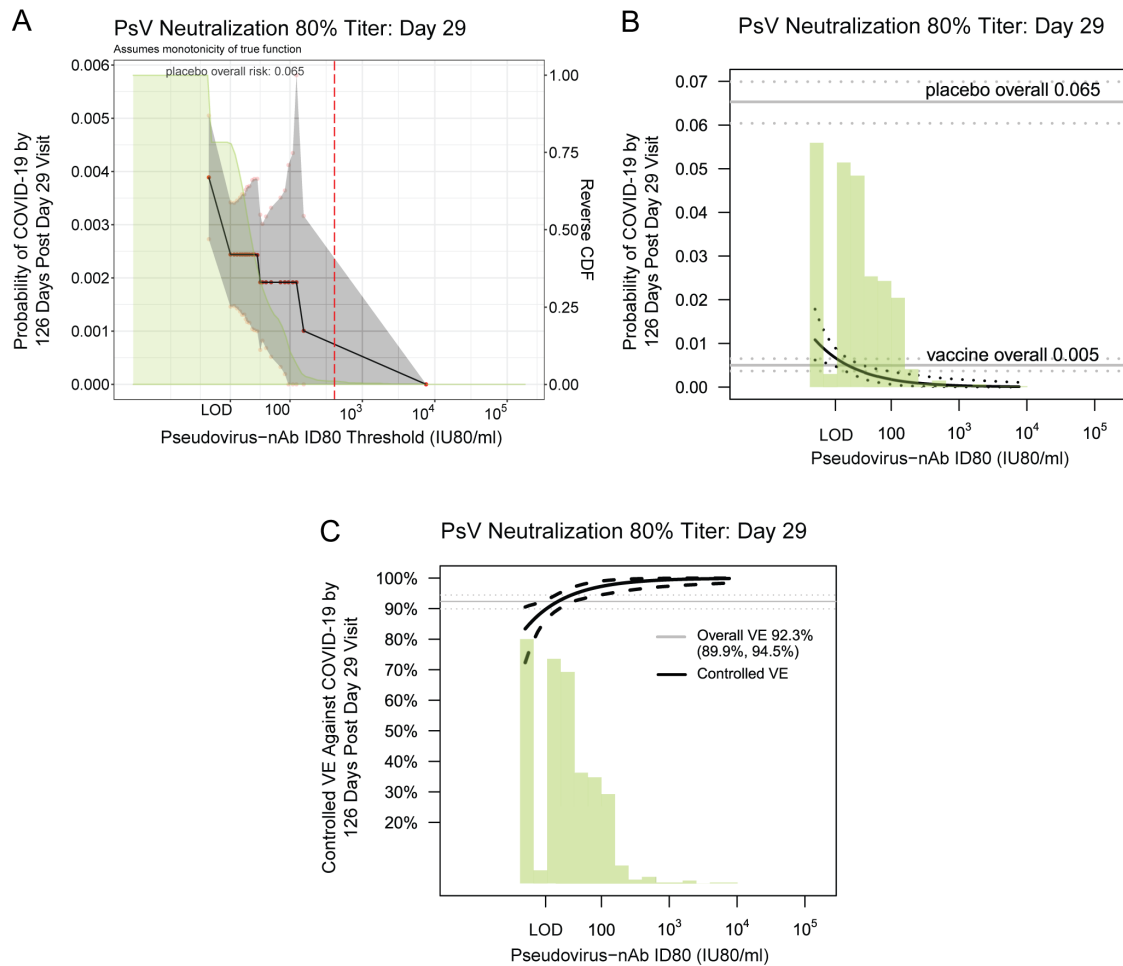


Fig. S26. Further analyses of Day 29 ID80 level as a correlate of risk and as a correlate of protection. (A) Covariate-adjusted cumulative incidence of COVID-19 by 126 days post Day 29 by vaccinated baseline SARS-CoV-2 negative per-protocol subgroups defined by Day 29 ID80 level above a threshold, with reverse cumulative distribution function (CDF) of Day 29 ID80 level overlaid in green. The red dots are point estimates at 35 threshold values equally spaced over quantiles of the observed marker values, linearly interpolated by solid black lines; the gray shaded area is pointwise 95% confidence intervals (CIs). The upper boundary of the green shaded area is the estimate of the reverse cumulative distribution function (CDF) of Day 29 ID80 level in baseline SARS-CoV-2 negative per-protocol vaccine recipients. The vertical red dashed line is the Day 29 ID80 threshold above which no post Day 29 COVID endpoints occurred. (B) Covariate-adjusted cumulative incidence of COVID-19 by 126 days post Day 29 by Day 29 ID80 level. The dotted black lines indicate bootstrap point-wise 95% CIs. The upper and lower horizontal gray lines are the overall cumulative incidence of COVID-19 from 7 to 126 days post Day 29 in placebo and vaccine recipients, respectively. (C) Vaccine efficacy (solid black line) by Day 29 ID80 level, estimated using the method of Gilbert, Fong, and Carone (28). The dashed black lines indicate bootstrap point-wise 95% CIs. The horizontal gray line is the overall vaccine efficacy from 7 to 126 days post Day 29, with the dotted gray lines indicating the 95% CIs (this number 92.3% differs from the 94.1% reported in (6), which was based on counting COVID-19 endpoints starting 14 days post Day 29). In (B) and (C), the green histograms are an estimate of the density of Day 29 ID80 level in baseline negative per-protocol vaccine recipients. LOD, limit of detection. Baseline covariates adjusted for: baseline risk score, at risk status, community of color status.

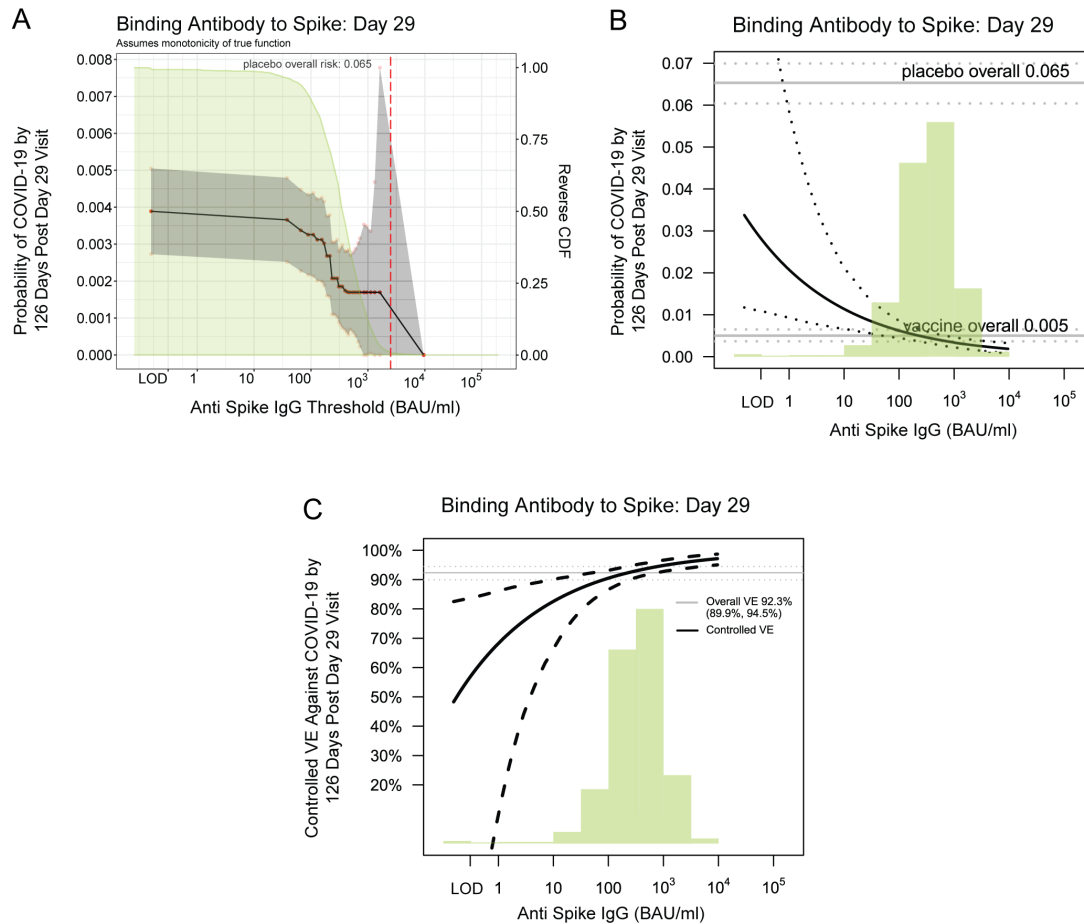


Fig. S27. Further analyses of Day 29 anti-spike IgG level as a correlate of risk and as a correlate of protection. (A) Covariate-adjusted cumulative incidence of COVID-19 by 126 days post Day 29 by vaccinated baseline SARS-CoV-2 negative per-protocol subgroups defined by Day 29 anti-spike IgG level above a threshold, with reverse cumulative distribution function (CDF) of Day 29 anti-spike IgG level overlaid in green. The red dots are point estimates at 35 threshold values equally spaced over quantiles of the observed marker values, linearly interpolated by solid black lines; the gray shaded area is pointwise 95% confidence intervals (CIs). The upper boundary of the green shaded area is the estimate of the reverse cumulative distribution function (CDF) of Day 29 anti-spike IgG level in baseline SARS-CoV-2 negative per-protocol vaccine recipients. The vertical red dashed line is the Day 29 anti-spike IgG threshold above which no post Day 29 COVID endpoints occurred. (B) Covariate-adjusted cumulative incidence of COVID-19 by 126 days post Day 29 by Day 29 anti-spike IgG level. The dotted black lines indicate bootstrap point-wise 95% CIs. The upper and lower horizontal gray lines are the overall cumulative incidence of COVID-19 from 7 to 126 days post Day 29 in placebo and vaccine recipients, respectively. (C) Vaccine efficacy (solid black line) by Day 29 anti-spike IgG level, estimated using the method of Gilbert, Fong, and Carone (28). The dashed black lines indicate bootstrap point-wise 95% CIs. The horizontal gray line is the overall vaccine efficacy from 7 to 126 days post Day 29, with the dotted gray lines indicating the 95% CIs (this number 92.3% differs from the 94.1% reported in (6), which was based on counting COVID-19 endpoints starting 14 days post Day 29). In (B) and (C), the green histograms are an estimate of the density of Day 29 anti-spike IgG level in baseline negative per-protocol vaccine recipients. LOD, limit of detection. Baseline covariates adjusted for: baseline risk score, at risk status, community of color status.

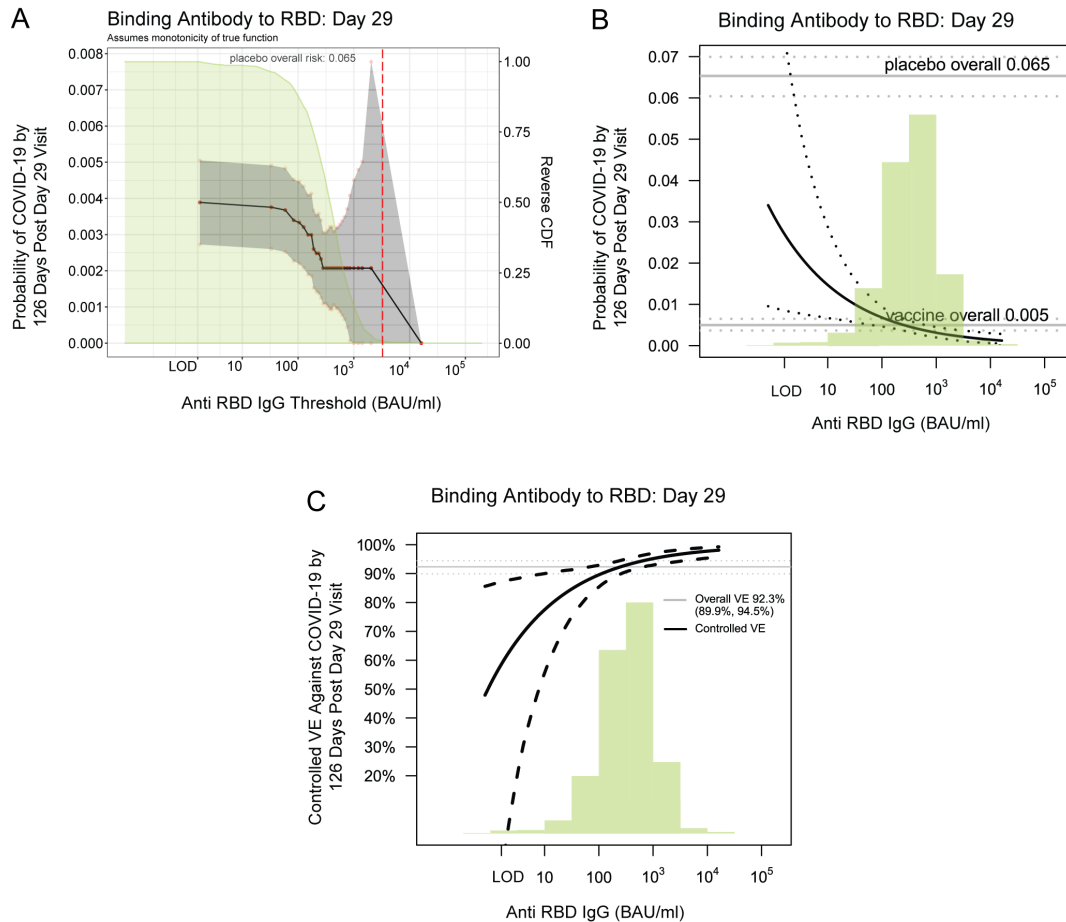


Fig. S28. Further analyses of Day 29 anti-RBD IgG level as a correlate of risk and as a correlate of protection. (A) Covariate-adjusted cumulative incidence of COVID-19 by 126 days post Day 29 by vaccinated baseline SARS-CoV-2 negative per-protocol subgroups defined by Day 29 anti-RBD IgG level above a threshold, with reverse cumulative distribution function (CDF) of Day 29 anti-RBD IgG level overlaid in green. The red dots are point estimates at 35 threshold values equally spaced over quantiles of the observed marker values, linearly interpolated by solid black lines; the gray shaded area is pointwise 95% confidence intervals (CIs). The upper boundary of the green shaded area is the estimate of the reverse cumulative distribution function (CDF) of Day 29 anti-RBD IgG level in baseline SARS-CoV-2 negative per-protocol vaccine recipients. The vertical red dashed line is the Day 29 anti-RBD IgG threshold above which no post Day 29 COVID endpoints occurred. (B) Covariate-adjusted cumulative incidence of COVID-19 by 126 days post Day 29 by Day 29 anti-RBD IgG level. The dotted black lines indicate bootstrap point-wise 95% CIs. The upper and lower horizontal gray lines are the overall cumulative incidence of COVID-19 from 7 to 126 days post Day 29 in placebo and vaccine recipients, respectively. (C) Vaccine efficacy (solid black line) by Day 29 anti-RBD IgG level, estimated using the method of Gilbert, Fong, and Carone (28). The dashed black lines indicate bootstrap point-wise 95% CIs. The horizontal gray line is the overall vaccine efficacy from 7 to 126 days post Day 29, with the dotted gray lines indicating the 95% CIs (this number 92.3% differs from the 94.1% reported in (6), which was based on counting COVID-19 endpoints starting 14 days post Day 29). In (B) and (C), the green histograms are an estimate of the density of Day 29 anti-RBD IgG level in baseline negative per-protocol vaccine recipients. LOD, limit of detection. Baseline covariates adjusted for: baseline risk score, at risk status, community of color status.

Supplementary Text S2: Controlled vaccine efficacy sensitivity analysis and mediation analysis

Controlled vaccine efficacy sensitivity analysis to assess robustness of the effect of antibody marker on preventing COVID-19 to unmeasured confounding

Fig. 2 reports results for estimation and inference for baseline covariate-marginalized COVID-19 risk ratios comparing vaccine recipients with Day 57 antibody marker in the third tertile vs. in the first tertile; denote this marginalized risk ratio by $RR_M(0,1)$, where 1 indicates the third tertile and 0 indicates the first tertile. As described in the SAP and Gilbert, Fong, and Carone (28), under the assumption of no unmeasured confounding of the effect of the antibody marker on COVID-19, the COVID-19 risk ratio $RR_M(0,1)$ equals a causal effect parameter $RR_C(0,1)$, the controlled effects risk ratio, which in turn equals $(1 - CVE(1))/(1 - CVE(0))$, where $CVE(1)$ is controlled vaccine efficacy for vaccine recipients with third tertile marker level and $CVE(0)$ is controlled vaccine efficacy for vaccine recipients with first tertile marker level. In sensitivity analysis, we allow for some unmeasured confounding that makes $RR_M(0,1) < RR_C(0,1)$. In particular, as specified in the SAP the first part of the sensitivity analysis reports E-values, both for the point estimate of $RR_C(0,1)$ and for the upper 95% confidence limit of $RR_C(0,1)$. The E-value is the minimum strength of association, on the risk ratio scale, that an unmeasured confounder would need to have with both the antibody marker (exposure) and the COVID-19 outcome in order to fully explain away a specific observed exposure-outcome association, conditional on the measured covariates (29). Here ‘fully explain away’ means that $RR_C(0,1) = 1$, or equivalently $CVE(0) = CVE(1)$, i.e., controlled vaccine efficacy does not differ by upper vs. lower tertile, which means no correlate of protection. Many epidemiologists recommend that E-values are always reported (or alternative sensitivity metrics) for causal inferences, given that it is not possible to guarantee that all confounders are controlled for in the analysis; thus by using E-values we are implementing best practice.

In addition, we apply the sensitivity analysis technique developed by Ding and Vanderweele (2016) (53), as implemented in the SAP and in Gilbert, Fong, and Carone (28) for the COVE trial correlates application, to estimate $RR_C(0,1) = (1 - CVE(1))/(1 - CVE(0))$ under a specified scenario of unmeasured confounding that makes it harder to conclude a correlate of protection. This sensitivity analysis specifies an amount of unmeasured confounding defined by $RR_{UD}(0,1) = RR_{EU}(0,1) = 2$, where these parameters are defined in Ding and Vanderweele (2016) (52) and in our SAP and Gilbert et al. If the 95% confidence interval for $RR_C(0,1) = (1 - CVE(1))/(1 - CVE(0))$ is less than 1 after accounting for this confounding that pushes the confidence interval upwards, it provides evidence for a correlate of protection with a degree of robustness to possible unmeasured confounding.

Table S8 shows results for the eight Day 57 and Day 29 antibody markers categorized by upper vs. lower tertile that were assessed as correlates. For example, the E-value of 9.3 for the Day 57 ID80 marker means that a marginalized risk ratio $RR_M(0,1)$ at the observed value 0.20 could be explained away (i.e., $RR_C(0,1) = 1.0$) by an unmeasured confounder associated with

both the exposure and the outcome by a marginalized risk ratio of 9.3-fold each, after accounting for the measured potential confounders (risk score, at-risk status, community of color indicator), but that weaker confounding could not do so. In addition, the E-value of 3.3 for the upper confidence limit UL indicates the strength of unmeasured confounding at which statistical significance of the inference that $CVE(1) > CVE(0)$ would be lost.

Table S8. Sensitivity analysis to assess Day 57 and Day 29 antibody markers categorized as upper vs. lower tertiles as controlled vaccine efficacy CoPs against COVID-19

Antibody Marker	Marginalized Risk Ratio $RR_{M(0,1)}^1$		Controlled Risk Ratio = $(1-CVE(1))/(1-CVE(0))^2$		E-values ³	
	Point Est.	95% CI	Point Est.	95% CI	For Point Est.	For 95% CI UL
Day 57 Spike IgG	0.24	0.06, 0.56	0.32	0.09, 0.75	7.9	3.0
Day 57 RBD IgG	0.28	0.08, 0.62	0.38	0.11, 0.83	6.5	2.6
Day 57 PsV ID50	0.31	0.08, 0.72	0.42	0.11, 0.96	5.9	2.1
Day 57 PsV ID80	0.20	0.03, 0.51	0.27	0.05, 0.68	9.3	3.3
Day 29 Spike IgG	0.19	0.06, 0.40	0.26	0.08, 0.53	9.8	4.5
Day 29 RBD IgG	0.29	0.10, 0.59	0.38	0.13, 0.79	6.5	2.8
Day 29 PsV ID50	0.33	0.13, 0.65	0.44	0.17, 0.86	5.5	2.5
Day 29 PsV ID80	0.22	0.07, 0.46	0.30	0.10, 0.61	8.5	3.8

¹This analysis estimates the Controlled Risk Ratio under the no-unmeasured confounding and positivity assumptions.

²Conservative (upper bound) estimate assuming unmeasured confounding at level $RR_{UD}(0, 1) = RR_{EU}(0, 1) = 2$ and thus $B(0, 1) = 4/3$ (notation as in Ding and vanderWeele (2016)).

³E-values are computed for upper tertile ($s = 1$) vs. lower tertile ($s = 0$) biomarker subgroups after controlling for baseline risk score, at risk or not, community of color or not; UL = upper limit.

A second sensitivity analysis was conducted to assess robustness of findings on correlates of vaccine efficacy as a function of the quantitative antibody marker level varying over its whole range, which builds on the analyses that assumed no-unmeasured confounding that were reported in **Fig. 4C** for ID50 titer and in **figs. S22-S28** for the other seven antibody markers. With details in the SAP and Gilbert, Fong, and Carone (28), the sensitivity analysis was done similarly to the analysis above for categorized markers, except now instead of specifying $RR_{UD}(0,1)$ and $RR_{EU}(0,1)$ for third tertile vs. first tertile, we specified $RR_{UD}(s^{15}, s^{85}) = 2$ and $RR_{EU}(s^{15}, s^{85}) = 2$ for s^{15} the 15th percentile of the antibody marker and s^{85} the 85th percentile of the antibody marker. We then specified unmeasured confounding across the whole range of antibody marker levels through the model

$$\log(RR_{UD}(s_1, s_2)) = [(s_2 - s_1) / (s^{85} - s^{15})] \log(RR_{UD}(s^{15}, s^{85})) \text{ for all } s_1 \leq s_2,$$

with the same model used for $RR_{EU}(s1, s2)$. The result of the sensitivity analysis is point estimates of controlled vaccine efficacy $CVE(s)$ over the range s of antibody marker levels, with 95% bootstrap pointwise confidence intervals, which build in robustness to unmeasured confounding by supposing bias that makes the estimate of the curve $CVE(s)$ flatter. **Figures S29 and S30** show the sensitivity analysis results for the eight antibody markers, for the markers at Day 57 and at Day 29, respectively. We interpret the results as follows. For both binding antibody markers at each time point (top panels), the point estimate of the $CVE(s)$ curve with measured confounding is considerably flatter than under no unmeasured confounding (solid red curve vs. solid pink curve), and it is possible to draw a horizontal line between the lower and upper 95% confidence limits without intersecting either limit curve. This suggests that at the specified amount of unmeasured confounding for this quantitative marker analysis, the evidence for a CoP is not robust. In contrast, for the Day 29 ID50 and ID80 titer markers, the point estimate of the $CVE(s)$ curve with posited measured confounding varies markedly, from 85% at the left-most point and 98% at the right-most point, constituting a 7.5-fold difference in efficacy level ($7.5 = (1-.85)/(1-0.98)$), and a horizontal line cannot be drawn between the lower and upper 95% confidence limits without intersecting either limit curve (where preferably the analysis would use simultaneous 95% confidence intervals). We conclude that the sensitivity analysis shows robustness of the Day 29 ID50 and ID80 neutralization titer markers as CoPs. The Day 57 ID50 and ID80 titer marker sensitivity analyses show less robustness of results compared to the Day 29 markers.

Mediation analysis

Table S9. Table of mediation effect estimates for quantitative markers with 95% confidence intervals.

Direct VE = VE comparing vaccine vs. placebo with marker set to distribution in placebo.
 Indirect VE = VE in vaccinated comparing observed marker vs. hypothetical marker under placebo.
 Prop. mediated = fraction of total risk reduction from vaccine attributed to antibody response.

Time	Assay	Direct VE	Indirect VE	Prop. mediated
Day 29	PsV Neutralization 50% Titer (ID50, IU50/ml)	0.560 (0.422, 0.665)	0.832 (0.769, 0.878)	0.685 (0.585, 0.784)
Day 29	PsV Neutralization 80% Titer (ID80, IU80/ml)	0.739 (0.601, 0.829)	0.717 (0.597, 0.801)	0.485 (0.345, 0.624)

In the main text, it was claimed that “Yet, under the reasonable assumption that the vaccine’s effect on the risk of COVID-19 operating through the Day 57 ID50 marker is non-negative, 68% may be a lower bound on the proportion of vaccine efficacy that is mediated through ID50 levels

at both Day 29 and Day 57.” The mathematical statement of this assumption is that $\beta \geq 0$, where

$$\beta = E[Y(1, M1(0), 1, M2(1, M1(0), 1))] - E[Y(1, M1(0), 1, M2(0, M1(0), 0))].$$

Here $Y(1, m1, 1, m2)$ is the potential COVID-19 outcome under assignment to both doses of the vaccine and if the Day 29 ID50 marker is set to $m1$ and the Day 57 ID50 marker is set to $m2$; $M1(0)$ is Day 29 ID50 marker under assignment to placebo (and hence equals $LOD/2$); and $M2(a1, m1, a2)$ is Day 57 ID50 marker under assignment of vaccine dose one to $a1$ and vaccine dose two to $a2$. The parameter β measures an effect of the vaccine operating only through the Day 57 antibody marker, with Day 29 antibody marker held fixed to what it would have been under assignment to placebo.

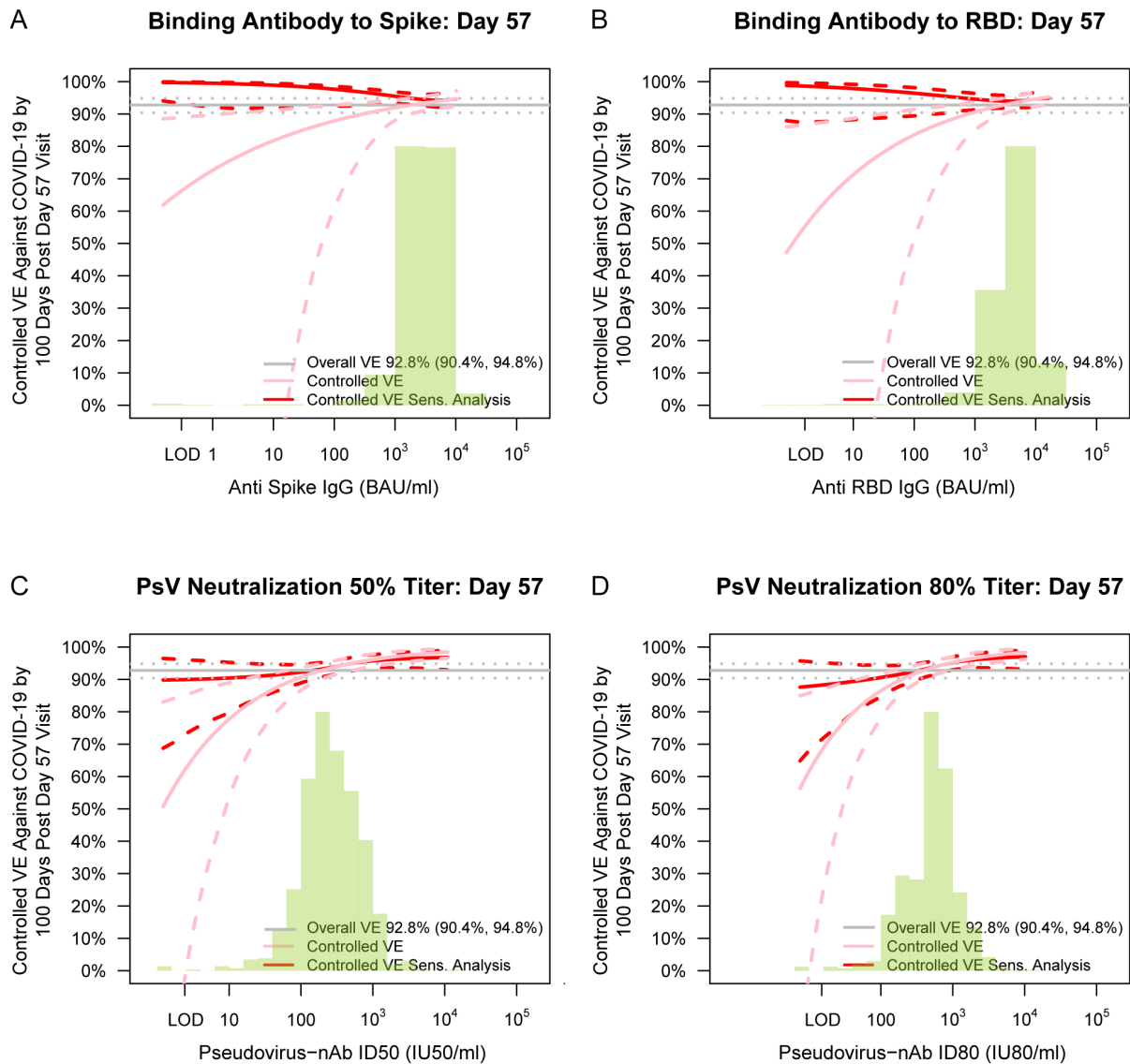


Fig. S29. Vaccine efficacy with sensitivity analysis by Day 57 (A) anti-spike IgG level, (B) anti-RBD IgG level, (C) ID50 level, or (D) ID80 level. Vaccine efficacy estimates were obtained using the method of Gilbert, Fong, and Carone (28). The upper boundary of the green shaded area is the estimate of the reverse cumulative distribution function of the marker in baseline SARS-CoV-2 negative per-protocol vaccine recipients. The pink solid line is point estimates assuming no unmeasured confounding; the dashed lines are bootstrap point-wise 95% CIs. The red solid line is point estimates assuming unmeasured confounding in a sensitivity analysis (dashed lines are bootstrap point-wise 95% CIs); see supplementary text S2 and the SAP (Section 12.1.2) for details of the sensitivity analysis. The horizontal gray line is the overall vaccine efficacy from 7 to 100 days post Day 57, with the dotted gray lines indicating the 95% CIs (this number 92.8% differs from the 94.1% reported in (6), which was based on counting COVID-19 endpoints starting 14 days post Day 29). LOD, limit of detection.

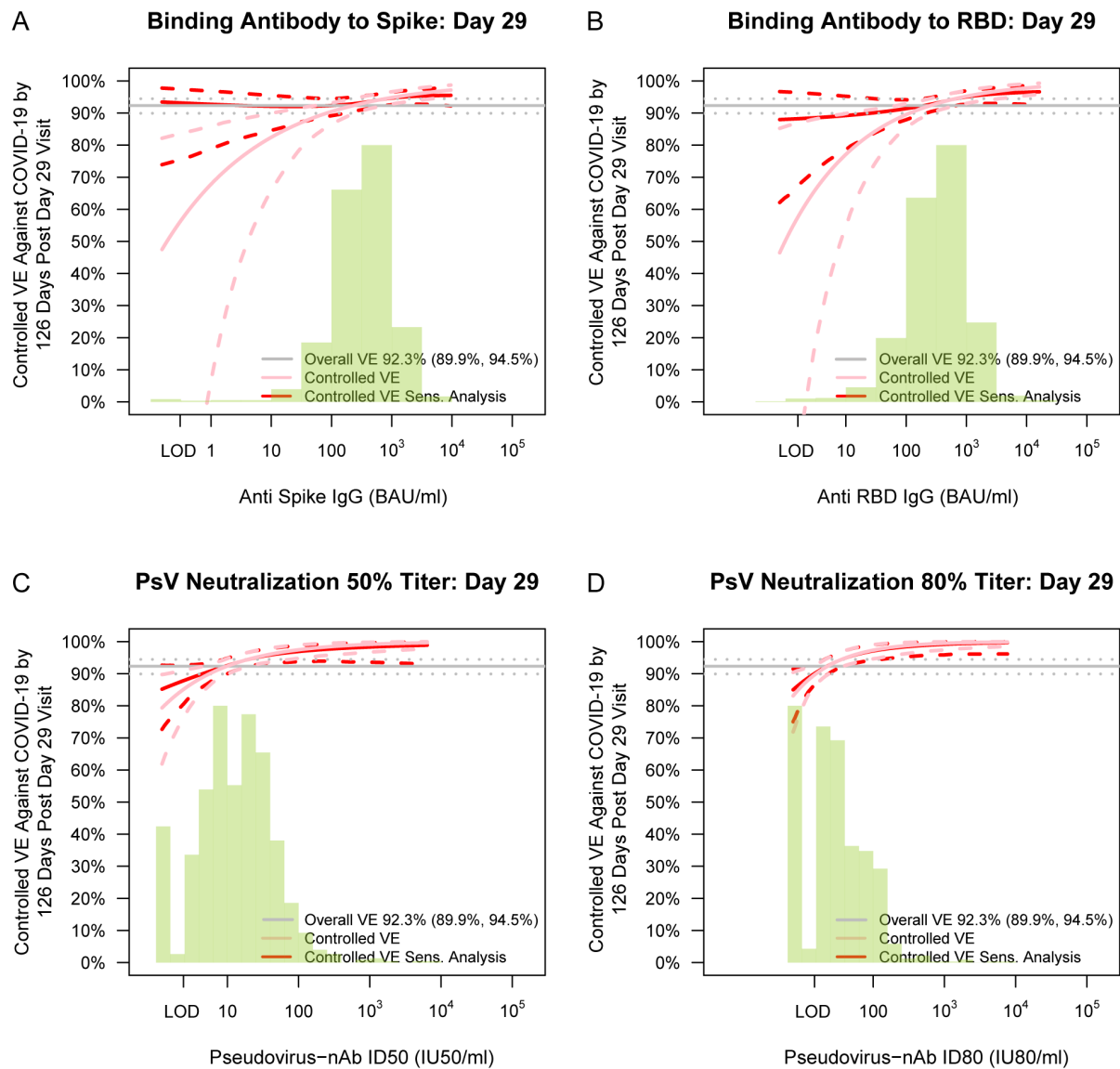


Fig. S30. Vaccine efficacy with sensitivity analysis by Day 29 (A) anti-spike IgG level, (B) anti-RBD IgG level, (C) ID50 level, or (D) ID80 level. Vaccine efficacy estimates were obtained using the method of Gilbert, Fong, and Carone (28). The upper boundary of the green shaded area is the estimate of the reverse cumulative distribution function of the marker in baseline SARS-CoV-2 negative per-protocol vaccine recipients. The pink solid line is point estimates assuming no unmeasured confounding; the dashed lines are bootstrap point-wise 95% CIs. The red solid line is point estimates assuming unmeasured confounding in a sensitivity analysis (dashed lines are bootstrap point-wise 95% CIs); see supplementary text S2 (and the SAP Section 12.1.2) for details of the sensitivity analysis. The horizontal gray line is the overall vaccine efficacy from 7 to 126 days post Day 29, with the dotted gray lines indicating the 95% CIs (this number 92.3% differs from the 94.1% reported in (6), which was based on counting COVID-19 endpoints starting 14 days post Day 29). LOD, limit of detection.